WL-TR-96-4018

CERAMIC BEARING DEVELOPMENT

VOL 4, TRIBOCHEMICAL FINISHING OF SILICON NITRIDE

S. R. HAH
TRAUGOTT E. FISCHER
CHARLES BURK

NORTON ADVANCED CERAMICS
DIV OF SGNICC
10 AIRPORT PARK ROAD
EAST GRANBY CT 06026

MARCH 1995

INTERIM REPORT FOR 08/01/92-10/01/94

MATERIALS DIRECTORATE
WRIGHT LABORATORY
AIR FORCE MATERIEL COMMAND
WRIGHT PATTERSON AFB OH 45433-7734

DISCLAIMER NOTICE

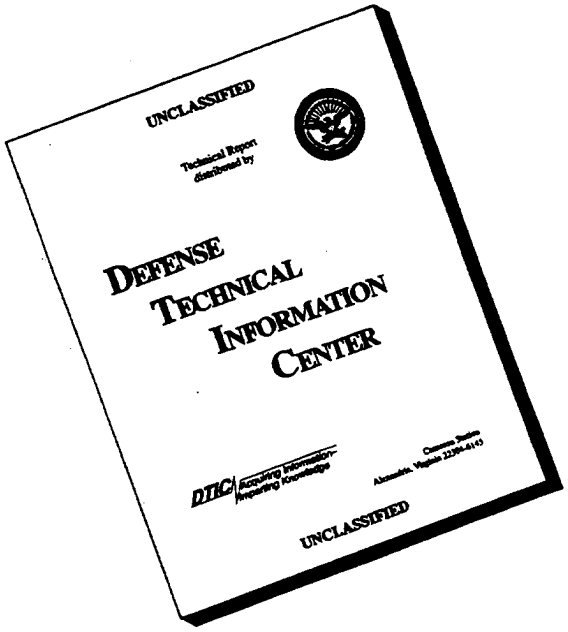

THIS DOCUMENT IS BEST QUALITY AVAILABLE. THE COPY FURNISHED TO DTIC CONTAINED A SIGNIFICANT NUMBER OF PAGES WHICH DO NOT REPRODUCE LEGIBLY.

NOTICE

When government drawings, specifications, or other data are used for any purpose other than in connection with a definitely related government procurement operation, the United States Government thereby incurs no responsibility nor any obligation whatsoever; and the fact that the government may have formulated, furnished, or in any way supplied the said drawings, specifications, or other data, is not to be regarded by implication or otherwise as in any manner licensing the holder or any other person or corporation, or conveying any rights or permission to manufacture, use, or sell any patented invention that may in any way be related thereto.

This report is releasable to the National Technical Information Service (NTIS). At NTIS, it will be available to the general public, including foreign nations.

This technical report has been reviewed and is approved for publication.

KARL R. MECKLENBURG, Project Engineer
Nonstructural Materials Branch
Nonmetallic Materials Division

KENT J. EISENTRAUT, Chief
Nonstructural Materials Branch
Nonmetallic Materials Division

CHARLES E. BROWNING, Chief
Nonmetallic Materials Division
Materials Directorate

If your address has changed, if you wish to be removed from our mailing list, or if the addressee is no longer employed by your organization, please notify WL/MLBT, Bldg 654, 2941 P Street, Suite 1, Wright-Patterson AFB OH 45433-7750 to help maintain a current mailing list.

Copies of this report should not be returned unless return is required by security considerations, contractual obligations, or notice on a specific document.

REPORT DOCUMENTATION PAGE

Form Approved
OMB No. 0704-0188

1. AGENCY USE ONLY *(Leave blank)*	2. REPORT DATE	3. REPORT TYPE AND DATES COVERED
	MAR 1995	INTERIM 08/01/92--10/01/94

4. TITLE AND SUBTITLE CERAMIC BEARING DEVELOPMENT

VOL 4, TRIBOCHEMICAL FINISHING OF SILICON NITRIDE

5. FUNDING NUMBERS

C F33615-92-C-5917
PE 62712
PR 8355
TA 00
WU 07

6. AUTHOR(S) S. R. HAH
TRAUGOTT E. FISCHER
CHARLES BURK

7. PERFORMING ORGANIZATION NAME(S) AND ADDRESS(ES)

NORTON ADVANCED CERAMICS
DIV OF SGNICC
10 AIRPORT PARK ROAD
EAST GRANBY CT 06026

8. PERFORMING ORGANIZATION REPORT NUMBER

9. SPONSORING/MONITORING AGENCY NAME(S) AND ADDRESS(ES)

MATERIALS DIRECTORATE
WRIGHT LABORATORY
AIR FORCE MATERIEL COMMAND
WRIGHT PATTERSON AFB OH 45433-7734

10. SPONSORING/MONITORING AGENCY REPORT NUMBER

WL-TR-96-4018

11. SUPPLEMENTARY NOTES

12a. DISTRIBUTION/AVAILABILITY STATEMENT

APPROVED FOR PUBLIC RELEASE; DISTRIBUTION IS UNLIMITED.

12b. DISTRIBUTION CODE

13. ABSTRACT *(Maximum 200 words)*

Tribochemical finishing of silicon nitride was developed by the Tribology Research Group at the Stevens Institute of technology. The finishing process produces ultrasmooth surfaces without mechanical defects.

Over 40 chemical solutions such as acids, bases, salts, inorganic and organic oxidizers were tested. Distilled water shows high volume removal rates but some solid wear debris are produced by surface fracture. Hydrogen peroxide, at 3 % or higher concentrations, produces high volume removal rates and pure tribochemical reaction. Chromic(VI) acid in all concentrations shows the best, purely tribochemical polishing results. Combinations of chromic oxides and hydrogen peroxides, also many of the chromates(VI) show outstanding efficiencies. Tribochemical polishing produces defect free, ultra smooth surfaces with Ra = 0.5 nm (0.02 μin) at 50 μm (0.002 in) cut-off, 2.0 nm (0.08 μin) at 0.8 mm (0.032 in) cut-off and 4.0 nm (0.16 μin) at 8 mm (0.320 in) cut-off .

Stainless steel and cast iron are effective tool materials for the tribochemical polishing of silicon nitride. Tribochemical polishing is easily adapted to most industrial finishing processes with minimal cost.

14. SUBJECT TERMS

Characterization of Silicon Nitride Ball Surfaces
Measurement of Residual Stress X-Ray Diffraction
Tribochemical Machining Tribochemical Polishing

15. NUMBER OF PAGES 113

16. PRICE CODE

17. SECURITY CLASSIFICATION OF REPORT	18. SECURITY CLASSIFICATION OF THIS PAGE	19. SECURITY CLASSIFICATION OF ABSTRACT	20. LIMITATION OF ABSTRACT
UNCLASSIFIED	UNCLASSIFIED	UNCLASSIFIED	SAR

Table of Contents

Table of Contents (continued)

List of Figures

List of Figures (continued)

List of Figures (continued)

List of Figures (continued)

List of Figures (continued)

List of Figures (continued)

List of Figures (continued)

List of Figures (continued)

List of Tables

Foreword

This work was performed by Traugott E. Fischer in cooperation with, and as a subcontractor to, Norton Advanced Ceramics Division of Saint Gobain/Norton Industrial Ceramics Corporation. It presents the results of several main tasks included in subcontract number 2882 of prime contract F33615-92-C-5917, issued by the United States Department of the Air Force, Air Force Systems Command, WPAFB, Ohio.

This written report is mainly the work of Traugott E. Fischer and Sangrok R. Hah, Ph.D. The contributing efforts of ARPA, for financial support, Norton Advanced Ceramics, for advice, technical support and provision of material. The following individuals provided technical advice and were key to the success of this program: Professor M. J. Kim of Arizona State University, Drs. David Cole and Jeff Schallenberger, of Evans East, Professor William Mayo of Rutgers University, Professors Bernard Gallois, Milos Seidl and H. J. Kwon of Stevens.

Several additions, changes, and edits were made to this report at Norton Advanced Ceramics.

1.0 Summary

Tribochemical Polishing (TCP) is a polishing process as a result of chemical reaction stimulated by simultaneous friction. It is capable of polishing hard materials. The technique is related to chemomechanical[1] polishing (CMP) or mechanochemical polishing MCP) used in the semiconductor industry, but it differs from these in that TCP does not use abrasives. Because of the absence of mechanical material removal, TCP is capable of producing surfaces that are very smooth, defect free, and have low residual stress. The material removal rate of TCP is similar to that of the finishing phases of dry (or mechanical) polishing. Silicon nitride is a widely used ceramic for high performance ball bearings and as an insulating interlayer in microelectronics. Tribochemical polishing of silicon nitride is a new technology developed by the Tribology Research Group at the Stevens Institute of Technology. In the framework of this program, the polishing process was further refined with the aim of producing the best possible surface quality at industrially useful removal rates. The variables explored were the contact pressure between tool and workpiece, the sliding speed of the tool, the chemical solutions and their concentrations, and materials that are effective tools.

For the purposes of the research, a ball-on-disc tribometer was used for the evaluation of material removal, friction coefficient, polishing rate and surface quality; a modified disc-on-disc tribometer was designed to study the feasibility of polishing large samples for industrial applications. The process is effective between the following two mechanical limits. At low sliding speed, application of a very high contact pressure introduces mechanical wear which results in rough surfaces and surface defects. A high sliding speed and low contact pressure favors hydrodynamic lubrication[2] where the surfaces are effectively separated by a fluid film and polishing stops.

Over 40 chemical solutions such as acids, bases, salts, inorganic and organic oxidizers were tested. Distilled water shows high volume removal rates but the mechanical wear limit is low so that some solid wear debris are produced by surface fracture. In various hydrogen peroxide concentrations, a minimum of 3 vol.% hydrogen peroxide is required to produce high volume removal rates and pure tribochemical reaction. Chromic(VI) acid in all concentrations less than the solubility limit shows the best, purely tribochemical polishing results. Combinations of chromic oxides and hydrogen peroxides, as well as many of the chromates(VI), show outstanding efficiencies. Tribochemical polishing in recommended chemical solutions produces defect free, ultra smooth surfaces with high volume removal rates. Some promising strong organic oxidants produce oxygen, but some of

them show 10-100 times lower volume removal rates. These fluids constitute interesting anti-wear reagents.

Tool materials for the tribochemical polishing of silicon nitride were explored for their use in manufacturing processes. It was found that stainless steel and cast iron are effective. Tribochemical polishing is a drop-in technology; it can be adapted in most industrial finishing processes with minimal cost and equipment modification.

The polished surfaces were examined by Nomarski differential interference contrast optical microscopy, Scanning electron microscopy, Energy dispersive X-ray spectroscopy, Profilometry, X-ray diffraction, Micro-Fourier transformed infrared spectroscopy, Chemical titration, X-ray photoelectron spectroscopy, Rutherford backscattering spectroscopy, Secondary ion mass spectroscopy and Atomic force microscopy. The primary reaction products, silicon dioxide and ammonia, are easily soluble in solvent to produce the secondary products: silicic acid and ammonium hydroxide. Surface stress analysis by X-ray diffraction shows no stress increase by tribochemical polishing. The method produces surfaces with a roughness Ra = 0.5 nm (0.02 μin) at 50 μm (0.002 in) cutoff, 2 nm (0.08 μin) at 0.8mm (0.032 in) cutoff and 6 nm (0.24 μin) at 8 mm (0.320 in) cutoff.

2.0 Introduction

The manufacture and finishing of ceramic bearing balls and other structural elements usually involves abrasive grinding and polishing with successively finer abrasive grains. Material removal occurs predominately by microfracture. This can produce cracks that penetrate to various depths into the surface, depending on the size of the abrasive grit. Surface cracks present an important limitation to the use and the reliability of ceramic structural elements because they can propagate through the material and cause failure. Morphological defects such as scratches, asperities or holes act as stress concentrators that limit the fatigue life and decrease the reliability of ceramics as well. The production of ceramic components with extremely smooth surfaces, devoid of cracks and other subsurface structural defects, is an important challenge to the ceramic industry.

In 1987, Professor Traugott E. Fischer found that, in the presence of water, silicon nitride wears by a tribochemical mechanism in which material is removed purely by chemical dissolution. This dissolution is accelerated by the simultaneous action of friction, thus the name "tribochemical". Since chemical dissolution took place only at contacting asperities where friction occurred, the asperities were removed tribochemically and the resulting surfaces were extremely smooth. The absence of mechanical removal also promised the achievement of surfaces without the cracks and other defects produced by the penetrating abrasives. Thus it was proposed, in the framework of this program, to explore the feasibility of tribochemical polishing to produce very smooth, defect free surfaces.

3.0 Characterization of Silicon Nitride Bearing Ball Surfaces, Subtask 3.4.1

The micro-topography of surfaces in as-received 5/32", 1/4", 7/16" and 19/32" diameter grade S NBD-200 silicon nitride bearing balls was characterized, and the surface defects and surface finish were quantitatively evaluated by means of optical microscopy, scanning electron microscopy and scanning force microscopy. The Tribochemical Polishing technique being investigated holds the promise of increasing the strength, fatigue resistance and reliability of ceramic workpieces. The machining technique being investigated holds the promise of increasing the strength, fatigue resistance and reliability of the ceramic workpieces. Commercially available silicon nitride ball surfaces were characterized and evaluated in terms of surface finish, defects such as holes (cavities of multiple-grain size), grain pullout, cracks, and residual stress. The measurement of surface residual stress of silicon nitride balls supplied by Norton Advanced Ceramics (previously Cerbec, Inc.) was performed in 1/4" and 19/32" diameter silicon nitride bearing balls and discs used as tool materials.

3.1 Examination and Evaluation of Silicon Nitride Bearing Ball Surfaces

Table 1 shows a typical chemical composition of Norton Advanced Ceramics NBD-200 Silicon Nitride. Table 2 shows the typical mechanical properties of NBD-200 Silicon Nitride.

Table 1.
Chemical Composition of
NBD-200 Silicon Nitride

Al	C	Ca	Fe	Mg	O	Si_3N_4
≤0.5	≤0.88	≤0.04	≤0.17	0.6-1.0	2.3-3.3	97.1-94.11

Table 2.
Mechanical and Thermal Properties of
NBD-200 Silicon Nitride

Property Of NBD-200 Silicon Nitride	Metric Units	English Units
Flexural Strength	800 MPa	116 ksi
Weibull Modulus	9.7	9.7
Tensile Strength	400 MPa	58 ksi
Compressive Strength	3.0 GPa	435 ksi
Hertz Compressive Strength	28 GPa	4060 ksi
Fracture Toughness (K_{1c})	4.1 MPa.$m^{1/2}$	3.7 ksi.$in^{1/2}$
Density	3.16 g/cm^3	0.117 lb/in^3
Elastic Modulus	320 GPa	46 x 10^6 psi
Poisson's Ratio	0.26	0.26
Hardness, Vickers	16.6 GPa	2.4 psi x 10^6
Hardness (H_{RC})	>70	>70
Thermal Expansion Coefficient (20°C-1000°C)	2.9 x 10^{-6}/°C	1.6 x 10^{-6}/°F
Thermal Conductivity at 500°C	21.3 W/m-K	147 (BTU-in/hr-ft^2-°F)
Thermal Conductivity at 1000°C	15.5 W/m-K	107 (BTU-in/hr-ft^2-°F)

Figure 1 shows 100x Nomarski differential interference contrast (NIC) optical microscopy of as-received 5/32", 1/4", 7/16" and 19/32" diameter silicon nitride bearing balls. Spots on the surface indicate that there are surface defects which are holes and/or single grain pull-out. As the ball diameter increases, the area density of surface defects becomes smaller. The density of surface defects in the 5/32" diameter bearing ball is higher than that of the 19/32" diameter bearing ball. NIC optical microscopic observation also reveals the presence of impurities. Figure 2 shows a 500x NIC micrograph of an as-received 1/4" diameter bearing ball. In Nomarski contrast, a different color indicates a different elevation of the surface (i.e. a topographic feature). A different intensity of a given

color represents a difference in reflectivity or chemistry. The background of Figure 2 was light blue. The spot indicated was dark blue. Figure 2 reveals the presence of impurities by the difference in intensity. The spot noted indicates the presence of an impurity.

For the identification of impurities, Energy dispersive spectroscopy (EDS) and Scanning electron microscopic elemental mapping (SEMEM) were used. In Figure 3(A), traces of Si, Mg, Pd and Au were detected in the spot. Si and Mg were evidence of silicon nitride and magnesium oxide respectively. Pd and Au were the conducting coated layer. Fe detected from EDS can be assigned to iron oxide (Fe_2O_3). After elemental analysis, Fe-mapping was conducted and the result is shown in Figure 3(B), which is magnified 7000x. Scattered white spots indicate the distribution of Fe in the form of iron oxide (Fe_2O_3).

For the quantitative evaluation of the density of surface defects in the as-received bearing balls, SEM analysis was performed at five different areas of the 5/32, 1/4, 7/16 and 19/32 inch balls. Figure 4 shows the morphology of selected surface areas of as-received bearing balls. The surfaces are generally smooth, but contain a number of surface defects that have the appearance of missing grains. These cavities have a diameter generally less than 0.5μm, their average diameter is 0.35±0.05μm on the surface of bearing balls. The area density of these cavities in the 5/32" ball is 22,500/mm^2; on the 1/4" ball, the area density is 20,000/mm^2, on 7/16, it is 18,000/mm^2. On the 19/32" balls, no surface defects similar to those on the smaller balls were found, but very fine finishing scratches (less than 0.5μm width) appear. Bright spots, indicative of iron-oxide impurities, are more numerous on the 19/32" diameter ball.

For the additional analysis of surface morphology of the as-received bearing balls, atomic force microscopy (AFM) was used. Figure 5(A, B, C, D) show the surface morphology by AFM of as-received bearing balls. The light shading direction for all micrographs is from the right. The scale bar in the left-upper corner indicates the angle between illuminated surface and incoming light. For hillocks, the right sides are brighter than the left sides and for holes the left side is brighter. The surfaces of as-received bearing balls are generally smooth, but they show a number of surface defects. The micrographs also show a number of dirt particles which are not relevant. The concentric circular shadowing on some micrographs is thought to be some sort of phase interference pattern, not related to the physical surface being measured. Apparently, as the diameter of the bearing ball increases, the number of surface defects decreases. This result corresponds to that of NIC optical microscopy and SEM. In the as-received bearing balls, surface scratches are also clearly visible. Table 3 shows the results of

AFM analysis on as-received bearing balls. The surface roughness was measured along lines that included and did not include surface defects. When measured on a line that avoids surface defects, the roughness of different diameter bearing balls is almost equal. When the surface defects are included, the roughness is about 3 to 10 times higher.

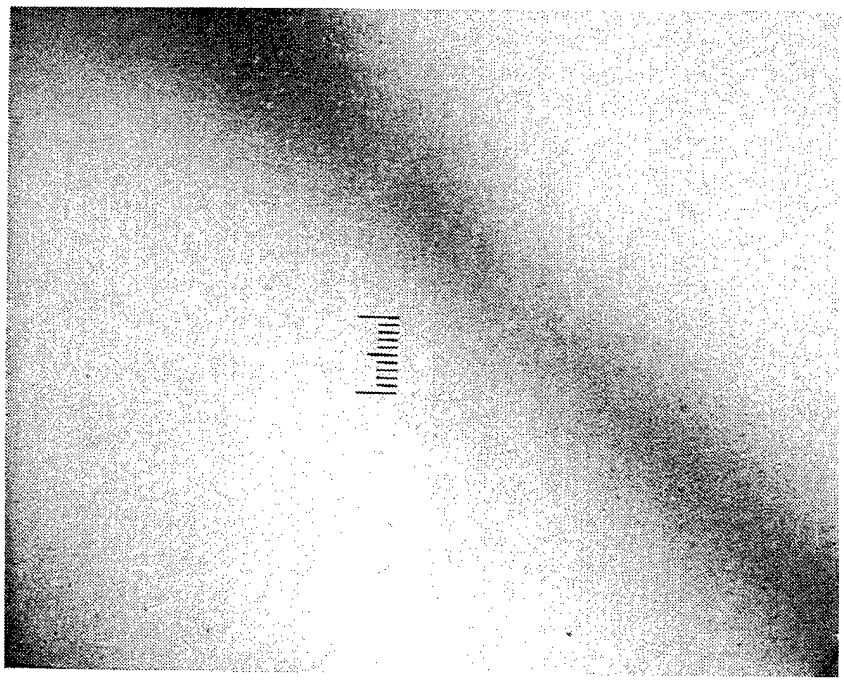

(A)

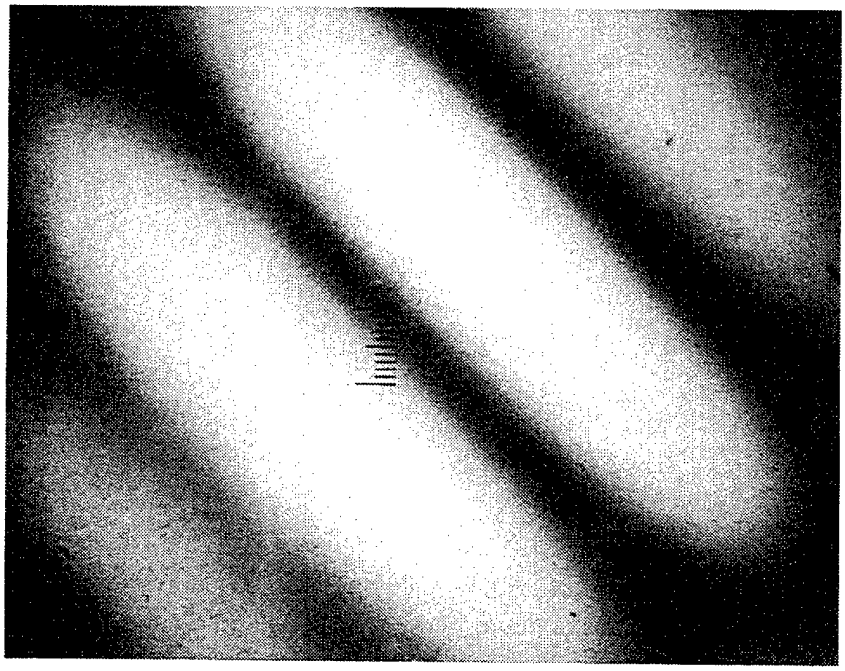

(B)

Figure 1 Surface morphology of commercially finished bearing balls (NBD 200) by Nomarski differential interference contrast (NIC) optical microscopy. The magnification of all micrographs is 100x: (A) 5/32", (B) 1/4" diameter ball.

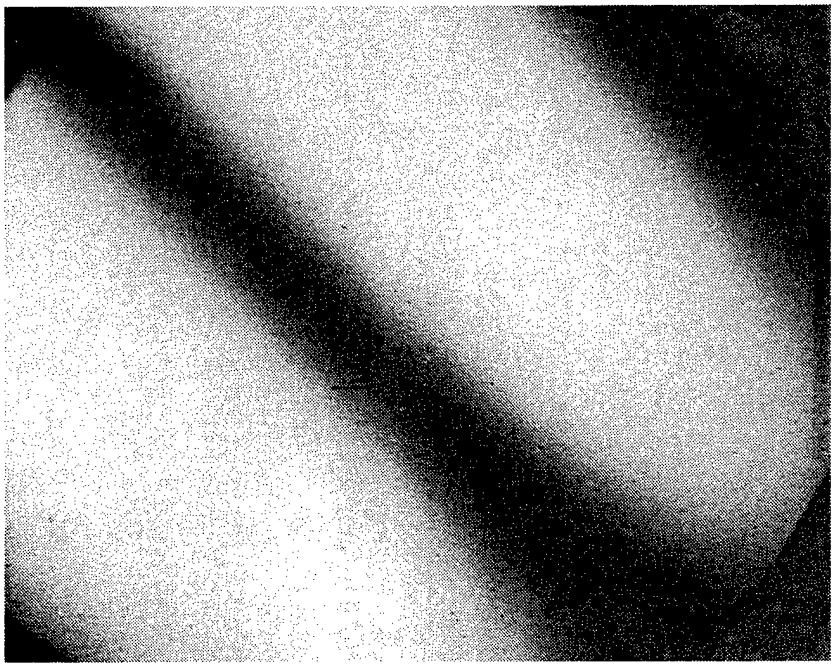

(C)

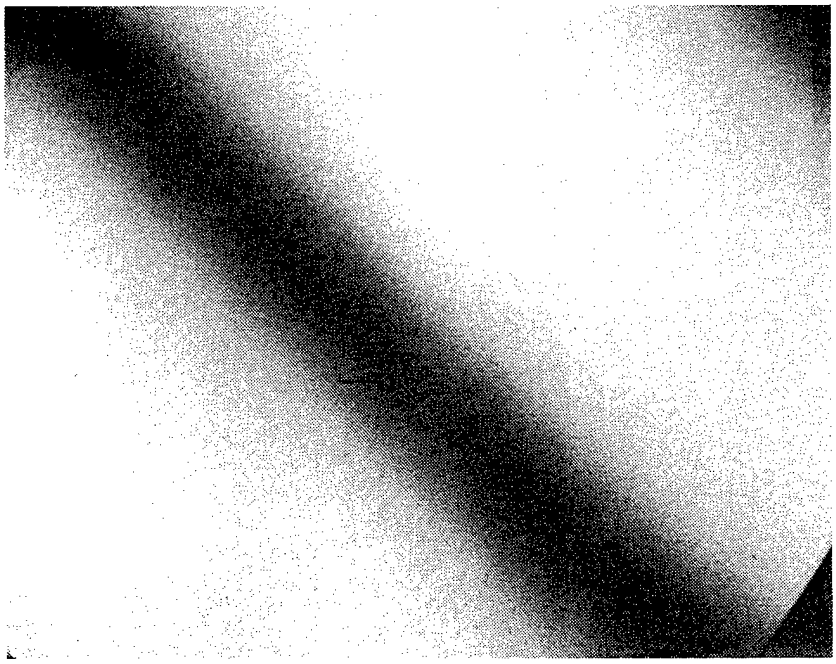

(D)

Figure 1 (continued) Surface morphology of commercially finished bearing balls (NBD 200) by Nomarski differential interference contrast (NIC) optical microscopy. The magnification of all micrographs is 100x: (C) 7/16" and (D) 19/32" diameter ball.

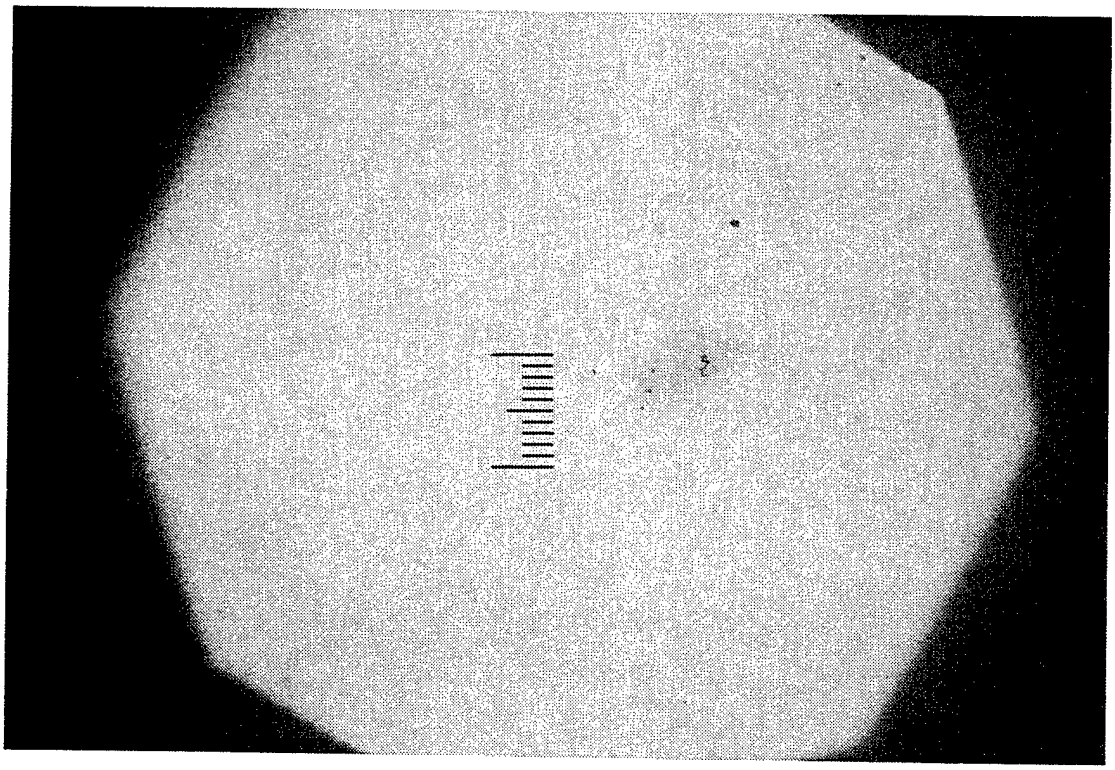

Figure 2 Surface morphology of commercially finished 1/4" diameter bearing ball by NIC optical microscopy 500x magnification. Dark spot indicates impurities.

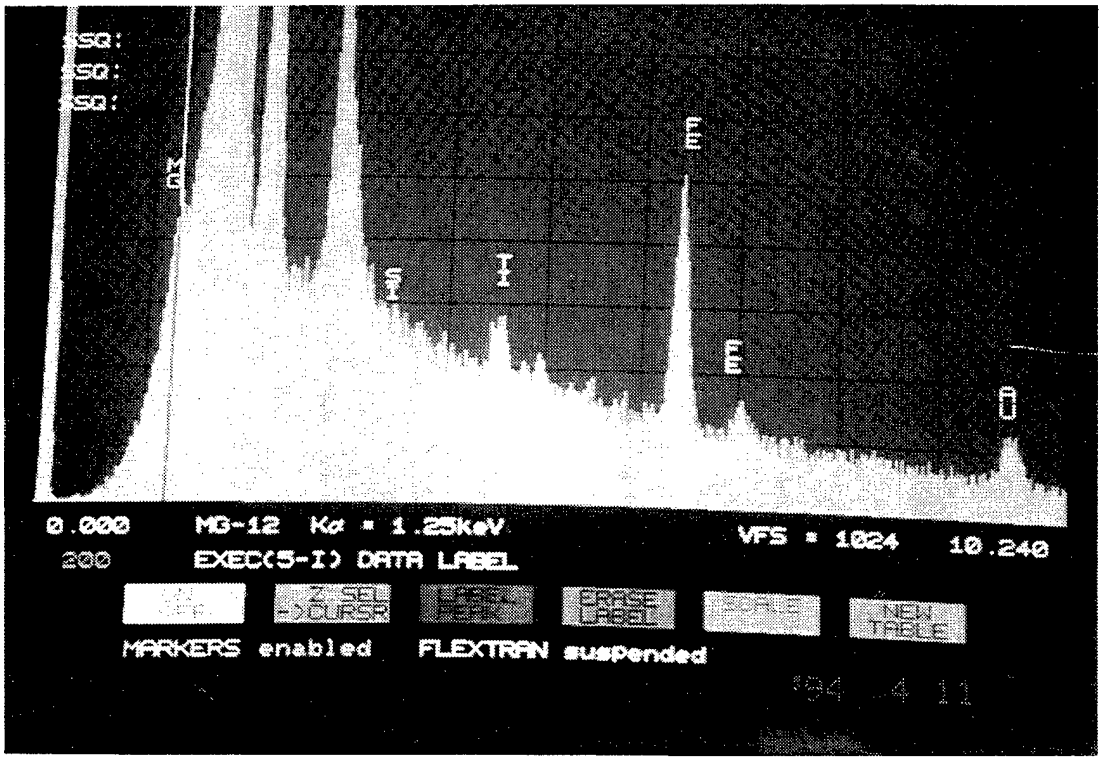

(A)

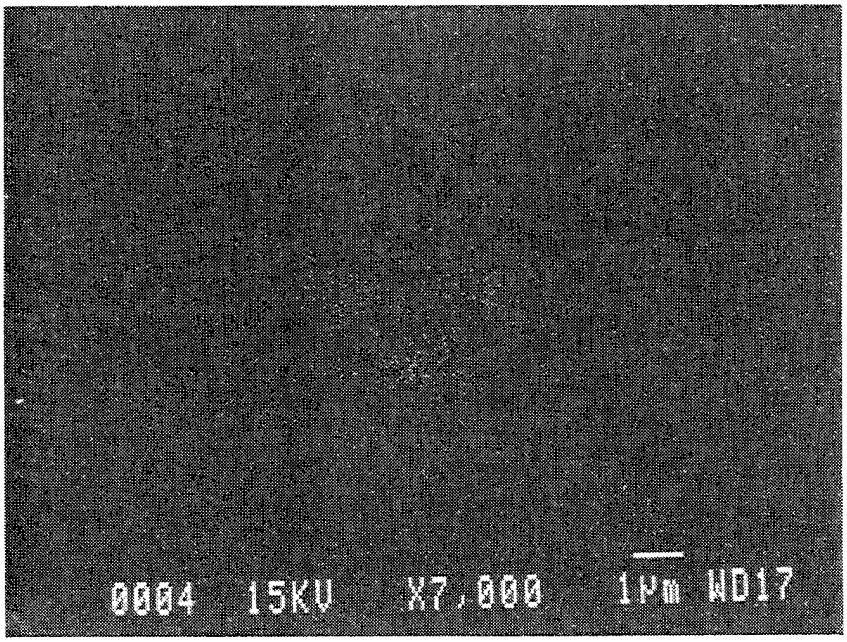

(B)

Figure 3 Energy Dispersive Spectroscopy (EDS) of the dark spot in Figure 2. (B) elemental mapping of Fe by SEM.

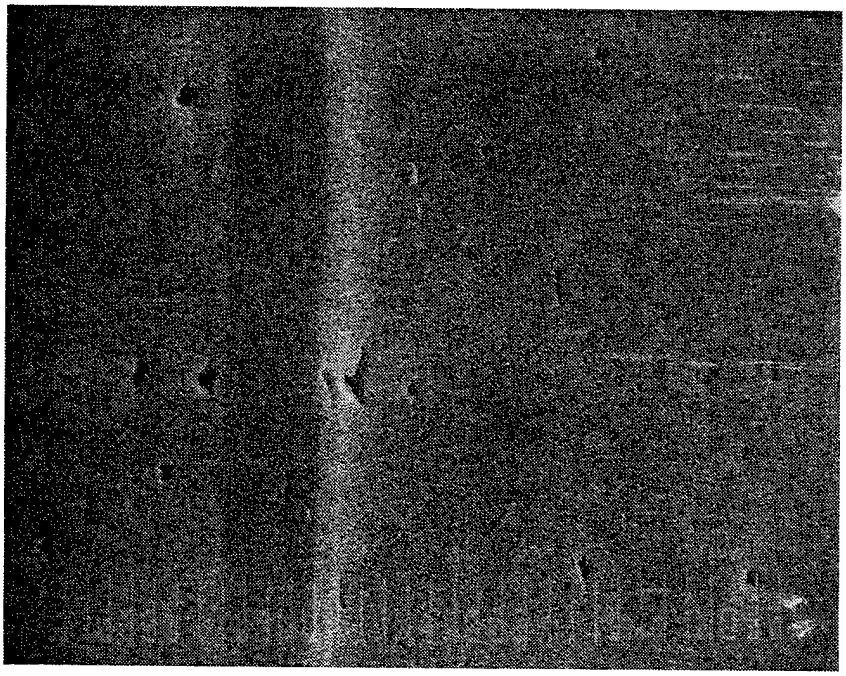

(A)

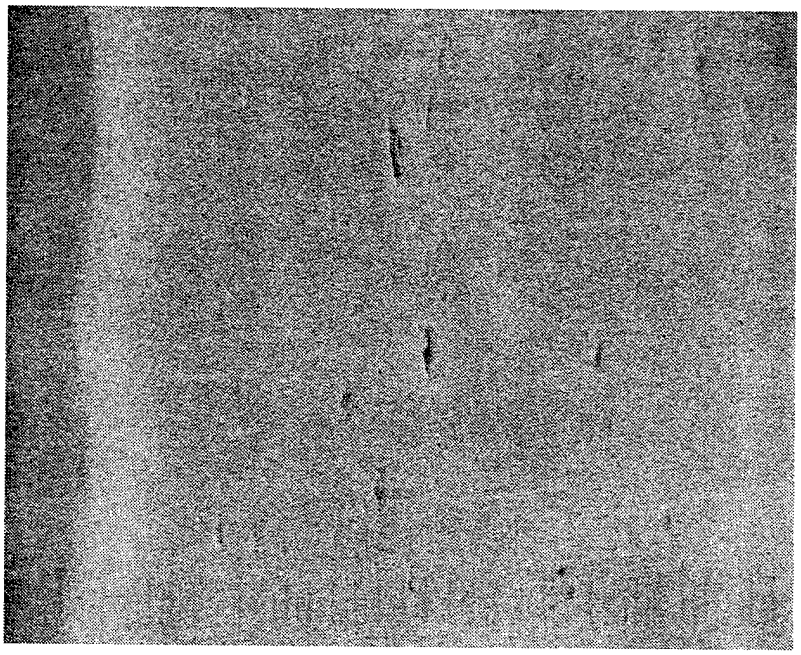

(B)

Figure 4 SEM micrographs of commercially finished bearing balls (NBD 200) by SEM: (A) 5/32" (400x magnification, tilting=43.8°), (B) 7/16" (4000x magnification, tilting=42.8°).

Figure 5 High resolution surface morphology of commercially finished bearing balls by Atomic Force Microscopy (AFM): (A) as-received 5/32" diameter ball.

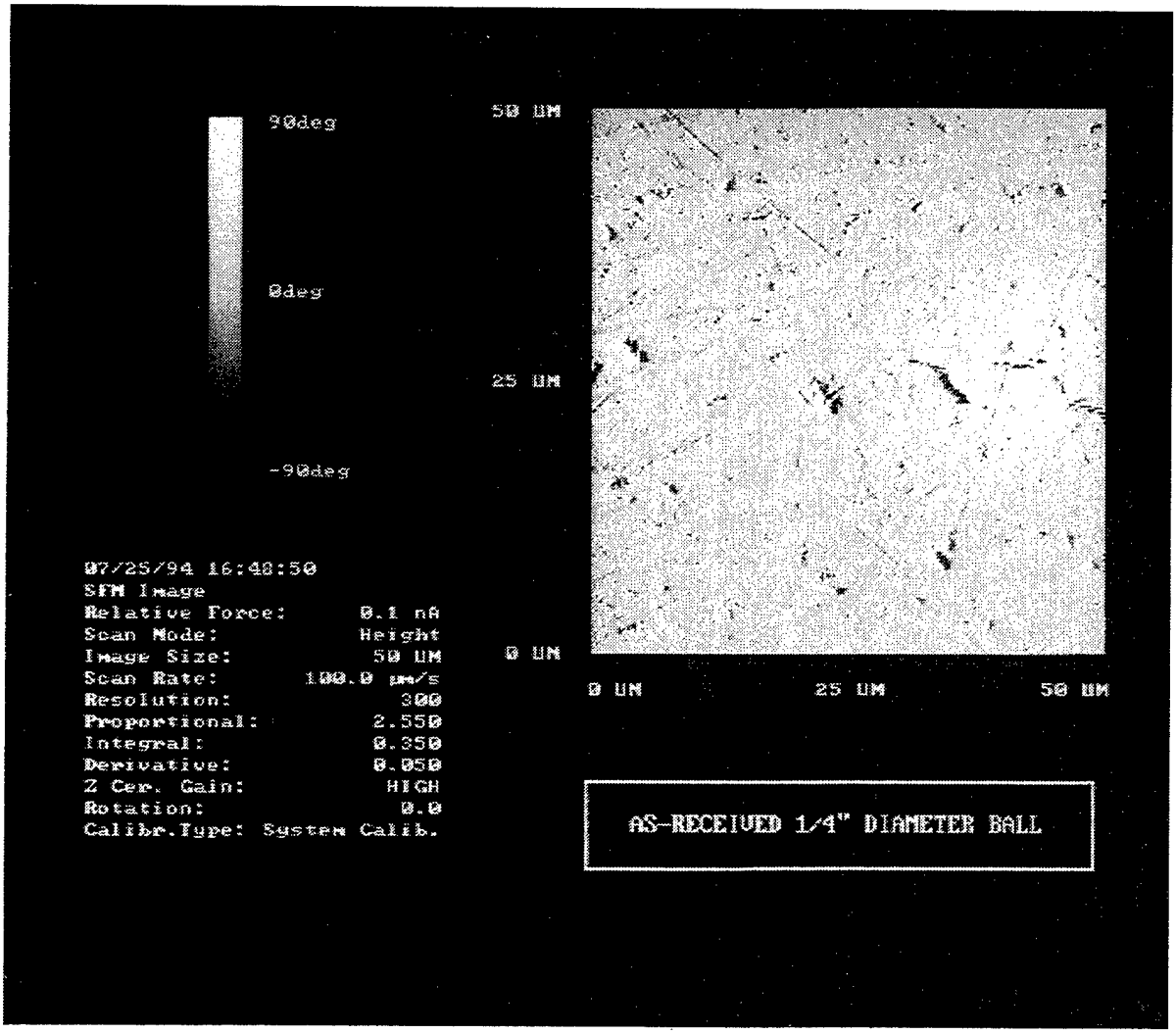

Figure 5 (continued) High resolution surface morphology of commercially finished bearing balls by Atomic For(continued)ce Microscopy (AFM): (B) as-received 1/4" diameter ball.

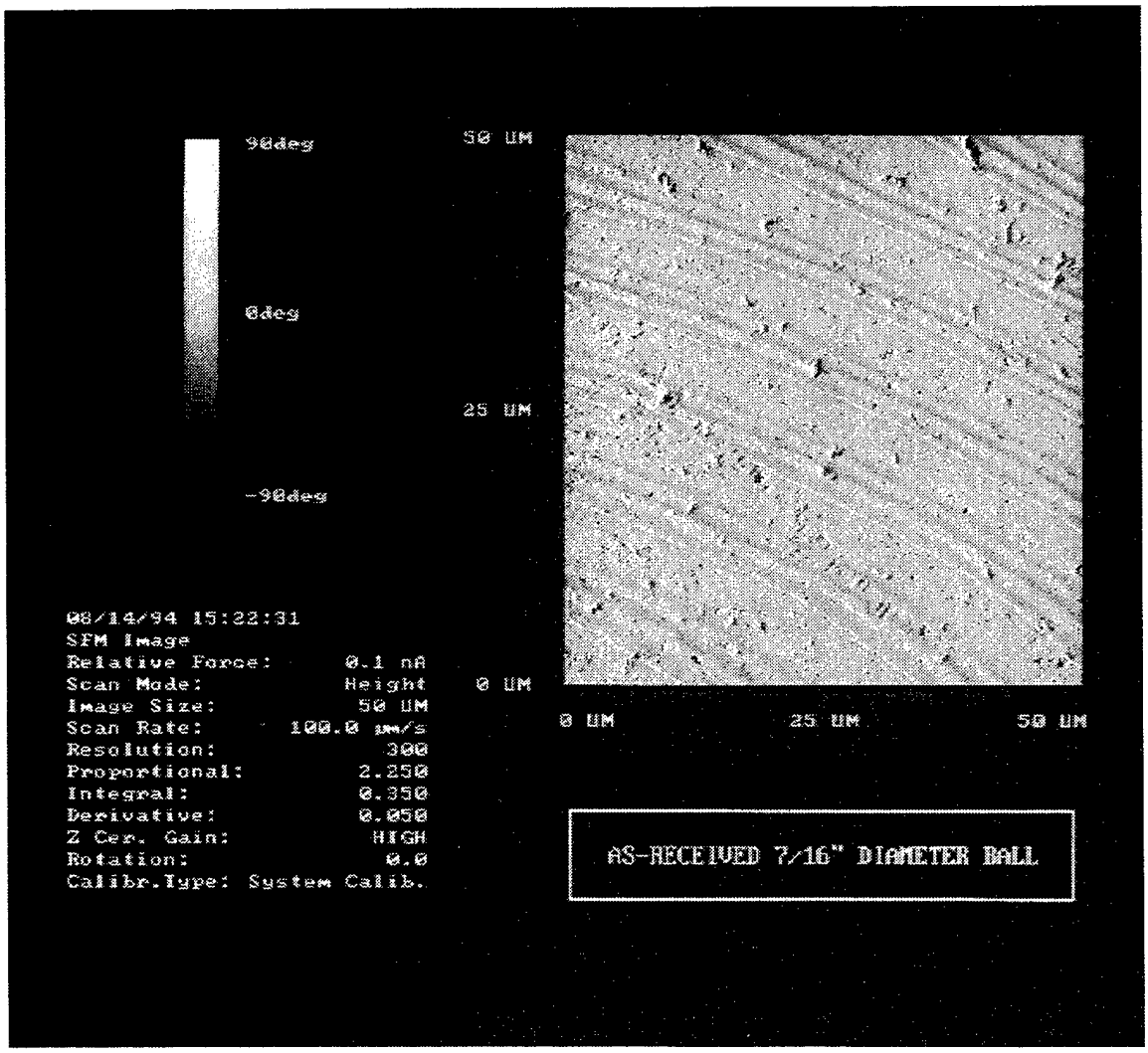

Figure 5 (continued) High resolution surface morphology of commercially finished bearing balls by Atomic Force Microscopy (AFM): (C) as-received 7/16" diameter ball.

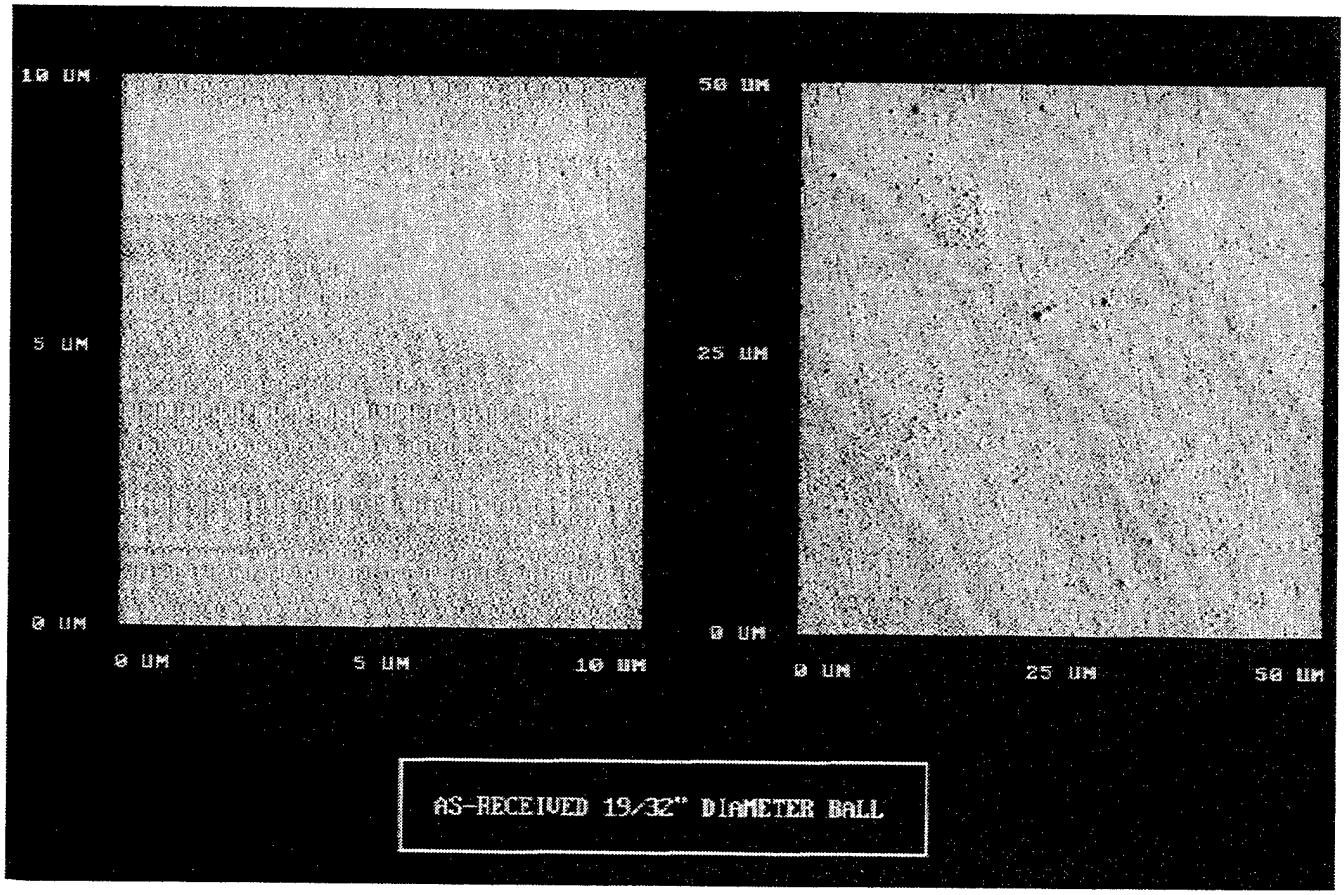

Figure 5 (continued) High resolution surface morphology of commercially finished bearing balls by Atomic Force Microscopy (AFM): (D) as-received 19/32" diameter ball.

Table 3.
Observation Results of Atomic Force Microscopy

Observation	As-received 5/32" ball	As-received 1/4" ball	As-received 7/16" ball	As-received 19/32" ball
Ra (nm) without defects	2.5 4.0	2.1-3.0	1.8-2.8	3.0-4.0
Defect Density	large	medium	medium	small
Defect Type	hole and grain fall-out	hole and grain fall-out	hole and grain fall-out	NA
Scratch[a] Mark	some	some	severe	some
Ra (nm) with defects	35-40	35-45	11-18	9-12

[a] Studies by AFM and SEM show that the mechanical polishing process will always produce surface defects.

3.2 Measurement of Residual Stress

Stresses present in a material always cause elastic deformation that is measurable as a variation of the lattice parameter. Nonuniform microstrain causes a broadening and shifting of the corresponding X-ray diffraction lines. It was thought that mechanical grinding and lapping processes could produce a tensile or compressive surface stress and influence the fatigue life of bearing balls. Tensile stresses at the surface of an object are usually harmful and contribute to brittle fracture. Compressive residual stresses at the surface usually increase fatigue strength.

3.3 X-Ray Diffraction Procedure

The standard procedure for the measurement of surface residual stresses at bearing ball surfaces, SAE J784a, was used for the present investigation. The two-exposure technique for the surface residual stress measurement was used. This requires several measurements, one with the diffractometer aligned in its normal position corresponding to the general 2θ measurement method, in which the incident and diffracted beam make the same

angle θ with the surface. The other measurements are performed with the specimen rotated at angles of θ degrees from its normal position. One of the basic equations derived and used in relating and calculating the stress from the displacement of the diffraction beam is:

$$\sigma\phi = \frac{-E}{2(1+\nu)} \cdot \frac{1}{\tan\theta} \cdot \frac{\partial(2\theta)}{\partial(\sin^2\varphi)} \quad (-tensile) \tag{1}$$

where φ is the angle between normal to the surface and the normal to reflecting planes, θ is the diffraction angle, σφ is the stress (compressive or tensile), the variable term $\frac{\partial(2\theta)}{\partial(\sin^2\varphi)}$ is the slope between 2θ in radian and $\sin^{2\phi}$, E is elastic modulus and ν is Poisson's ratio.

For the accurate measurement of 2θ peaks, the testing process should follow the specific requirements of residual stress measurement by x-ray diffractometer. The first requirement is to preserve focusing conditions; this means that whenever φ is established, the focusing circle of the diffracted beam should be altered by the following equation:

$$\frac{D}{R} = \frac{\sin(\theta-\varphi)}{\sin(\theta+\varphi)} \tag{2}$$

where D is the distance from the center of the reflecting plane to the focusing circle of the diffracted beam and R is the radius of the diffractometer circle. The second requirement is to modify the 2θ data detected, whether it is φ=0 or φ≠0, by the Lorentz-polarization factor and the absorption factor as shown in equation (3).

LPA-Factor = (LP factor).(Absorption factor)

$$= \left(\frac{1+\cos^2 2\theta}{\sin^2\theta}\right) \cdot (1-\tan\varphi\cdot\cot\theta) \tag{3}$$

Surface residual stress measurements were performed on as-received 1/4" and 19/32" diameter balls, 20mm x 20mm x 3mm discs, and TCP 1/4" balls and TCP discs. CuKα radiation at 40 KV and 20 mA, and (001) graphite monochromator were used. Before measuring surface residual stress, pre-scanning from 10° to 140° was performed to identify the silicon nitride used and to find the highest diffraction angle, as shown in Figure 6.

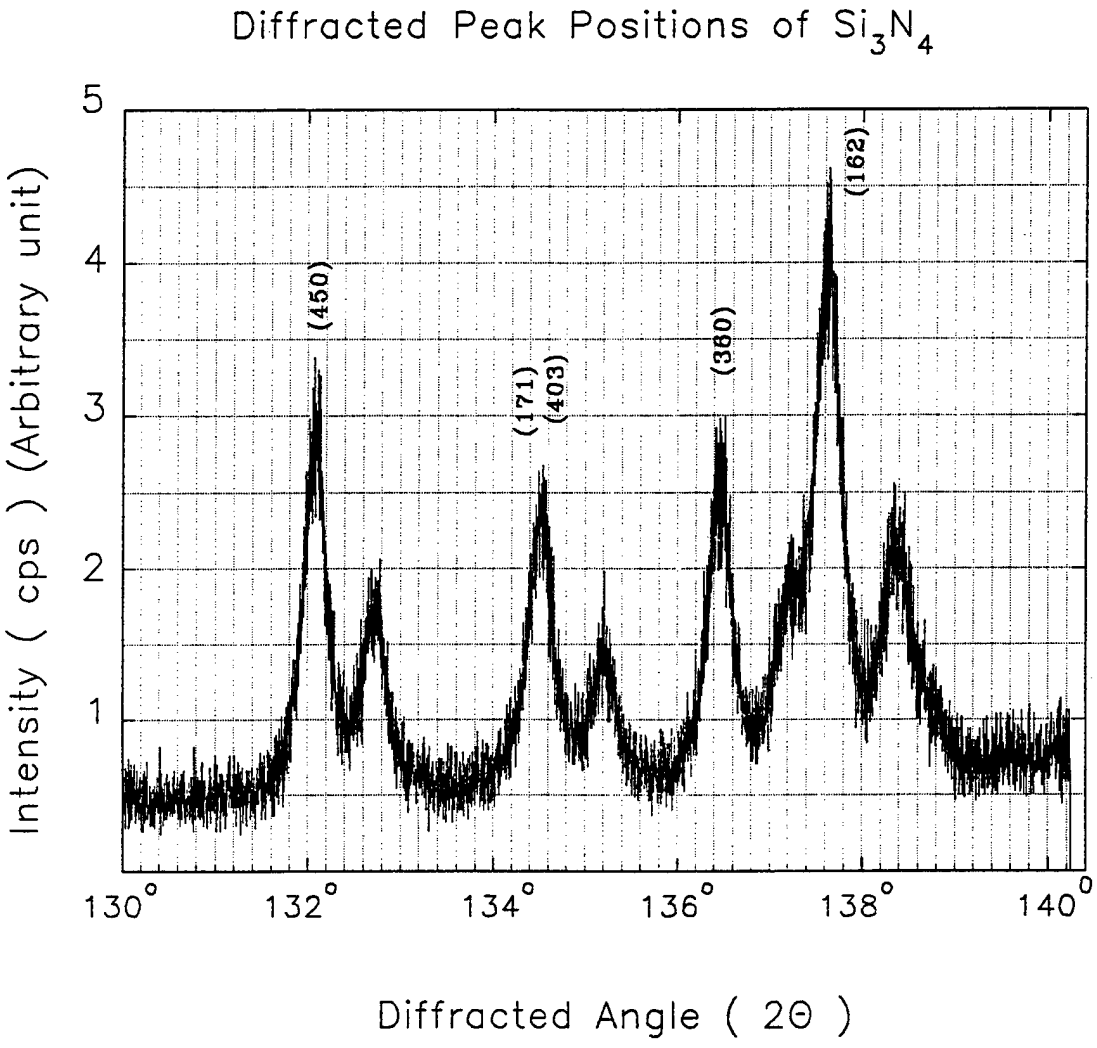

Figure 6 Diffracted peak positions of HIP'd silicon nitride (NBD 200) by X-Ray diffractometer: (A) from 130° to 140°.

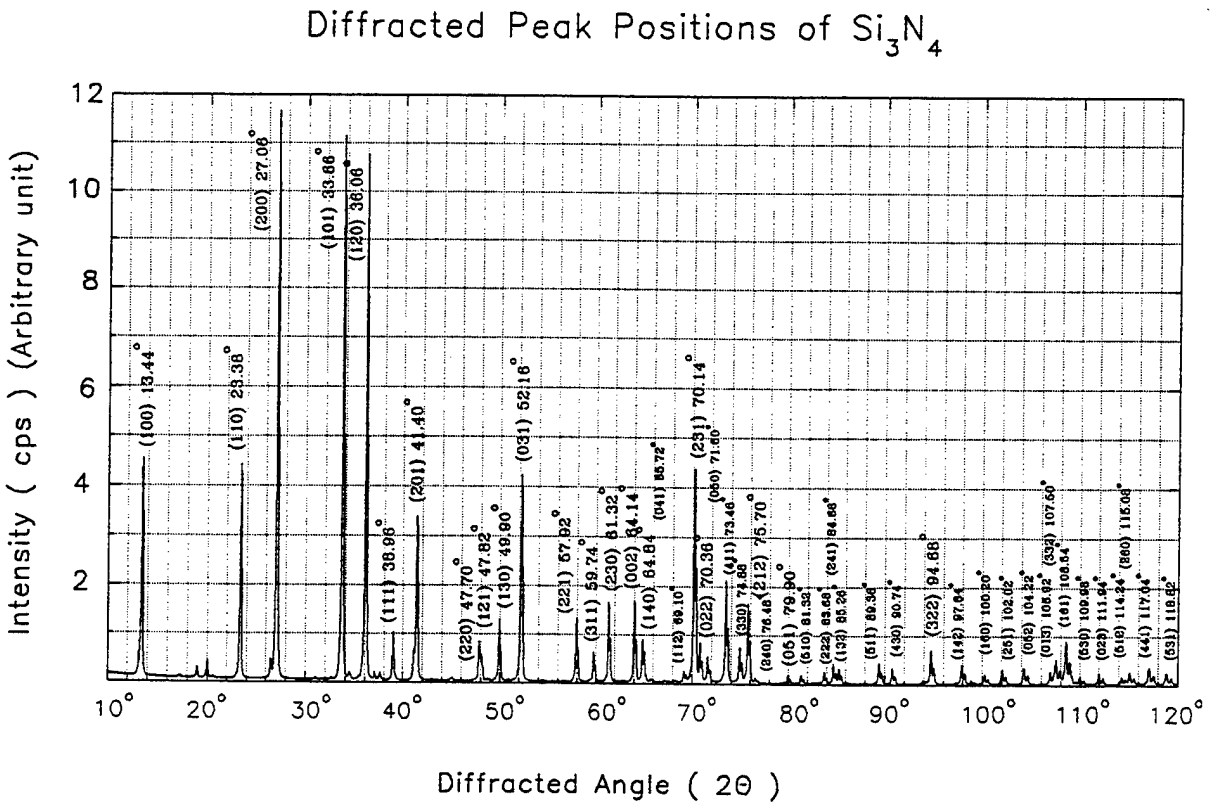

Figure 6 (continued) Diffracted peak positions of HIP'd silicon nitride (NBD 200) by X-Ray diffractometer: (B) from 10° to 120°.

The (450) crystalline plane was selected with a diffraction angle of $2\theta \approx 132^\circ$. This is the largest detectable angle within the limits of the Rikagu DXR 3000 system. A 0.02°/min scanning speed and scanning angles from 131.5° to 132.5° were adopted. Calibration of correct peak position by quartz as the standard sample before any measurement was conducted and the focusing circle was aligned whenever φ was established. After all the measurements at φ=0°, 60°, 45°, 30° and 15°, all data was modified by the LPA-factor and a polynomial curve fitting method was adopted to find the exact position of each peak.

Table 4 shows the average results of surface residual strain and stress measurements for bearing balls and discs before and after tribochemical polishing.

Table 4.
Average Surface Residual Strain and Stress Measurements

Component Measured	Average strain	Average stress MPa (ksi)
As-received 1/4" ball	$8.4\pm0.3 \times 10^{-4}$	55±5 (7.97±0.725)
After tribochemical polishing 1/4" ball	$7.4\pm0.2 \times 10^{-4}$	50±4 (7.25±0.58)
As-received 19/32" ball	$1.2\pm0.2 \times 10^{-4}$	37±3 (5.36±0.435)
As-received disc	$9.0\pm0.5 \times 10^{-4}$	55±6 (7.97±0.870)
After tribochemical polishing disc	$8.7\pm0.5 \times 10^{-4}$	53±5 (7.69±0.725)

The surface residual stresses of all the samples are very small: thus there is little opportunity for significant reduction by tribochemical polishing. The residual stress of the large diameter bearing balls (19/32") is smaller than that of the small diameter balls (1/4"). We recall that, according to NIC optical microscopy, SEM and AFM, the density of surface defects is smaller for the larger balls. This suggests that the surface residual stress may be proportional to the surface defect density.

4.0 Tribochemical Machining, Subtask 3.4.2

4.1 Material Removal

Tribochemical polishing is characterized by the fact that material is not removed by a mechanical process such as abrasion, plastic deformation or fracture, but by chemical dissolution of the silicon nitride in a liquid. This dissolution is stimulated by friction and occurs only at the friction contact. Consequently, contacting asperities are preferentially dissolved and the surface acquires a high degree of polish.

The process consists simply of rubbing the workpiece against a suitable surface in the presence of the dissolving liquid. In the experiments that led to the discovery of tribochemical polishing, the liquid was water and both solid surfaces were silicon nitride. It was the purpose of the present investigation to find more convenient and less expensive surfaces rubbing against the silicon nitride and to find dissolving fluids that would produce a higher removal rate and/or a smoother surface. During the exploratory phase of the present work, the workpiece was a bearing ball of NBD-200 silicon nitride provided by Norton Advanced Ceramics (previously Cerbec, Inc.) and the polishing surfaces were alumina, silicon nitride, cast iron, and stainless steel. The latter three were found to be equally adequate. Alumina was unsatisfactory because of low silicon nitride removal rates and failure to produce a smooth polished surface. Worn Alumina particles were found at the edges of the polished areas of the workpiece.

4.1.1 Tribochemical Polishing Process and Material Removal Rates

The polishing was performed on standard pin-disc tribometers. The stationary silicon nitride ball was pressed with various loads from 3 to 20 Newtons against the moving polishing disc. The silicon nitride and metal discs were used in the as-ground condition. No particular care was taken to polish them.

The first series of experiments were conducted to establish the optimum conditions of load pressing the surfaces together and sliding speed of the polishing disk in distilled water, hydrogen peroxide and chromic acid. Figure 7 shows the amount of silicon nitride removed in distilled water as a function of total sliding distance at various loads and speeds. The "tool" surface is silicon nitride. The middle set of lines shows that the friction coefficient is independent of the process variables, μ=0.5±0.05. The lower set shows that the volume removed is proportional to the load and sliding distance; this allows us to define a polishing or wear rate in mm^3/Nm which is independent of

mechanical process variables and is 1-2x10^{-5} mm^3/Nm. Note that, at 60 mm speed and 3.92 N load, no more material is removed beyond 200 m sliding. This is caused by hydrodynamic lubrication from a very thin water film which forms on the extremely smooth silicon nitride surface.

Figure 8 shows the Nomarski interference optical micrographs of the silicon nitride surfaces obtained at 19.6, 9.8, 3.92 and 2.45 Newtons. The surfaces are smooth with 3.92 and 2.45 N but rough at the higher loads, showing that polishing is purely tribochemical at the low loads and at least partly mechanical at high loads. Figure 9 shows material removal, friction coefficient and polishing rates in hydrogen peroxide. A large number of loads, speeds and concentrations were examined.

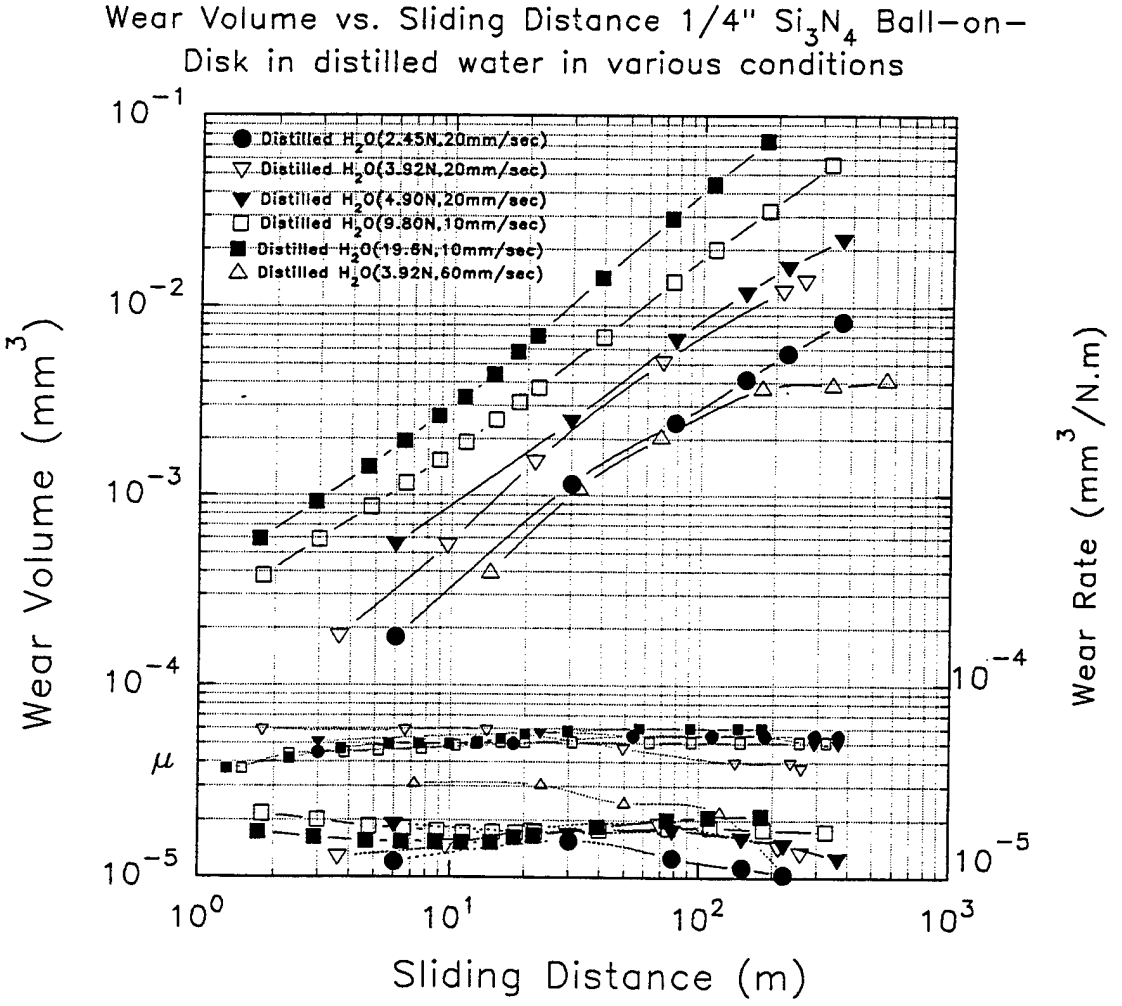

Figure 7 Material removal, friction coefficient and polishing rate (wear rate) of silicon nitride as a function of sliding distance in distilled water at various conditions.

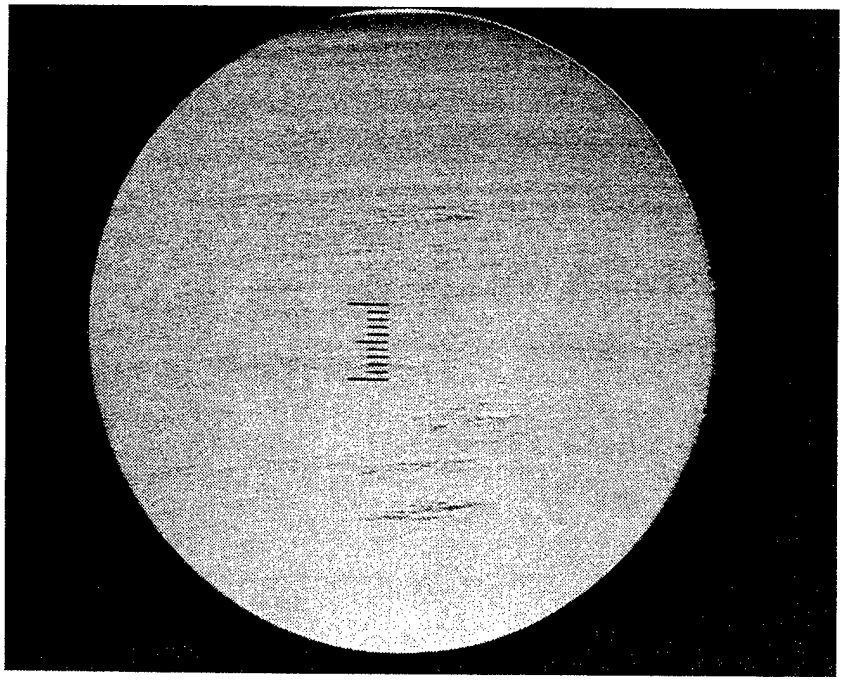

(A)

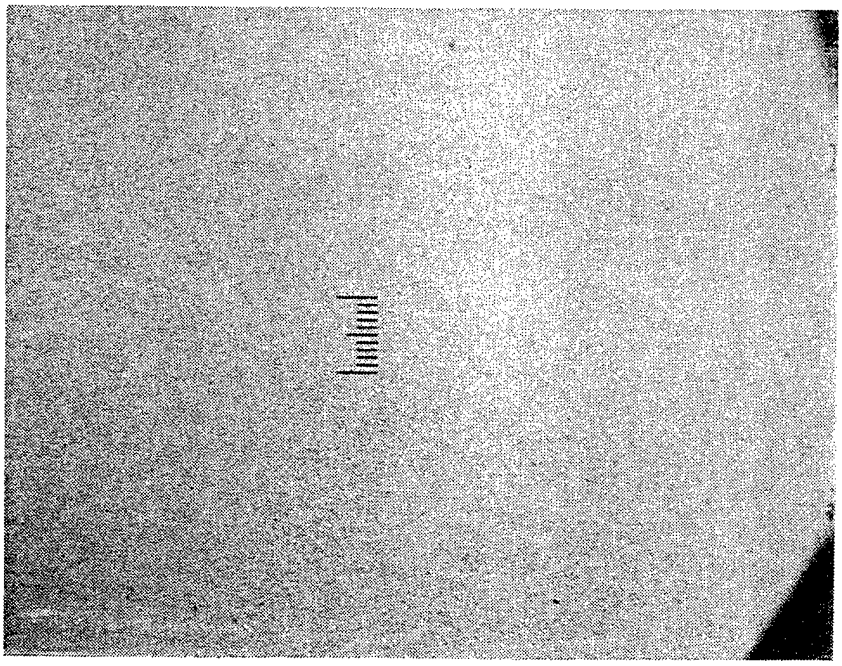

(B)

Figure 8 NIC optical micrographs of tribochemically polished surfaces in distilled water: (A) 19.6 N 50x, at 320m, (B) 9.8 N 200x, at 300m sliding distance.

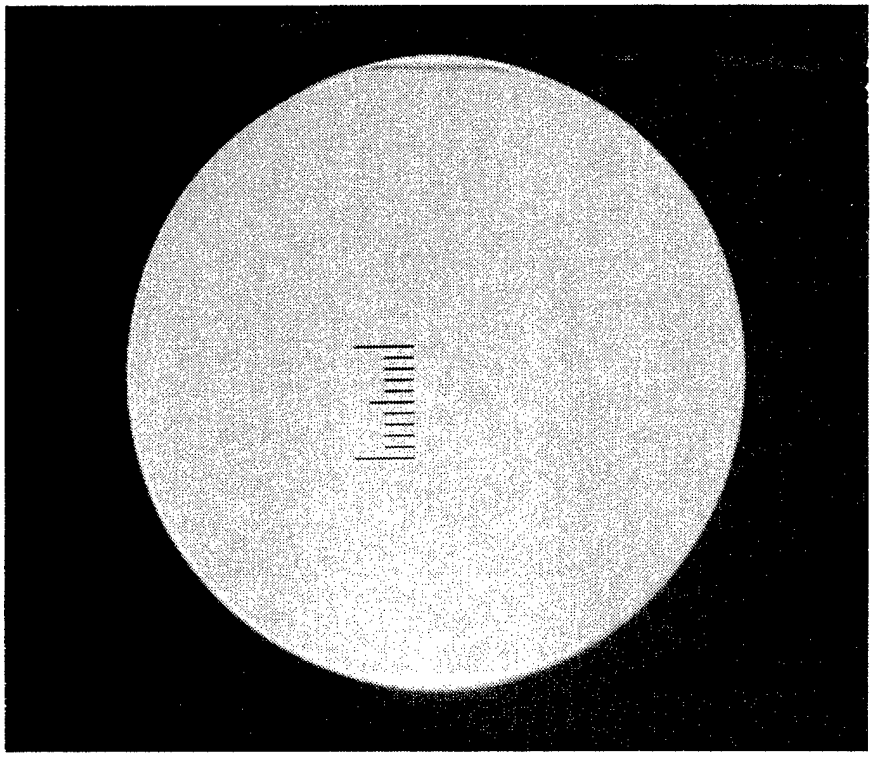

(C)

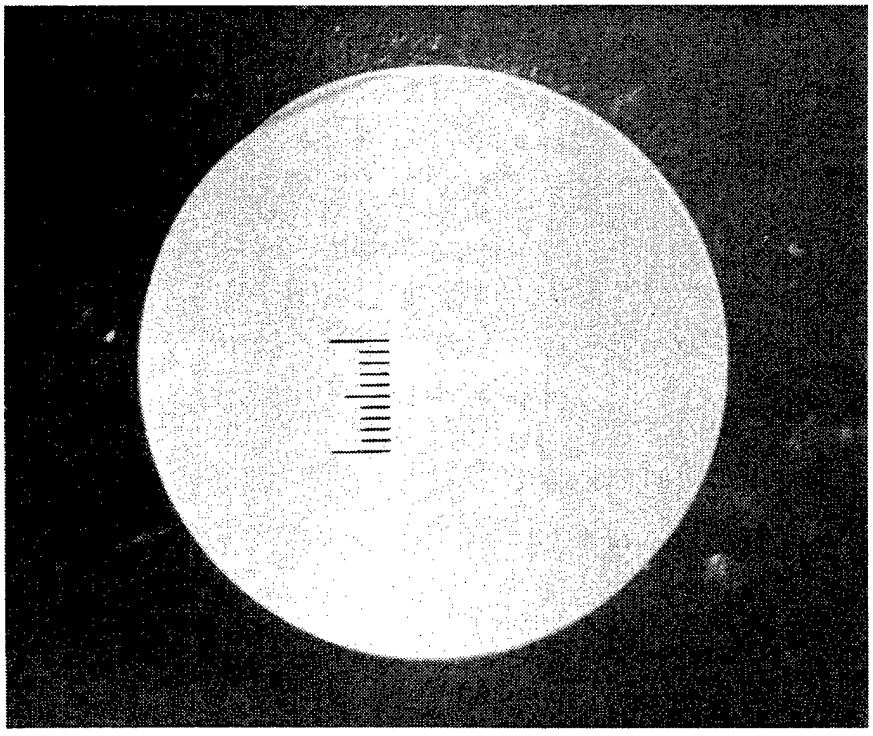

(D)

Figure 8 (continued) NIC optical micrographs of tribochemically polished surfaces in distilled water: (C) 3.92 N 50x, at 600m, (D) 2.45 N 50x, at 800m sliding distance.

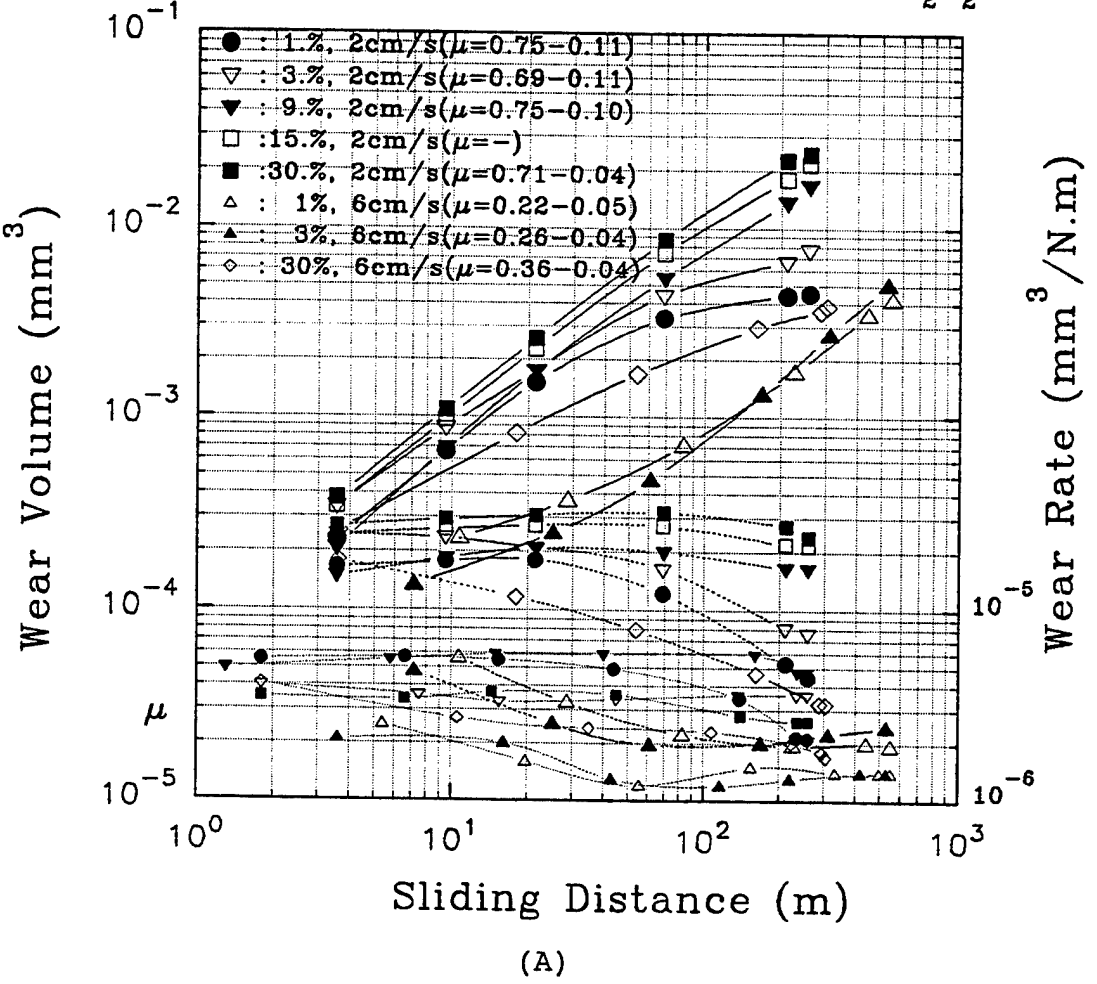

(A)

Figure 9 Material removal, friction coefficient and polishing rate (wear rate) of silicon nitride as a function of sliding distance in hydrogen peroxides. (A), Middle set indicates polishing rate.

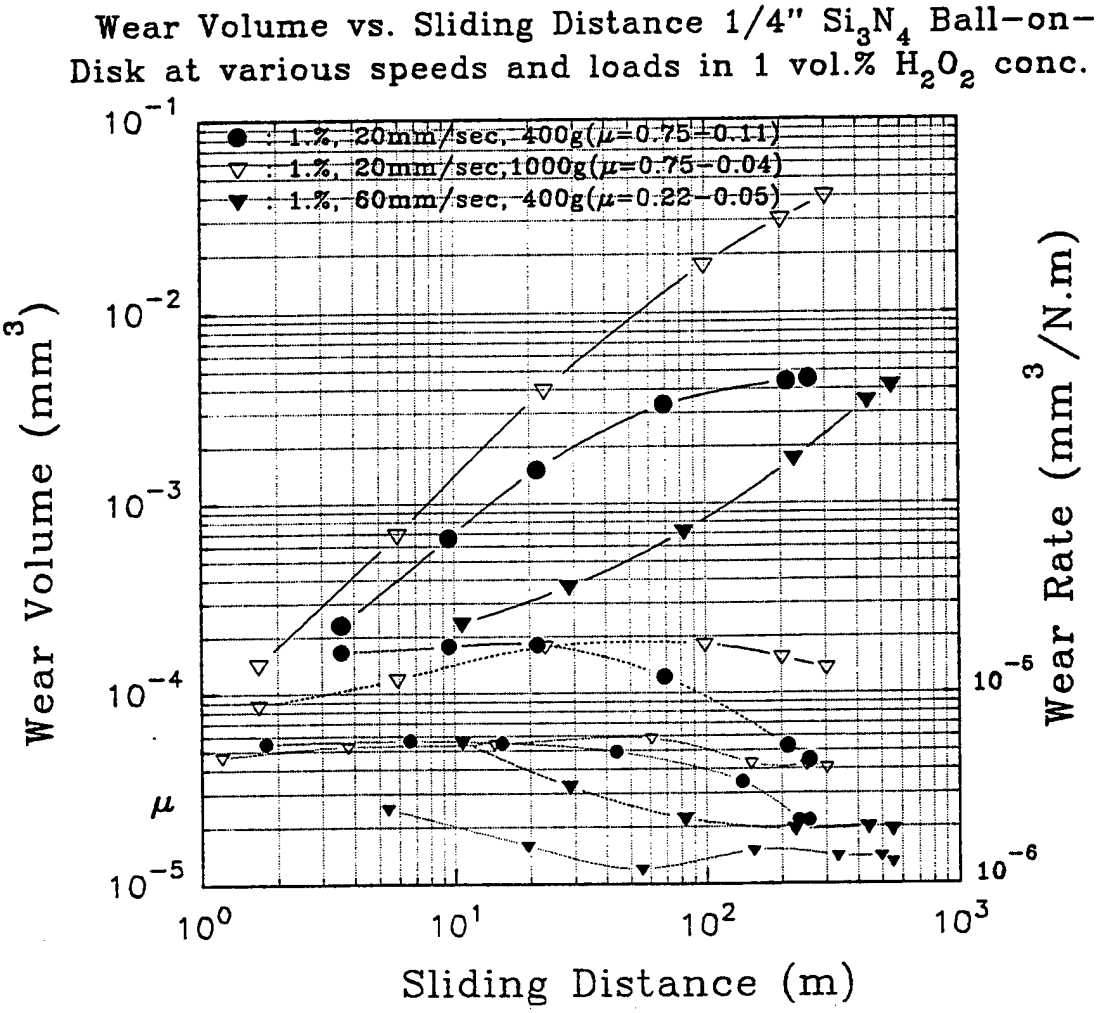

(B)

Figure 9 (continued) Material removal, friction coefficient and polishing rate (wear rate) of silicon nitride as a function of sliding distance in hydrogen peroxides. (B), Middle set indicates polishing rate.

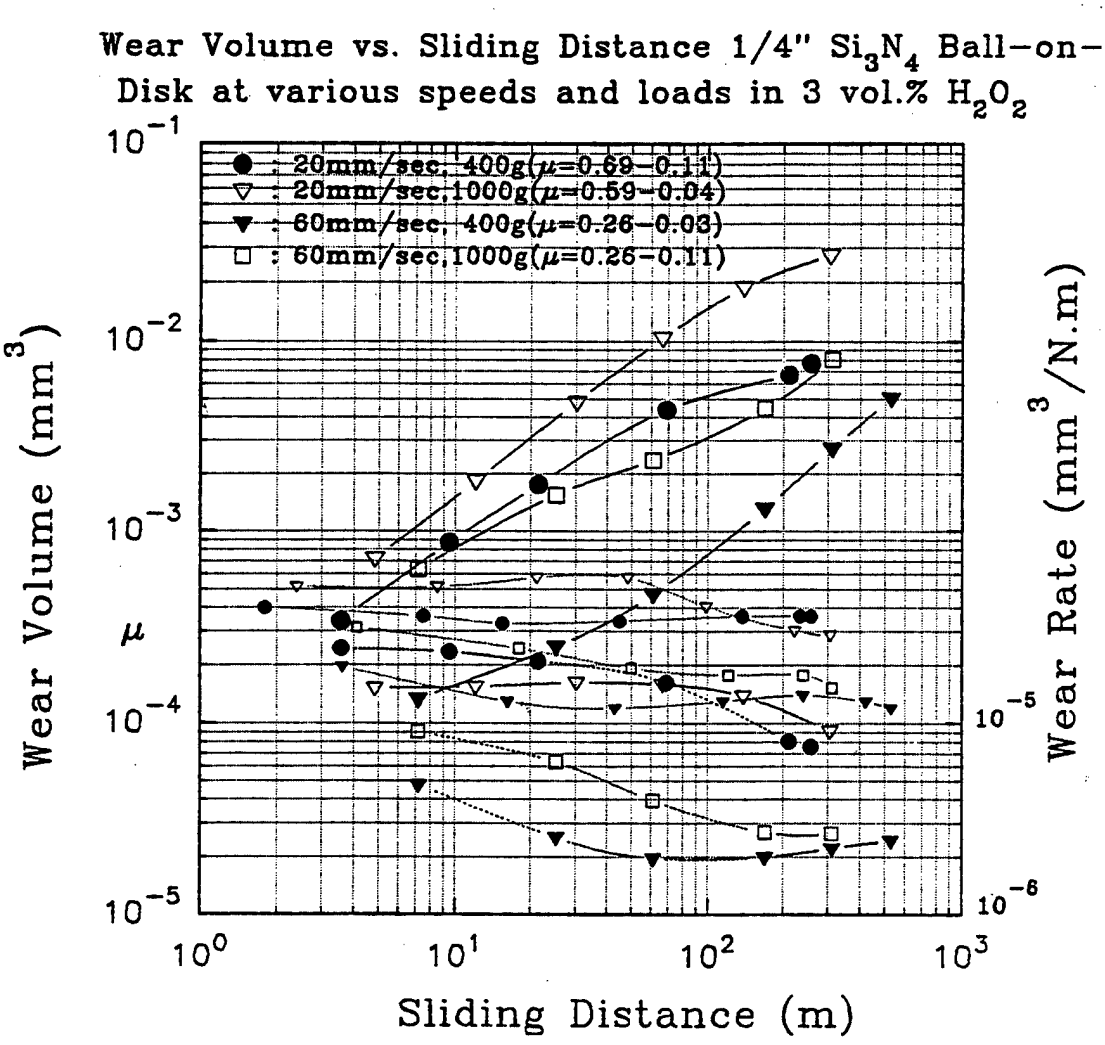

(C)

Figure 9 (continued) Material removal, friction coefficient and polishing rate (wear rate) of silicon nitride as a function of sliding distance in hydrogen peroxides. (C), Middle set indicates friction coefficient.

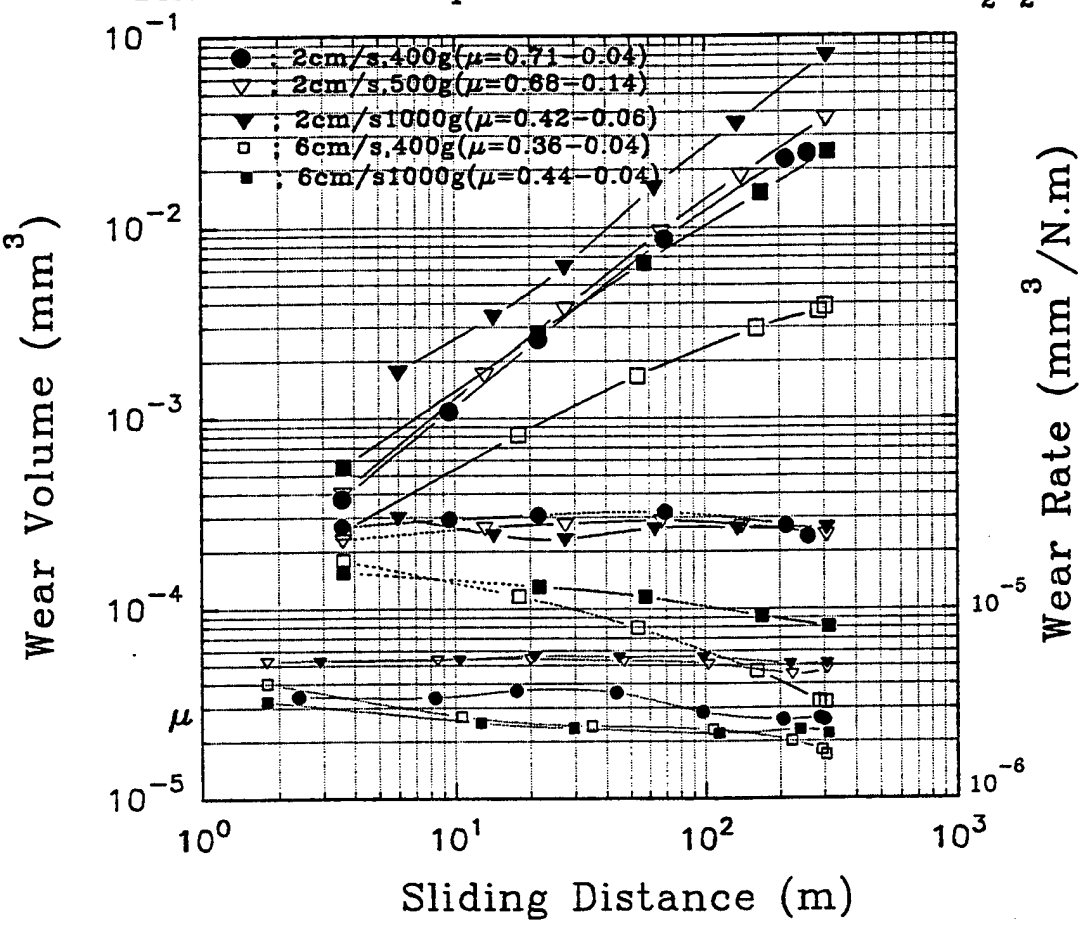

(D)

Figure 9 (continued) Material removal, friction coefficient and polishing rate (wear rate) of silicon nitride as a function of sliding distance in hydrogen peroxides. (D), Middle set indicates polishing rate.

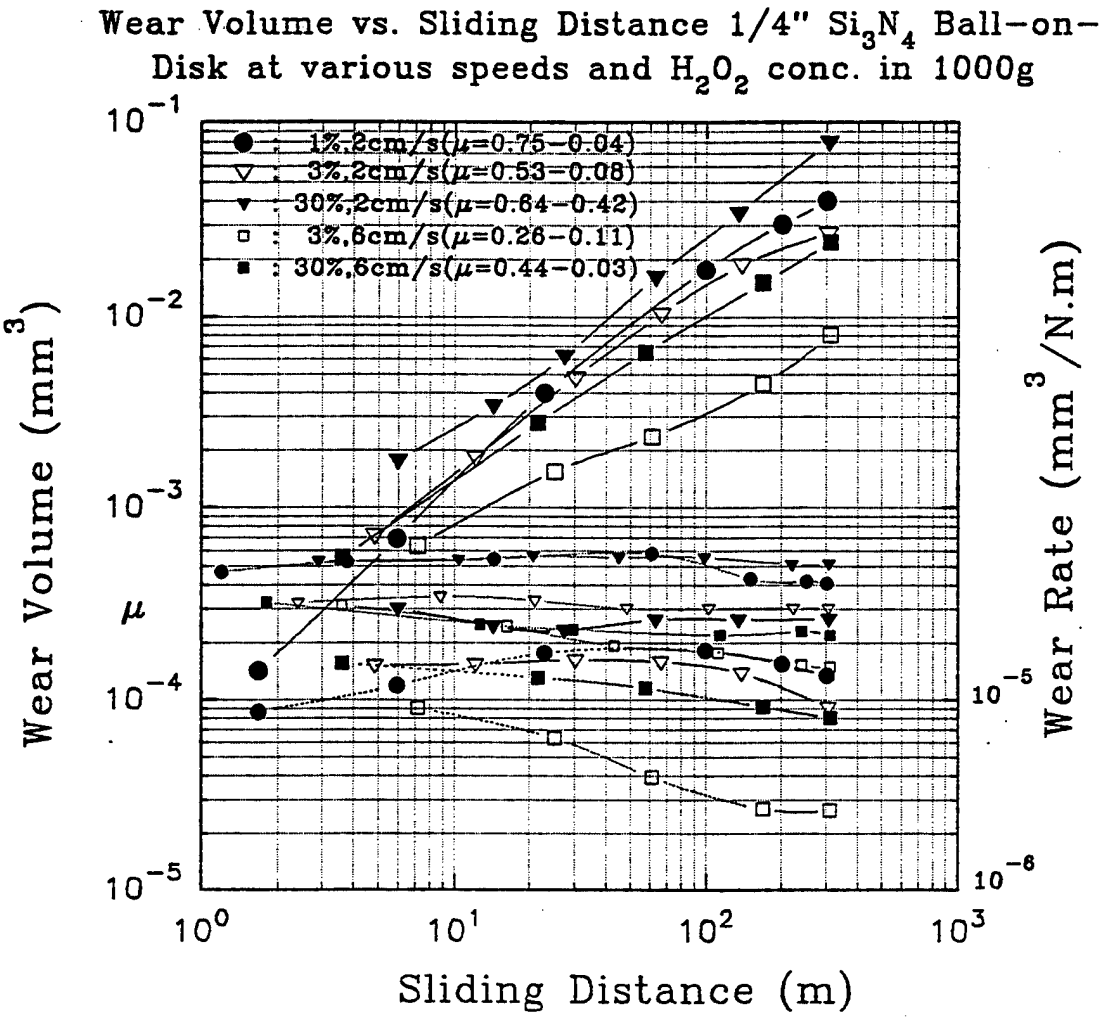

(E)

Figure 9 (continued) Material removal, friction coefficient and polishing rate (wear rate) of silicon nitride as a function of sliding distance in hydrogen peroxides. (E), middle set indicates friction coefficient.

Several corresponding surface morphologies are shown in Figure 10. The conclusion of this work is that material removal is proportional to load and increases with peroxide concentration. Material removal rate is higher than in water above 3 vol.% hydrogen peroxide and lower than in water for lower concentrations. All concentrations above 1 vol.% produce smooth surfaces when the load is less than 4 Newtons. Hydrogen peroxide produces smoother surfaces than water. Figures 11 and 12 show the results obtained with chromic acid CrO_3. The removal rate is slightly lower than with water and is independent of concentration; the surface quality is superior to those obtained with water and hydrogen peroxide. An optimum set of mechanical process parameters for the exploration of other polishing fluids is a speed of 20 mm/sec and a load of 4.4 Newtons (0.8 pound). Figure 13 shows the results obtained with various chromates, a number of acid solutions characterized by their pH, basic solutions, and organic oxidizers. The solutions used with their pH values are given in Table 5. None of the solutions shown in Figure 13 gave removal rates as high as those of water, nor did they produce surfaces with a satisfactory polishing, with the exception of the chromates. All of the organic oxidizers show so low a removal rate that they can be considered as effective anti-wear reagents. A patent application to this effect has been submitted.

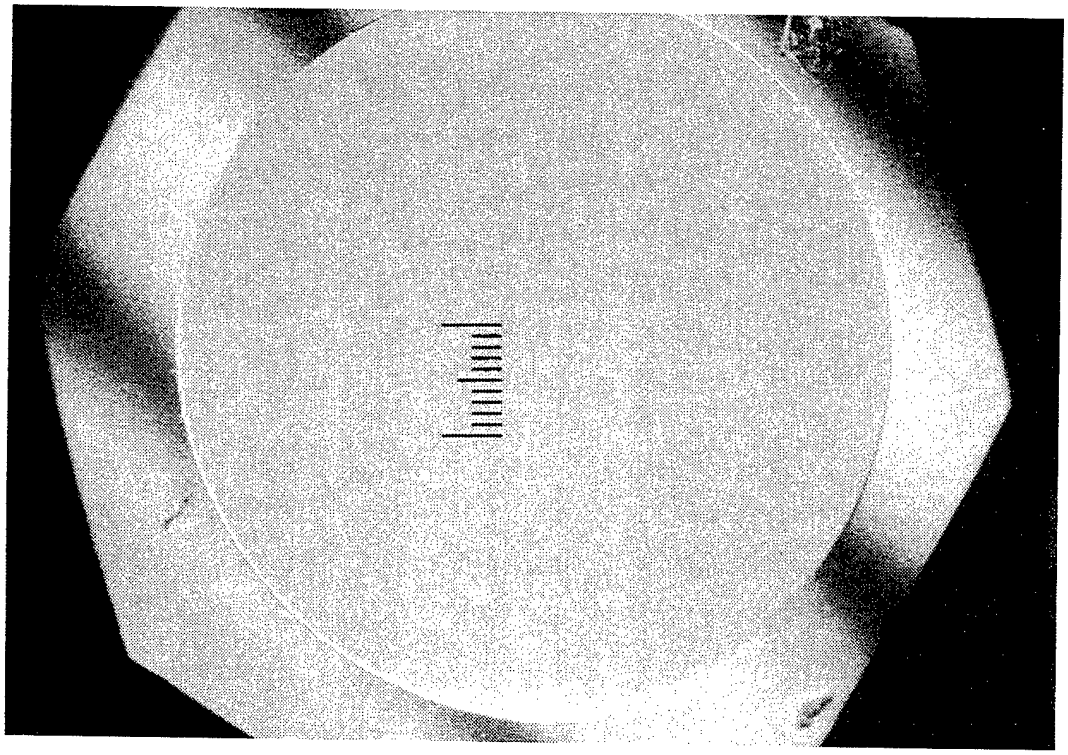

(A)

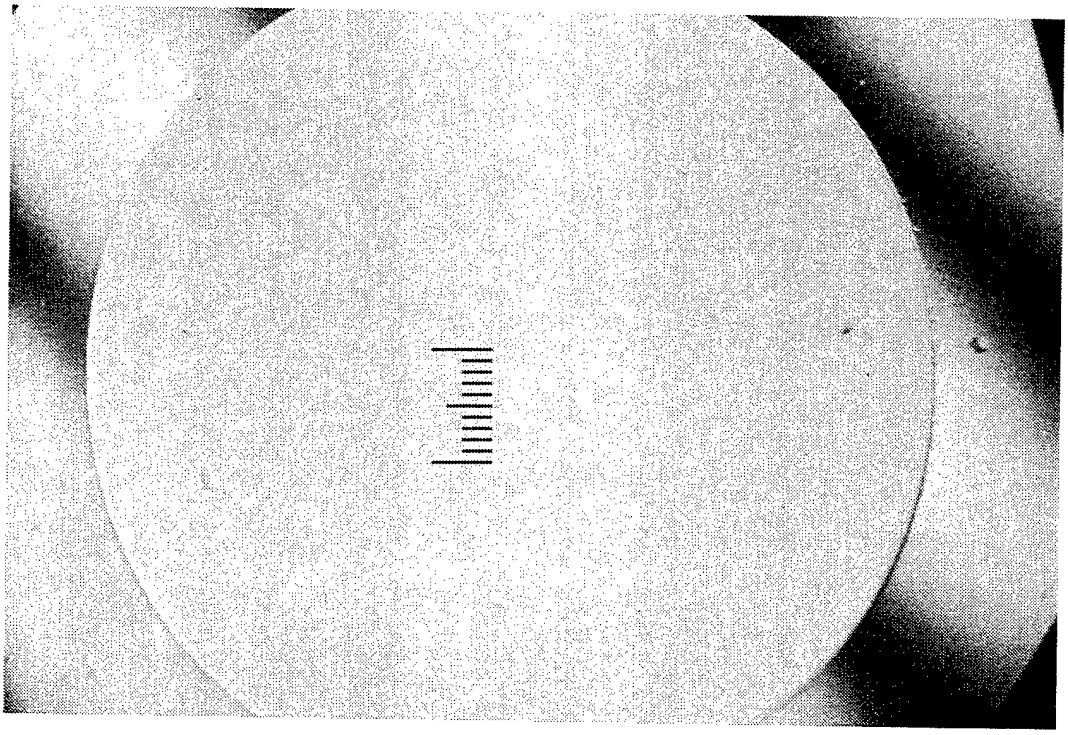

(B)

Figure 10 Surface morphology by NIC optical microscopy of tribochemically polished surfaces in hydrogen peroxides: (A) 3 vol.%, 3.92N, 100x, 20mm/sec, at 30mm. (B) 30 vol.%, 3.92 N, 100x, 20mm/sec, at 300m.

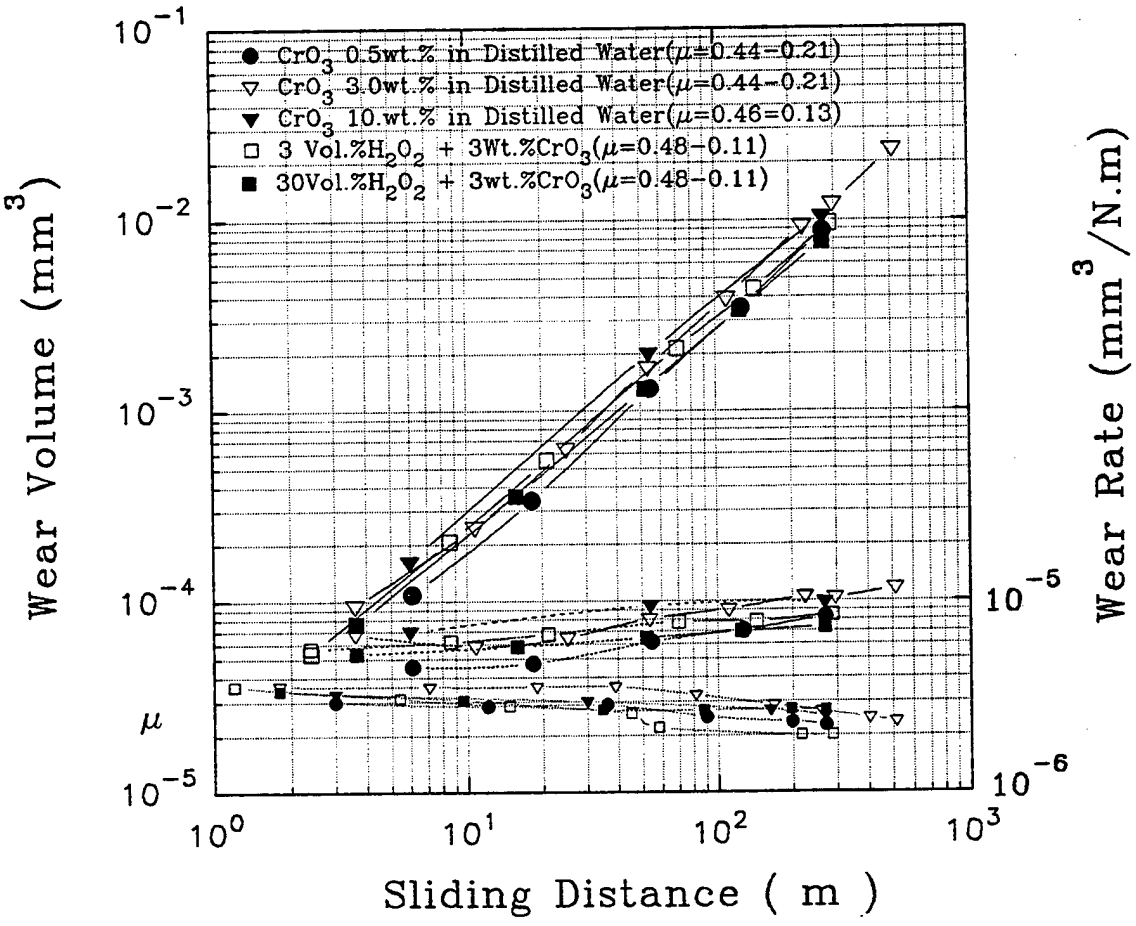

(A)

Figure 11 Material removal, friction coefficient and polishing rate (wear rate) in chromic acids. Lower set indicates friction coefficients.

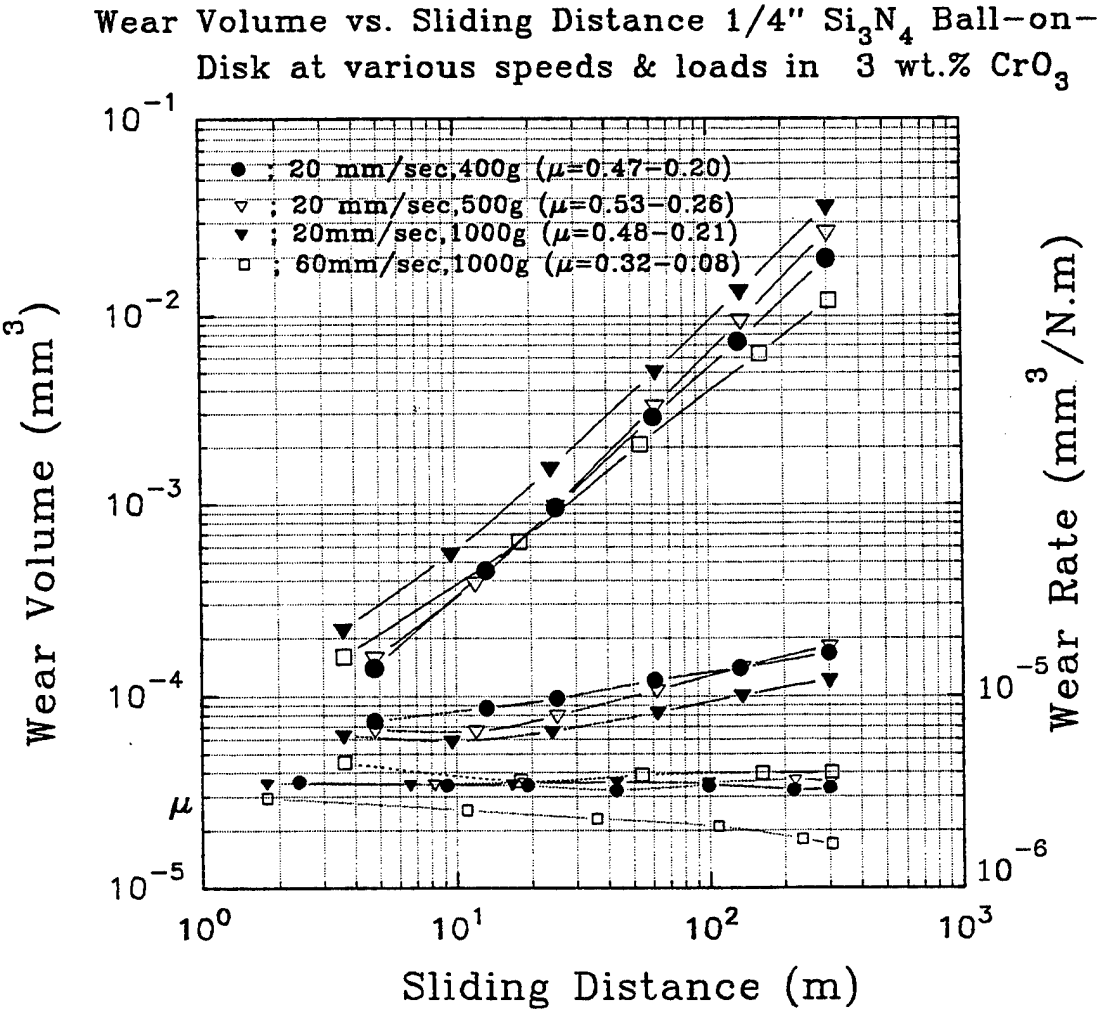

(B)

Figure 11 (continued) Material removal, friction coefficient and polishing rate (wear rate) in chromic acids. Lower set indicates friction coefficients.

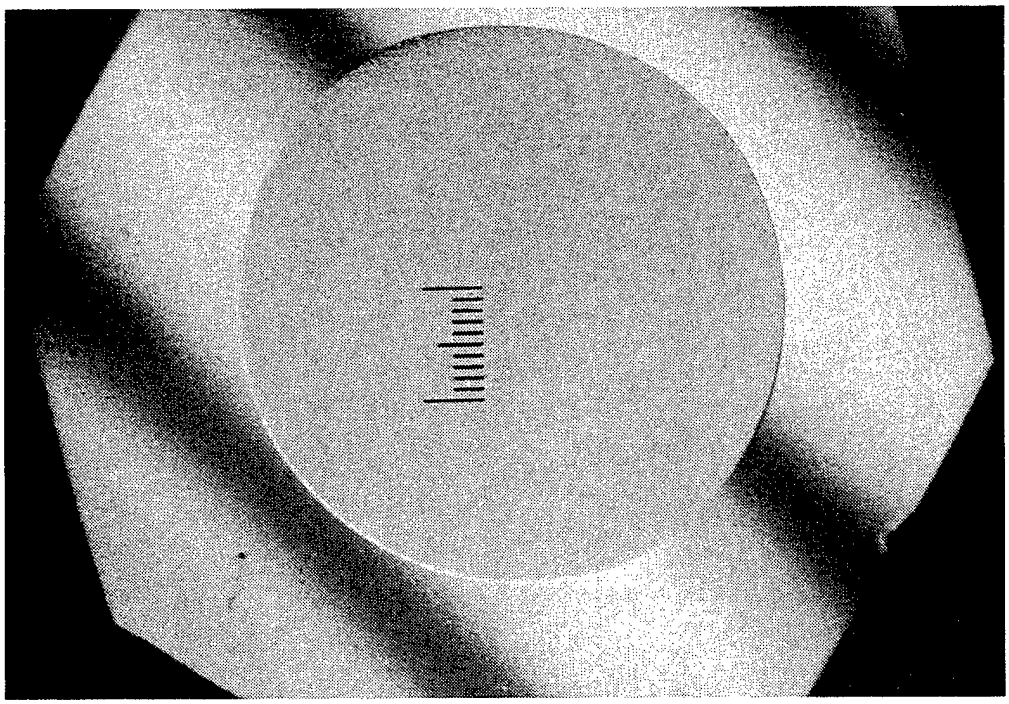

(A)

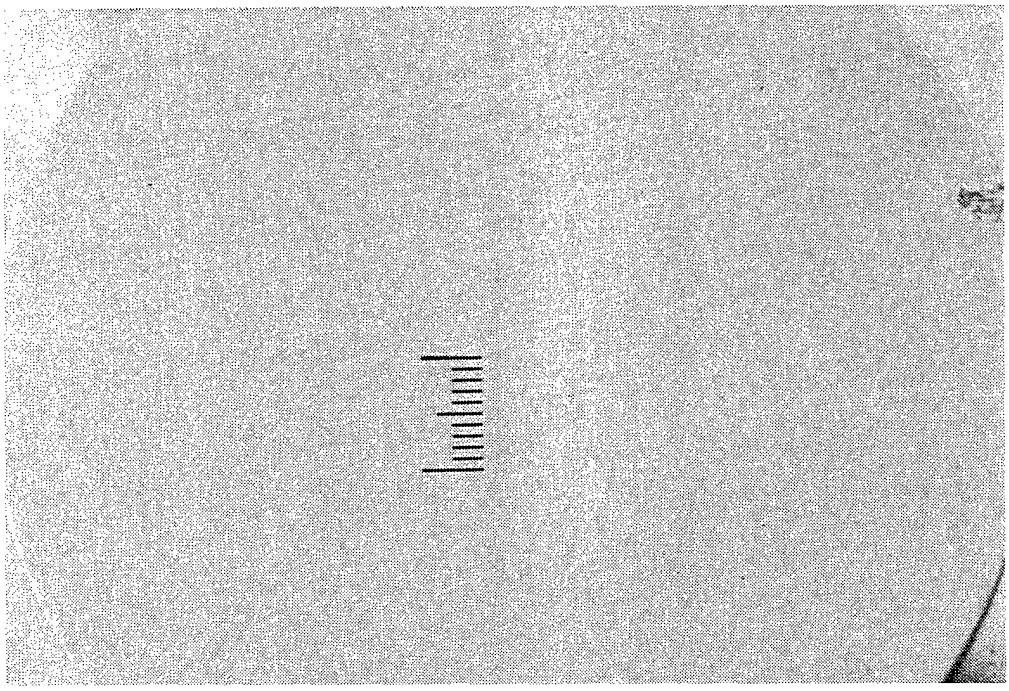

(B)

Figure 12 Surface morphology by NIC optical microscopy of tribochemically polished surfaces in chromic acids.(A) 3 wt.%, 3.92 N, x100, 20mm/sec, at 21.6m, (B) 3 wt.%, 9.8 N, x100, 60mm/sec, at 306m sliding distance.

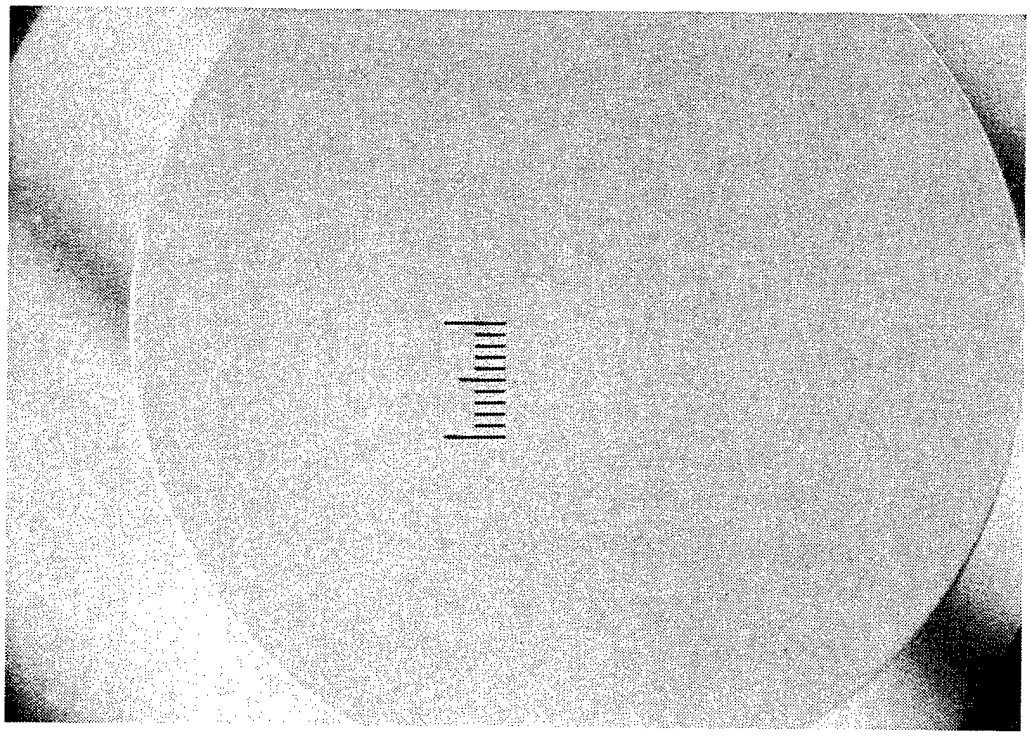

(C)

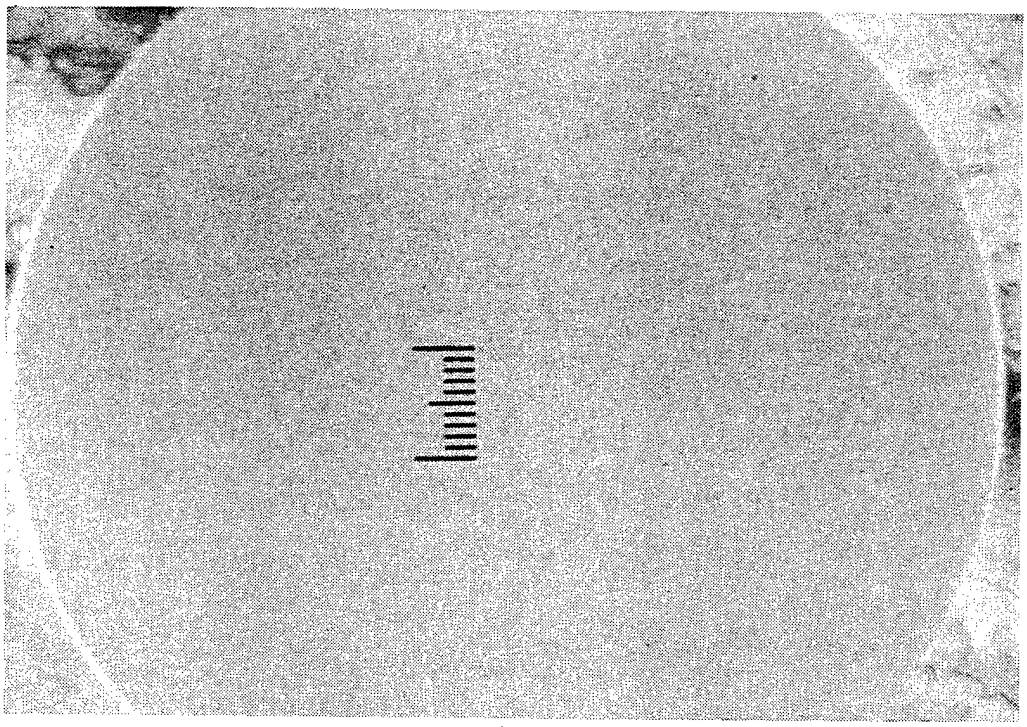

(D)

Figure 12 (continued) Surface morphology by NIC optical microscopy of tribochemically polished surfaces in chromic acids.(C) 3 wt.%, CrO_3+3vol.%H_2O_2 9.8 N, 100x, at 162m, (D) 0.5 wt.%, 3.92 N, 100x, 20mm/sec, at 290m sliding distance.

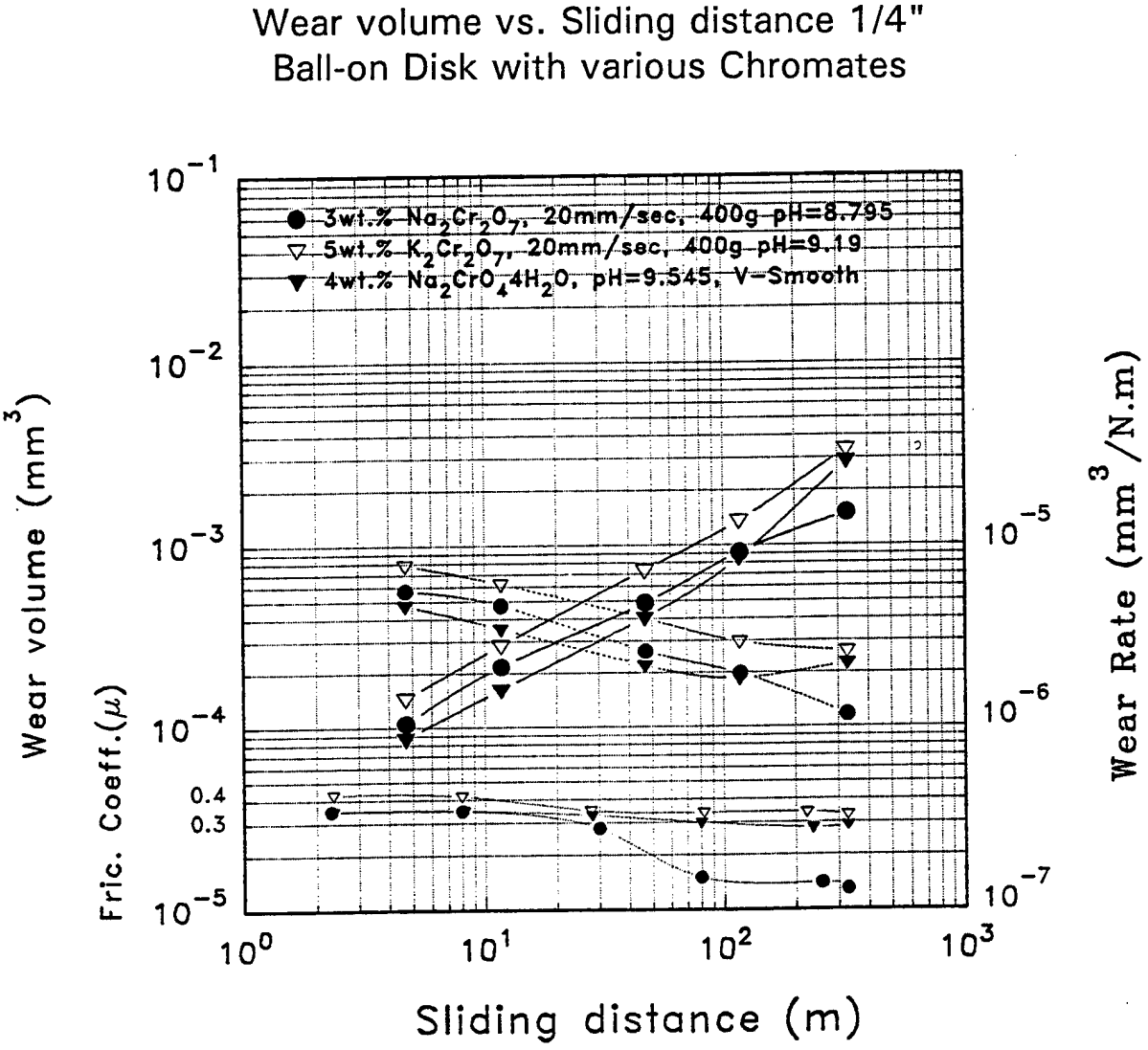

(A)

Figure 13 Material removal, friction coefficient and polishing rate (wear rate) in various polishing fluids, (A) Chromate.

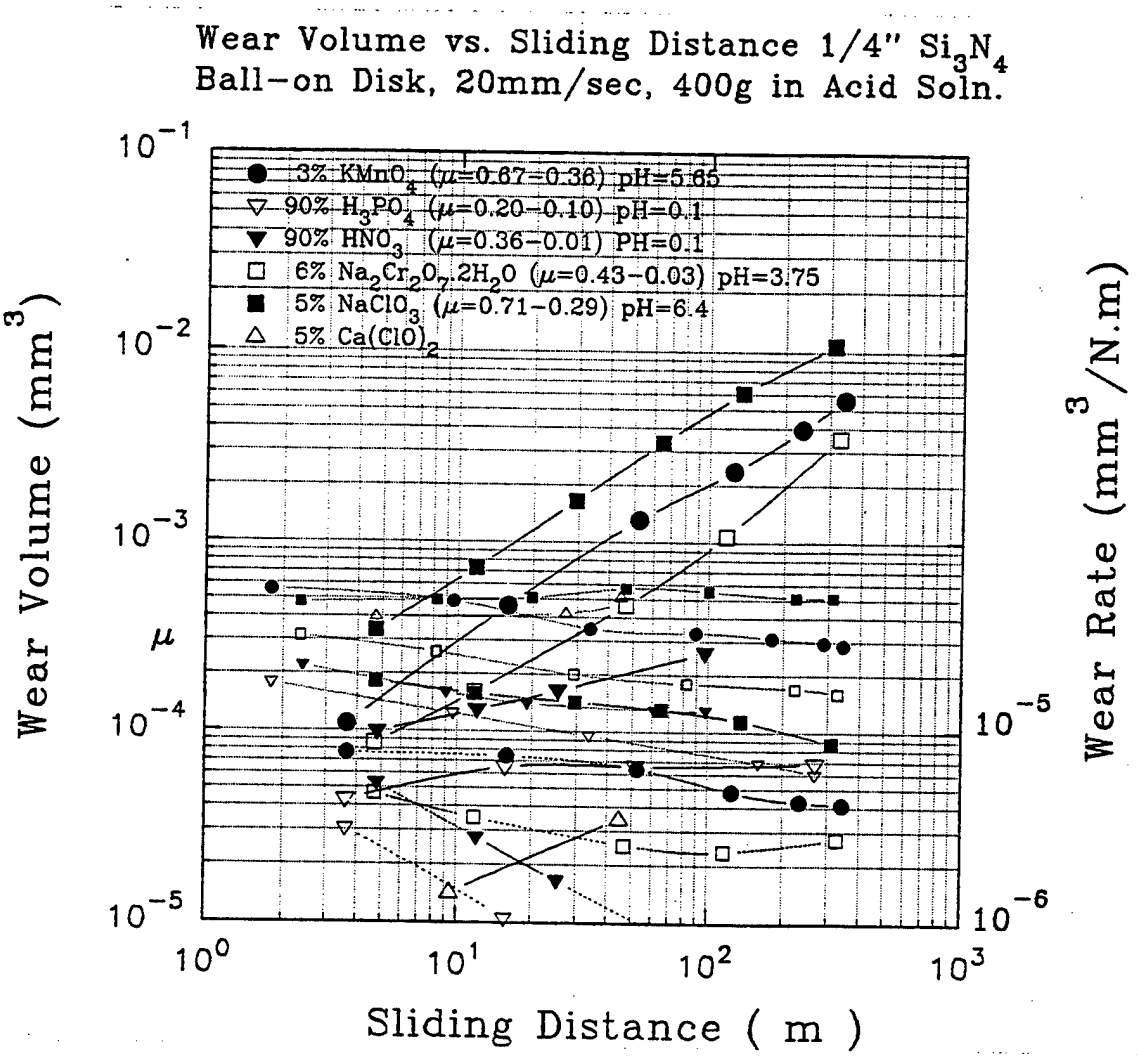

(B)

Figure 13 (continued) Material removal, friction coefficient and polishing rate (wear rate) in various polishing fluids, (B) acidic solution.

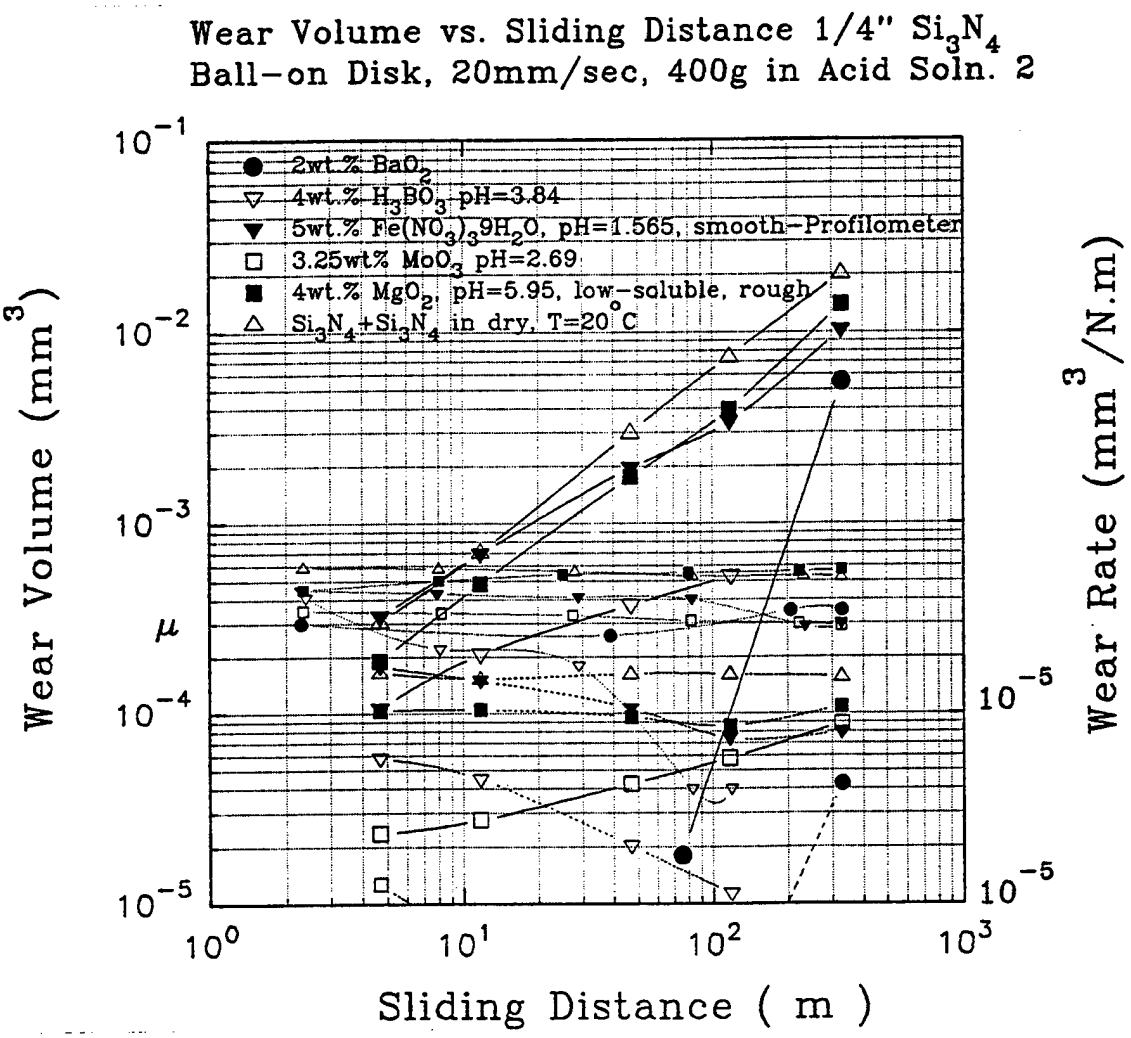

(C)

Figure 13 (continued) Material removal, friction coefficient and polishing rate (wear rate) in various polishing fluids, (C) acidic solution.

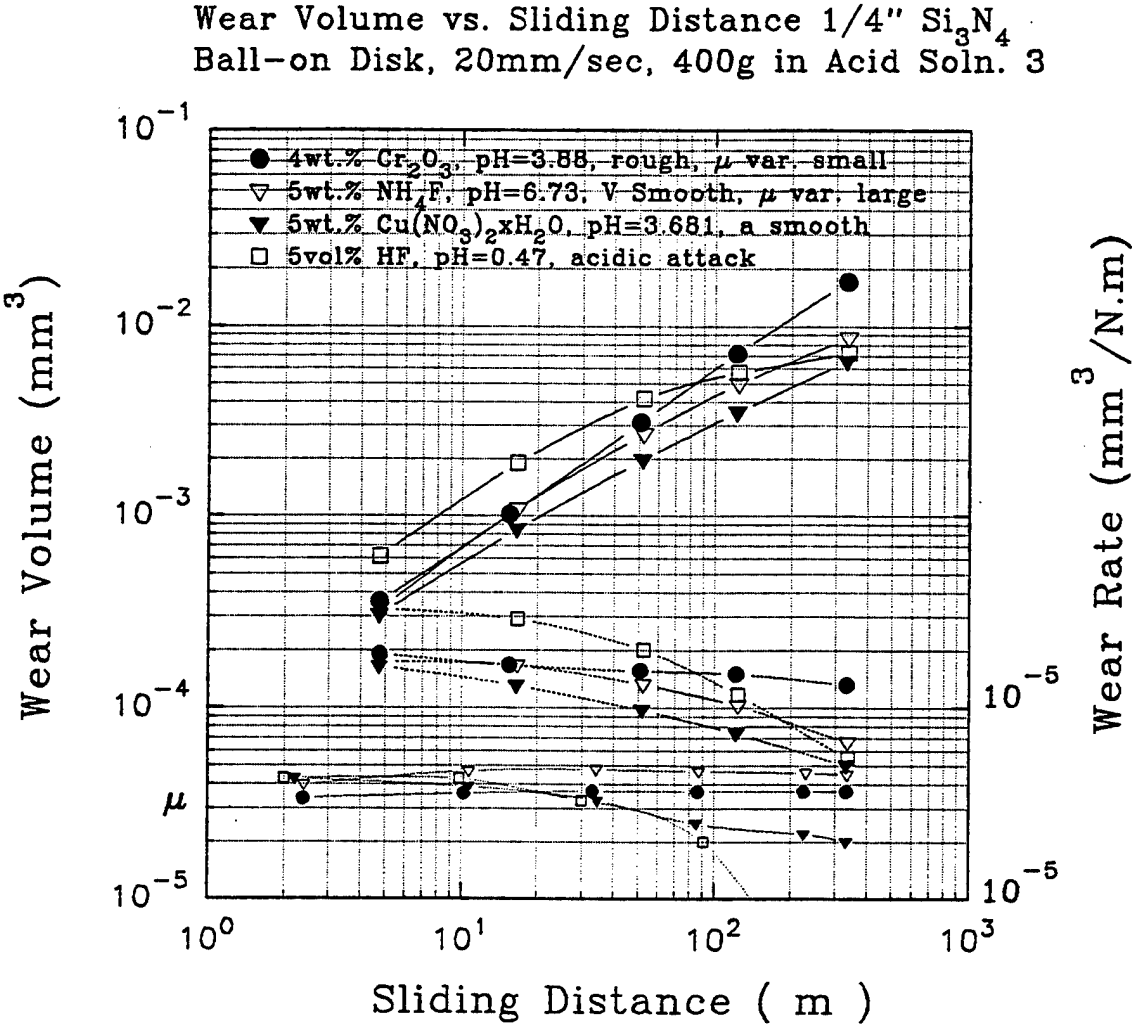

(D)

Figure 13 (continued) Material removal, friction coefficient and polishing rate (wear rate) in various polishing fluids, (D) acidic solution.

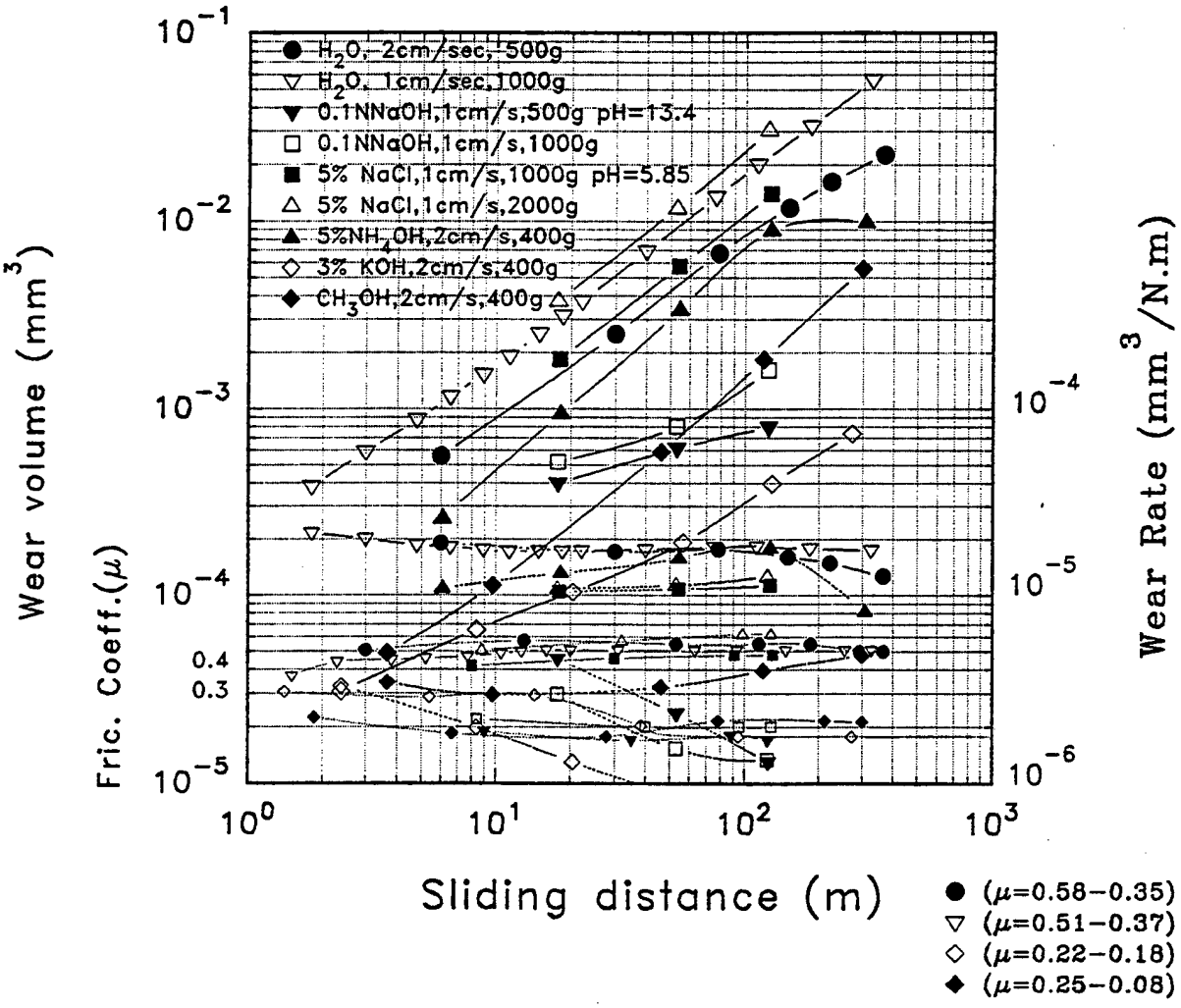

(E)

Figure 13 Material removal, friction coefficient and polishing rate (wear rate) in various polishing fluids, (continued) (E) basic solution.

Wear volume vs. Sliding distance 1/4" Si_3N_4
Ball-on-Disk at 20mm/sec, 400g and basic soln. 2.

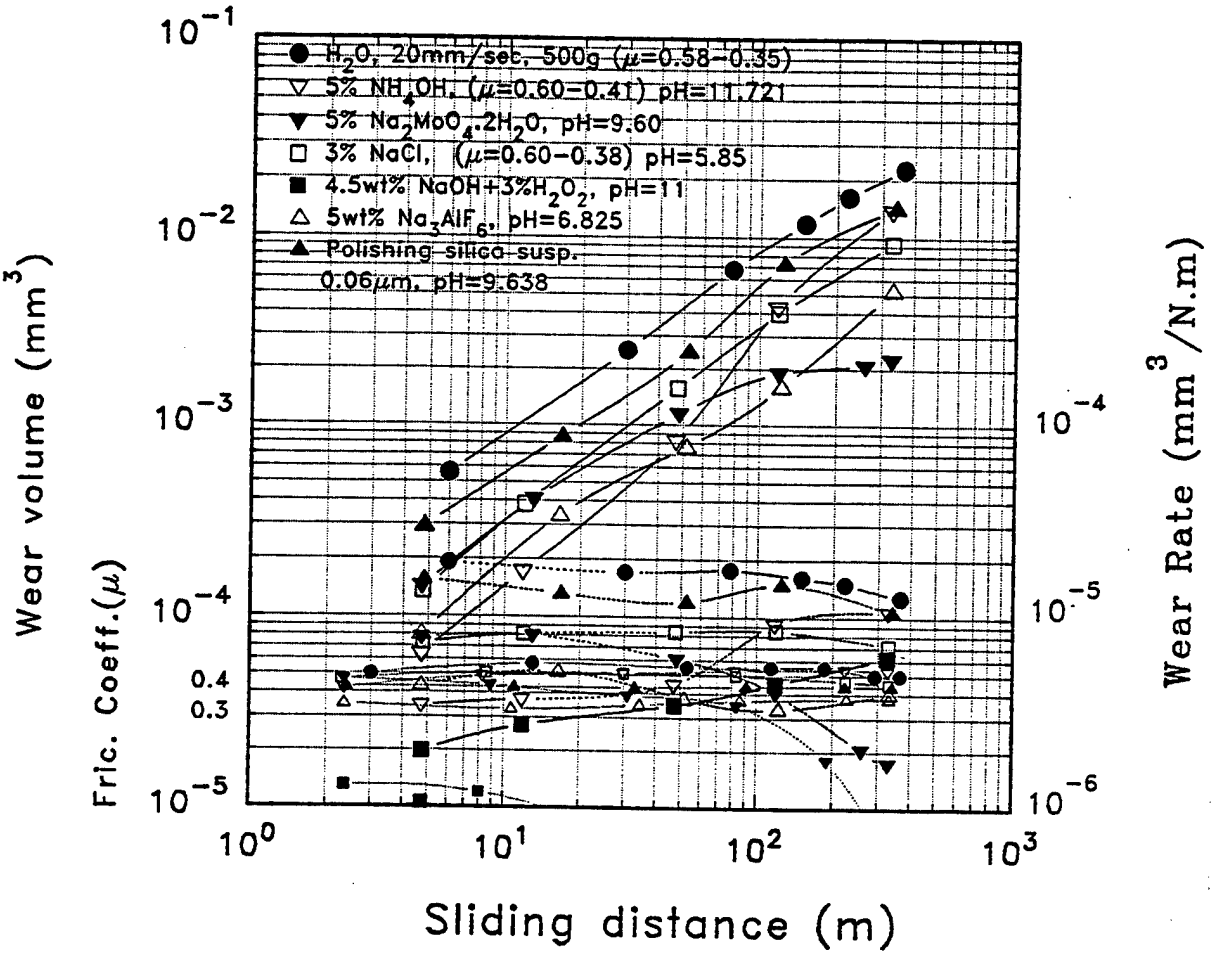

(F)

Figure 13 (continued) Material removal, friction coefficient and polishing rate (wear rate) in various polishing fluids, (F) basic solution.

Table 5.
pH Measurement Results

Number	Solution	pH Accumet	Comments
1	10wt% CrO_3	0.255-0.260	Very dark orange
2	5wt% CrO_3	0.47-0.48	Some dark orange
3	3wt% CrO_3	1.04-1.05	Dark orange
4	0.5wt% CrO_3	1.47-1.48	Orange
5	3wt% CrO_3+3%H_2O_2	2.44-2.45	Heat of reaction is great, bubbling dark brown
6	2.5vol% HF	1.16-1.17	Clear, transparent
7	5wt% $Fe(NO_3)_39H_2O$	1.56-1.57	Light yellow, no precipitates
8	3.25wt% MoO_3	2.69	White colloidal, large precipitates
9	3% Chloro-peroxybenzoic Acid	3.30	------
10	5wt% $Cu(NO_3)2xH_2O$	3.680-3.682	Light blue, clear
11	6wt% $Na_2Cr_2O_72H_2O$	3.70-3.71	------
12	5wt% H_3BO_3	3.84	------
13	4wt% Cr_2O_3	3.87-3.89	Large precipitates
14	3wt% Sodium Periodate	4.70	------
15	30vol% H_2O_2	5.07-5.08	------
16	3wt% $KMnO_4$	5.6-5.7	Whole soluble, dark violet
17	13wt% NaC	5.8-5.9	------
18	4wt% MgO_2	5.90-6.00	Not many precipitates, suspension
19	3vol% H_2O_2	6.6-6.7	------
20	5wt% NH_4F	6.730	Clear solution

Table 5. (continued)
pH Measurement Results

Number	Solution	pH (Accumet)	Comments
21	5wt% Na_3AlF_6	6.80-685	Clear, transparent, small precipitates Shaking→opaque→pH check
22	Tap Water	7.01	------
23	3wt% Silicic Acid	7.24-7.25	Large, white precipitates
24	CH_3OH	7.6-7.7	------
25	Distilled Water	7.7	------
26	3wt% $Na_2Cr_2O_7$	8.79-8.80	Light yellow
27	5wt% $K_2Cr_2O_7$	9.18-9.20	Light yellow
28	4wt% $Na_2CrO_4 4H_2O$	9.54-9.55	Light yellow
29	5wt% $Na_2MoO_4 2H_2O$	9.60	------
30	Silica Suspension	9.638	Light blue suspension
31	5vol% NH_4OH	11.721	Slight odor
32	19.8wt% NaOH	13.38-13.42	------

4.1.2 Surface Morphology

The surfaces of tribochemically polished bearing balls were examined by NIC optical microscopy, Profilometer, SEM and AFM. NIC optical micrographs in distilled water, hydrogen peroxide and chromic acid are shown in Figures 8, 10 and 12. Figure 14 shows optical micrographs by NIC of surfaces tribochemically polished in selected polishing fluids (as shown in Figure 13). The tribochemically polished surfaces in various chromates show smooth and defect-free surfaces. The surfaces tribochemically polished in acidic solutions show generally rough surfaces which are believed to be due to acid attack. Figure 15 shows the profilometer trace of a tribochemically polished flat in 3 wt.% chromic acid. The surface is smooth with a roughness less than 0.4 nm over a length of 0.25 mm. Figure 16 shows the surface morphology observed by SEM of a tribochemically polished flat. The surface morphology of a tribochemically polished surface can be compared with a commercially finished bearing ball as shown in Figure 4. Commercially finished balls present a number of surface defects such as holes and scratches. No such surface defects are found on the tribochemically polished surface. The

crack in Figure 16(A) was made artificially because the surface was too smooth for focusing without it. Figures 16(B), (C) and (D) show the corresponding optical micrographs at low (100x and 200x) and high (500x) magnification. High-resolution morphology studies were performed with the Atomic force microscope (AFM). The technique has been described in subtask 3.4.1. Figure 17 shows the surface morphology of the commercially finished 1/4" ball. Grain pull-outs and surface scratches are visible. Figure 17(B) shows a perspective image of Figure 17(A). The shading direction of light was from the right in both figures.

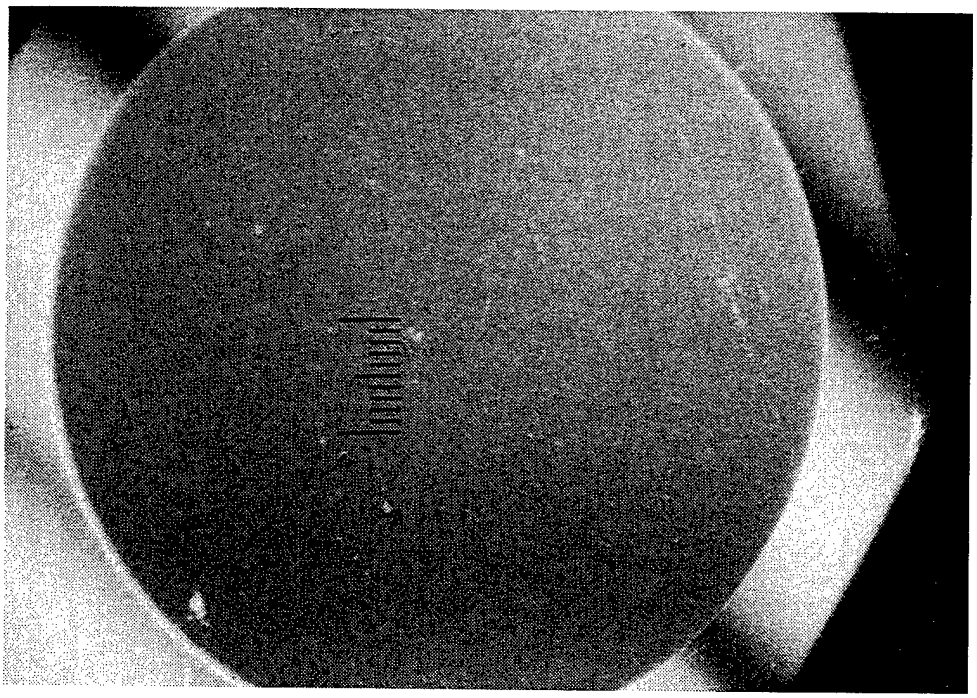

(A)

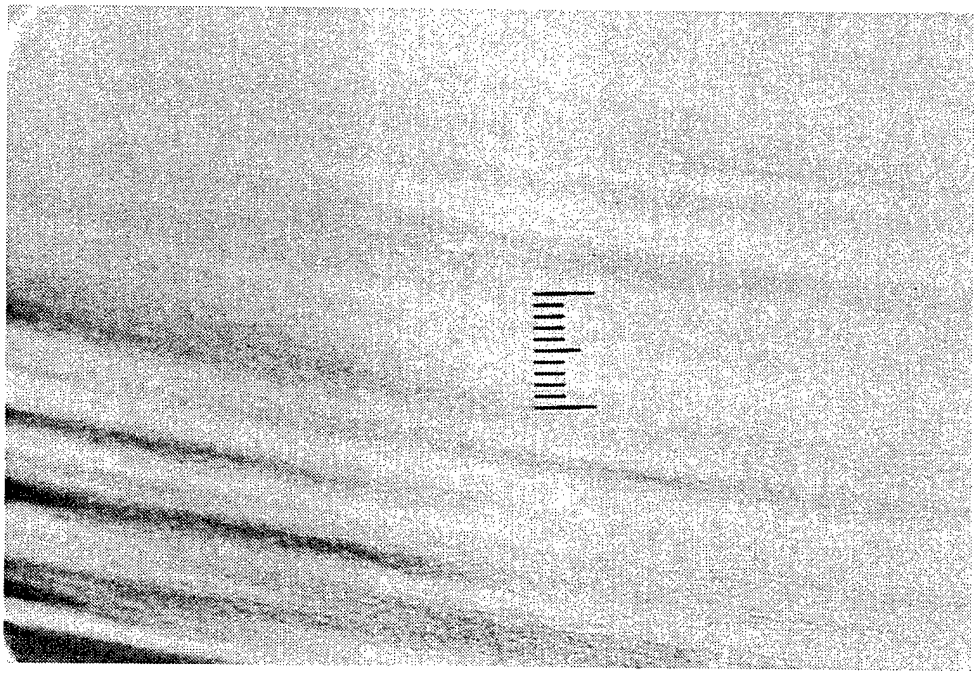

(B)

Figure 14 Surface morphology by NIC optical microscopy of tribochemically polished surfaces in selected fluids: (A) 6wt.% $Na_2Cr_2O_72H_2O$, 3.92N, 100x, 20mm/sec at 328m sliding distance, very smooth, (B) 4 wt.%CR_2O_3, 3.92N, 100x, 20mm/sec, at 333m sliding distance.

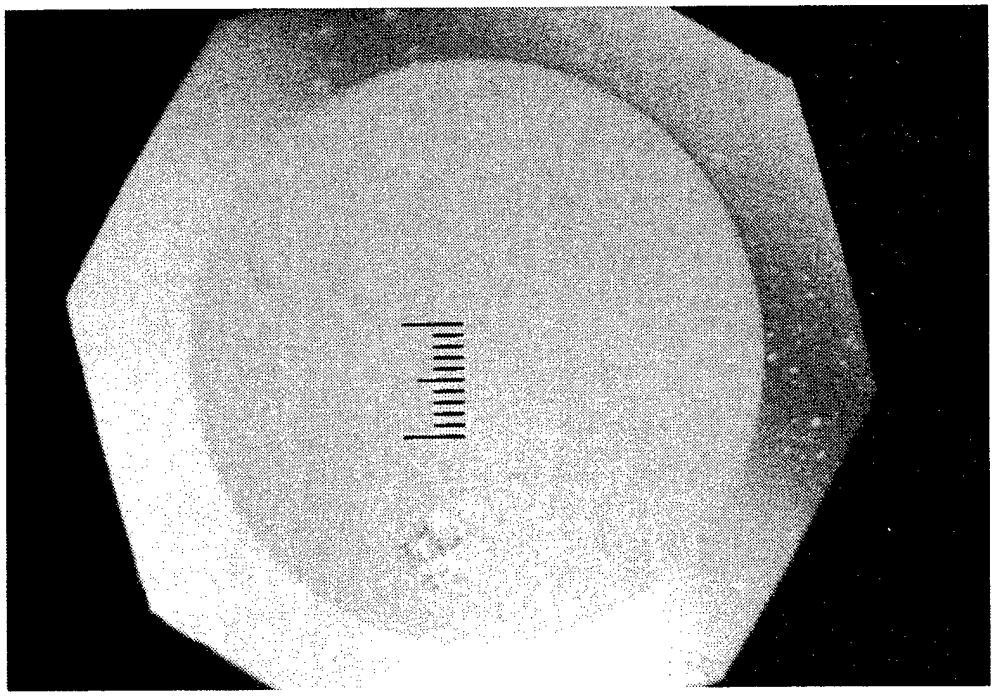

(C)

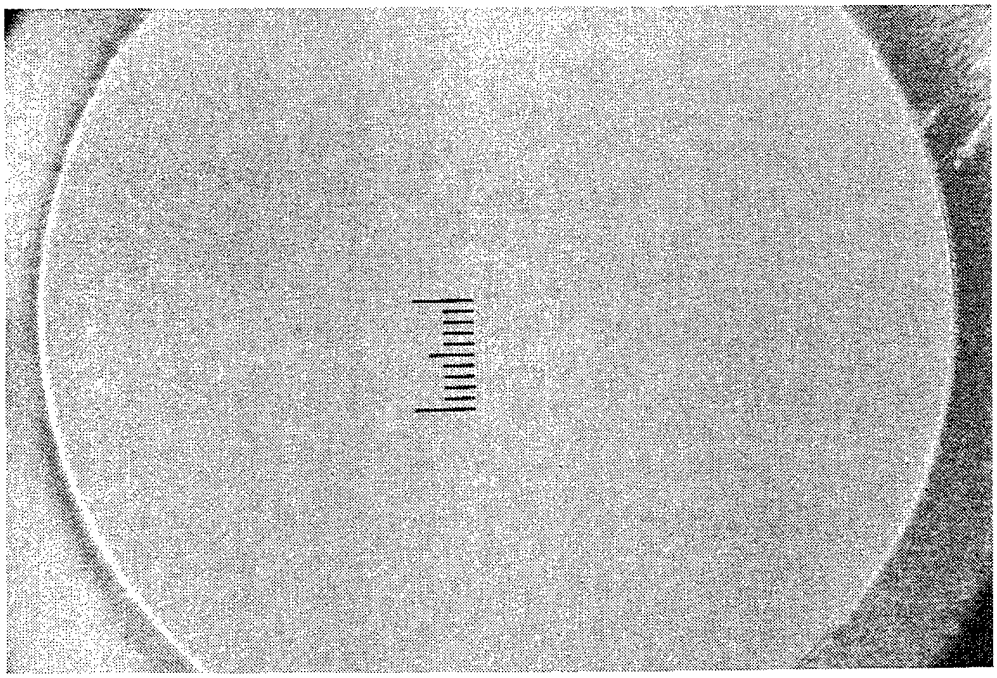

(D)

Figure 14 (continued) Surface morphology, by NIC optical microscopy, of tribochemically polished surfaces, in selected fluids: (C) 15 vol.% H_3PO_4, 50x, 3.92N, 20mm/sec, at 268m sliding distance, (D) 5 vol.% HF, 3.92N 100x, 20mm/sec, at 337m sliding distance.

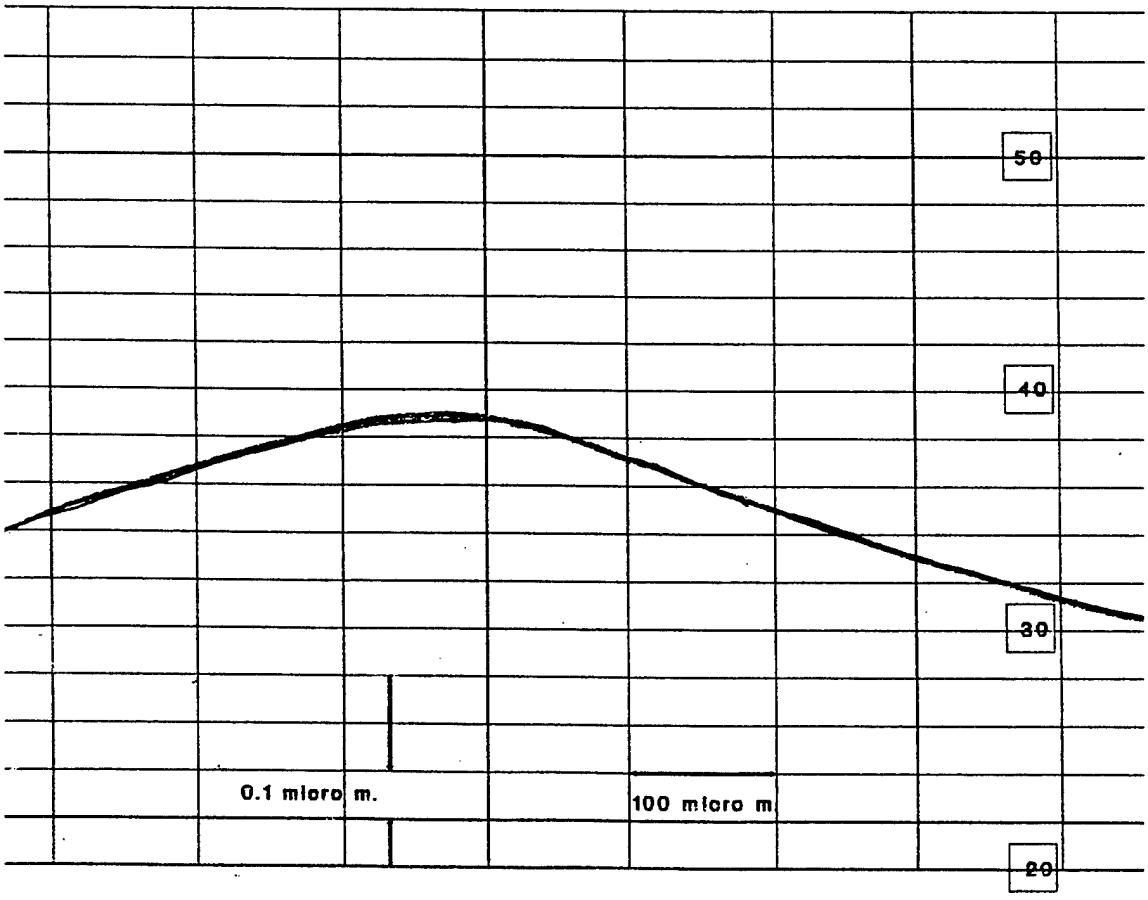

Figure 15 Profilometer trace of a tribochemically polished flat surface in 3 wt.% CrO_3. Vertical resolution: 0.1μm = 100nm.

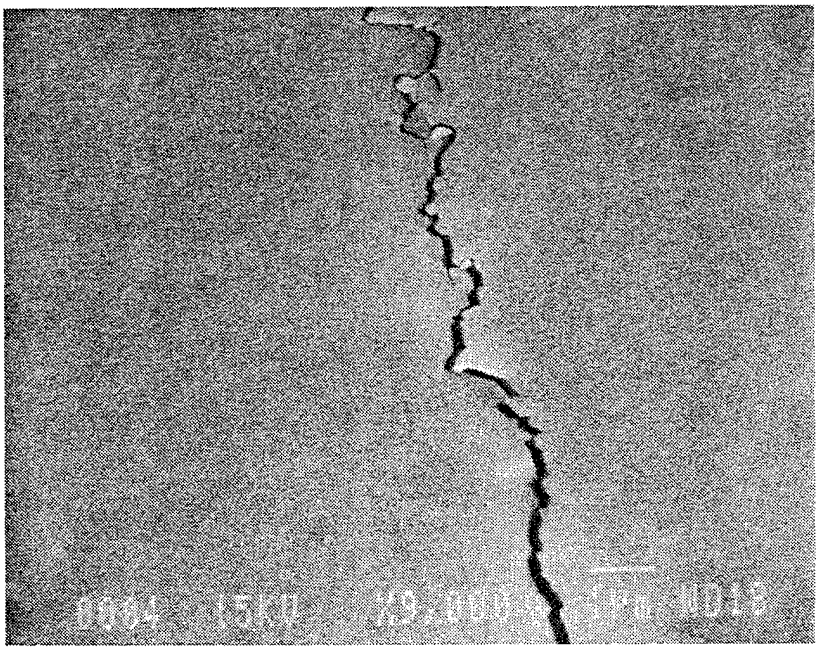

(A)

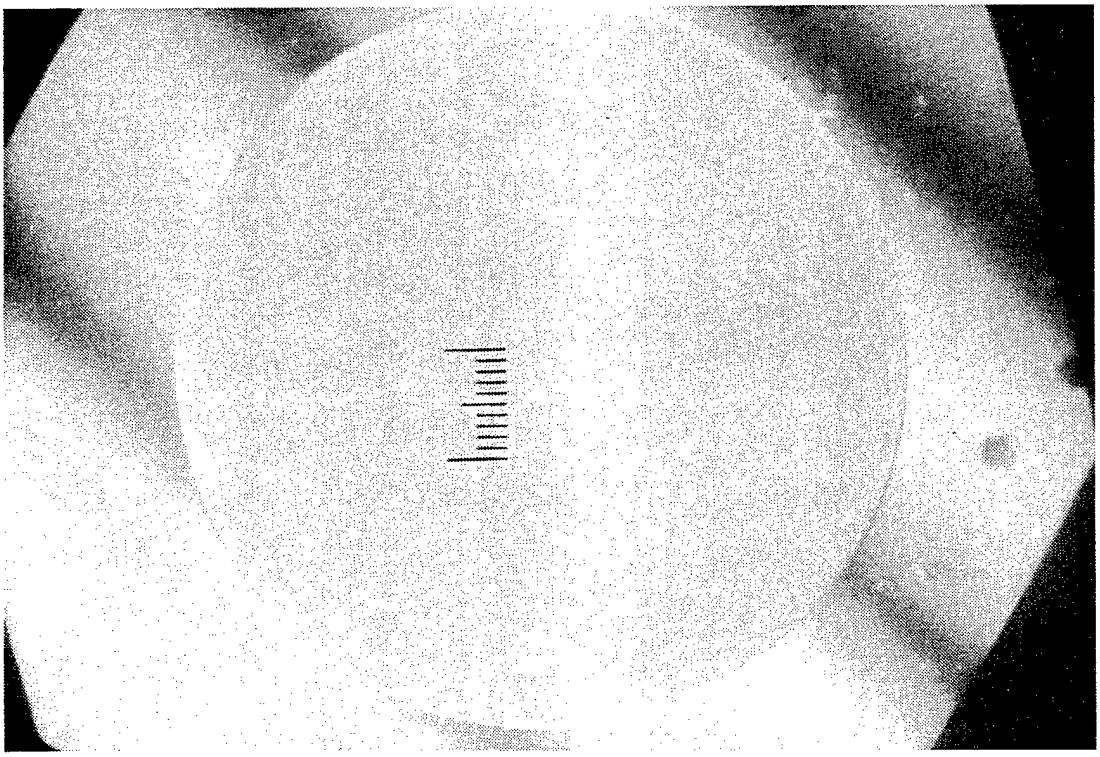

(B)

Figure 16 Surface morphology of tribochemically polished flat surface in 3wt.% CrO_3: (A) SEM micrograph (surface crack artificially made to aid focusing of SEM), (B) NIC optical micrograph 100x, at 61m sliding distance.

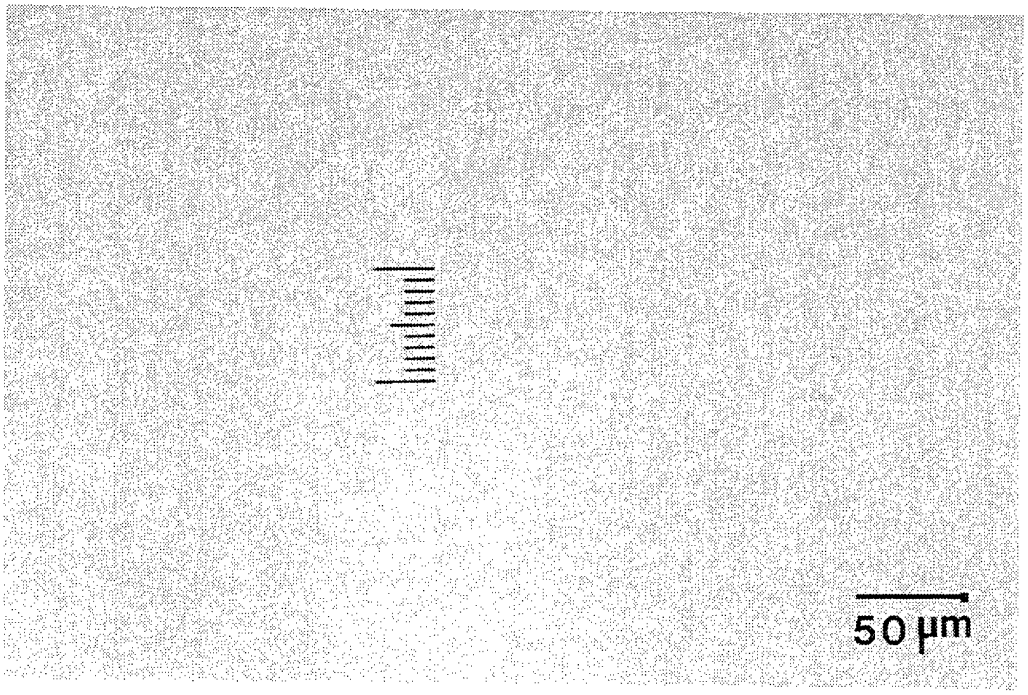

(C)

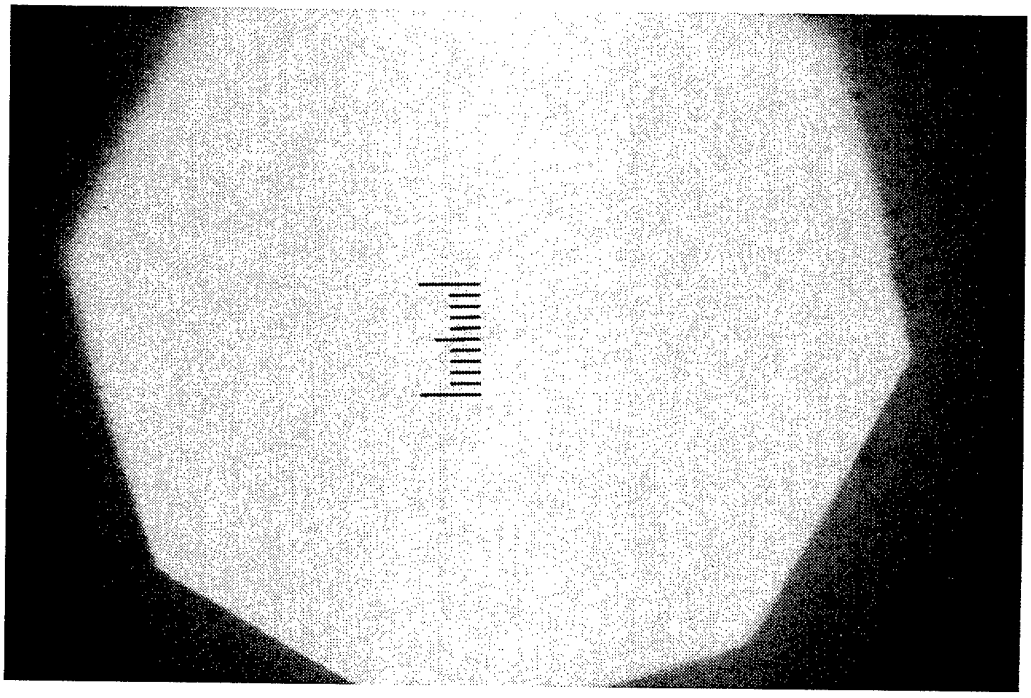

(D)

Figure 16 (continued) Surface morphology of tribochemically polished flat surface in 3wt.% CrO_3: (C) NIC optical micrograph 200x, at 300m sliding distance , (D) NIC optical micrograph 500x, at 311m sliding distance.

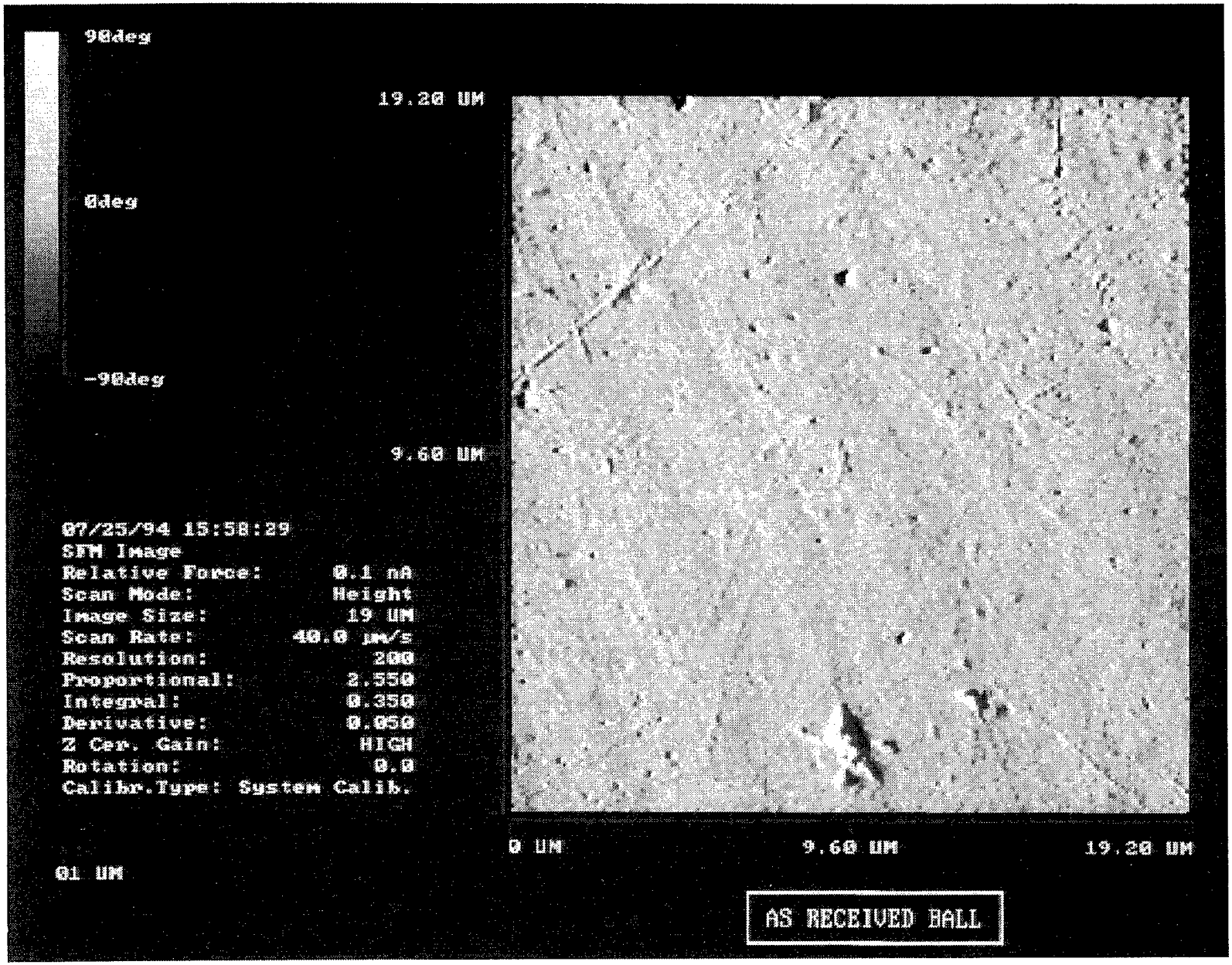

Figure 17 High resolution surface morphology, by Atomic Force microscopy, of a commercially finished 1/4" diameter ball: (A) 2-D mapping.

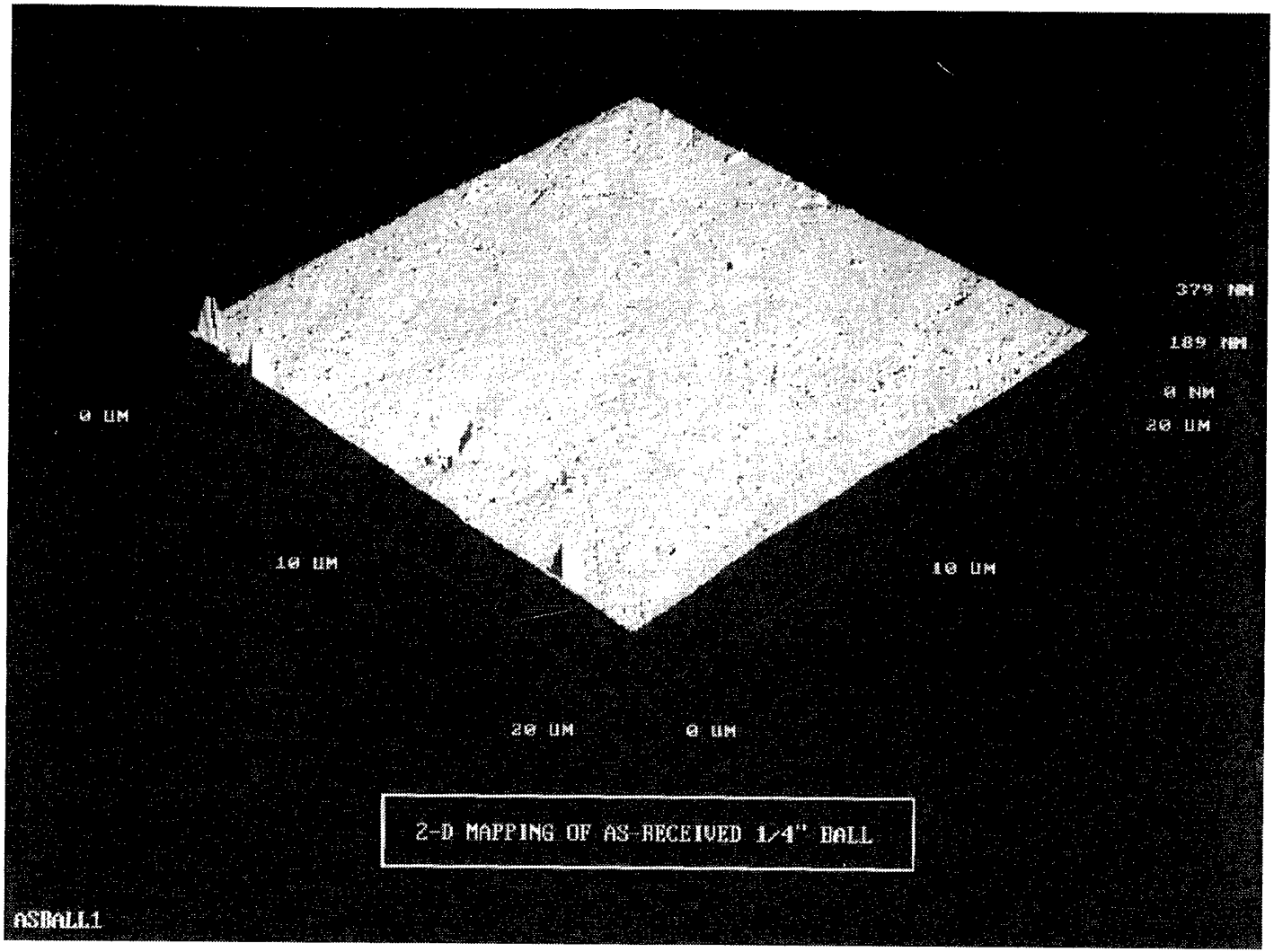

Figure 17 High resolution surface morphology, by Atomic Force (continued)microscopy, of a commercially finished 1/4" diameter ball: (B) 3-D mapping (corresponding perspective view of Figure 17(A)).

Figure 18 shows the AFM images of the surface tribochemically polished in 3 wt.% chromic acid. The direction of light is again from the right, which means that for hillocks such as surface dirt, the right sides are brighter than the left sides and for holes the left side is brighter. The surface morphology shown in Figure 18 is perfectly smooth and no surface defects such as holes, grain fall-out or scratch are apparent. The direction of light indicates that the bright spots on the surfaces represent dirt particles on the surface because this AFM measurement was performed in ambient conditions. Figure 19 shows the image and the result of surface roughness measurement: Ra = 0.5 nm (5Å). The surface roughness was measured at three different areas. Table 6 is a comparison of the roughnesses and surface defects. It is apparent that tribochemical polishing of silicon nitride in the appropriate liquid fluids can produce defect-free, perfectly smooth surfaces of higher quality than state-of-the-art abrasive polishing.

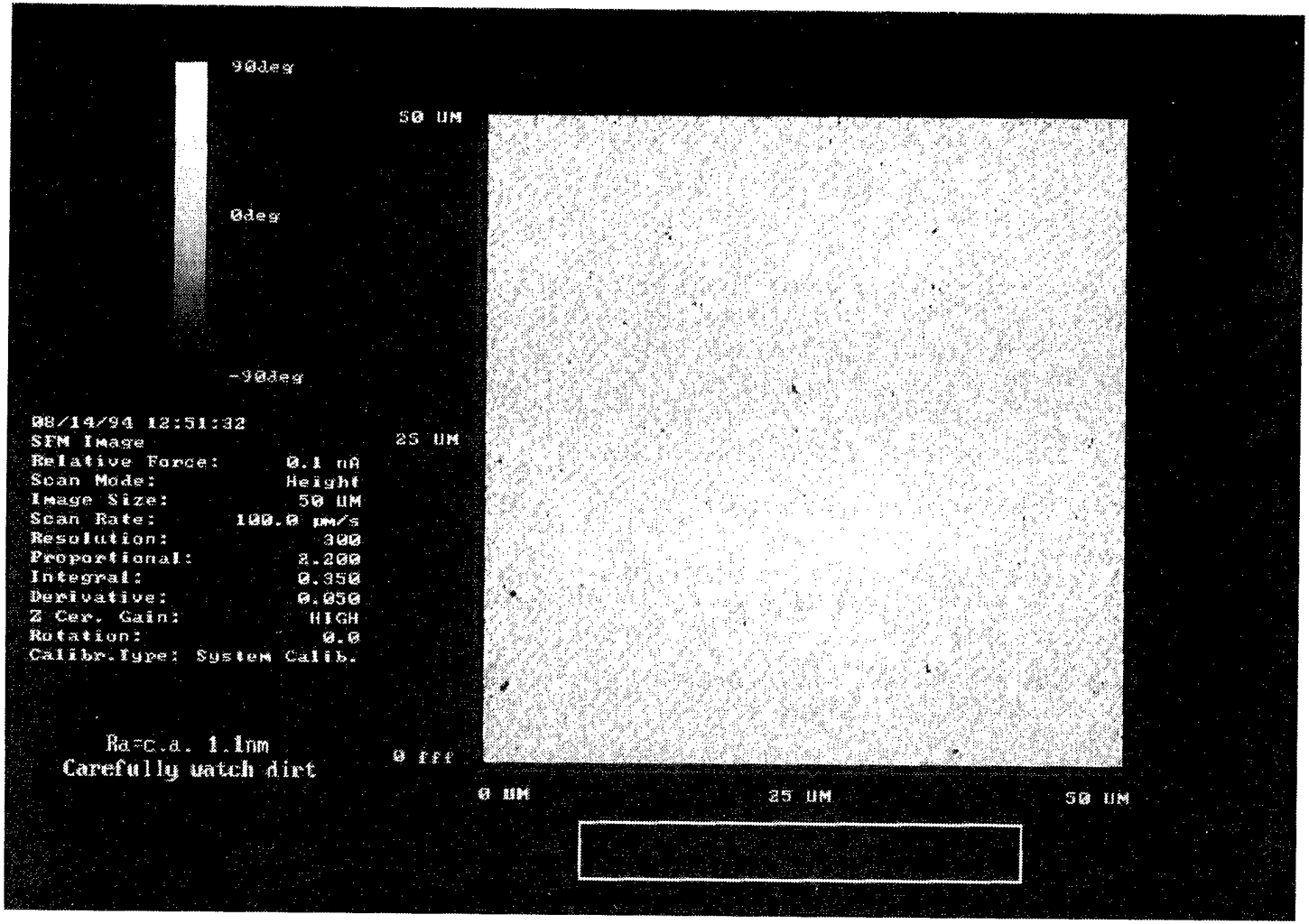

Figure 18 High-resolution surface morphology, by Atomic Force Microscopy, of a tribochemically polished, 1/4" ball, in 3 wt.% CrO_3.

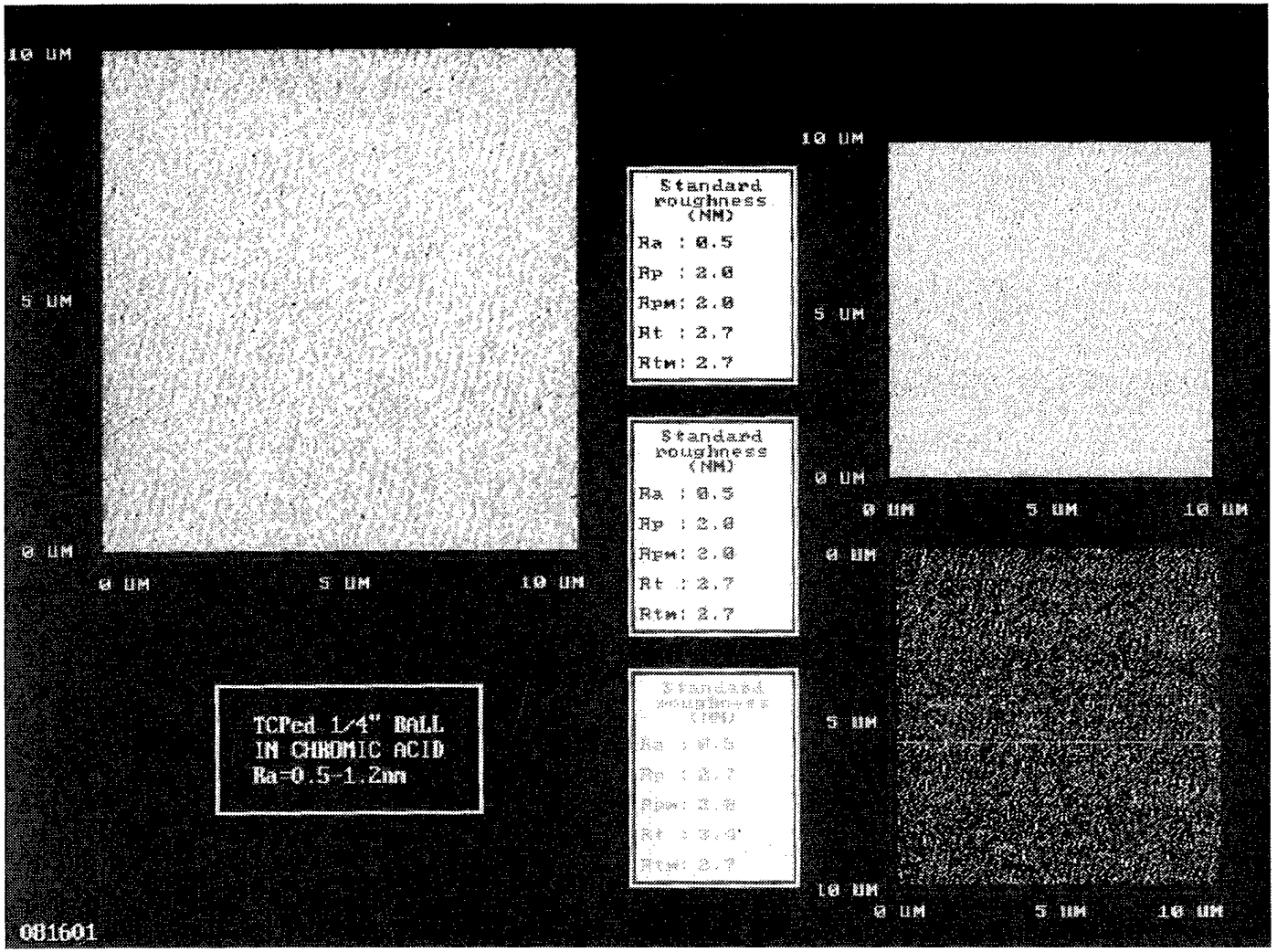

Figure 19 Surface morphology and roughness, by Atomic Force Microscopy, of a tribochemically polished, 1/4" ball, in 3 wt.% CrO_3.

Table 6.
Comparison of the AFM Measurement Results

Ball Quality Items	As-Received 1/4" ball	TCP'd 1/4" ball
Ra nm (μin) Without Defects	2.1-3.0 (0.083-0.118)	0.5-2.0 (0.020-0.079)
Defect Density	Large	None
Defect Type	Scratch and Grain Fall-Out	N/A
Scratch Mark	Some	None
Ra nm (μin) Without Defects	75-85 (2.953-3.346)	0.5-2.0 (0.020-0.079)

4.1.3 Elemental Analysis

Tribochemical polishing (TCP) is a polishing process based on simultaneous chemical reaction and friction. It is related to, but somewhat different from chemomechanical[3] polishing (CMP or Chemical-Mechanical[4,5] Polishing) or mechanochemical (MCP or Mechanical-Chemical Polishing) polishing known in the semi-conductor industry. CMP and MCP use chemical solutions which are normally pH-controlled water-based basic solutions for the chemical reactions and suspensions of abrasive particles.

The abrasive particles are nanometer size alumina, chromium oxide (Cr_2O_3), silica, diamond, or silica-encapsulated diamond. CMP and MCP require a porous polyurethane polishing pad to hold abrasives during polishing. The presence of abrasives may cause undesirable surface defects such as scratches or cavities. The reported major problem of CMP with abrasives is the surface damage from the abrasives. Tribochemical polishing does not require abrasives and the material removal is entirely chemical, simply stimulated by friction.

Since we utilize chromic acid for the polishing and that chromium is considered harmful for the performance of silicon nitride, the composition of the polished surface is important. In addition, it is often stated that polishing produces a foreign film with different structure (presumably amorphous) and different composition. Thus we considered it important to analyze the properties of the tribochemically polished surfaces. For this purpose, Rutherford Backscattering Spectroscopy (RBS), Secondary Ion Mass Spectroscopy (SIMS), and X-ray photo Electron Spectroscopy (ESCA) were performed to analyze the surface. In RBS, one bombards the sample with ions of known high energy and

measures the energy of the back-scattered ions. The technique measures the composition and thickness of a thin layer on the substrate. Bulk scattering analysis provides the ability to distinguish the atomic masses of elements and their distribution in depth as a function of detected energy. The detection of elements uses the following equation:

$$E_M = K_M \times E_o, \quad K_M = \left(\frac{M-m}{M+m}\right)^2 \qquad (4)$$

where E_M is energy of element M, K_M is constant, E_o is incident beam energy, M is unknown mass element, and m is 4 for He. The RBS measurements were performed by Professor M. J. Kim at Arizona State University. He used a 2 MeV He+ tandem accelerator and a beam collimator with magnetic analyzer. The beam incidence was normal at 200,000 total counts read on a multi-channel analyzer at less than 1% statistical error under 10^{-5} to 10^{-6} torr vacuum pressure. The target spot size was about 1mm and the detection limit was about 0.1 at.%. Three samples were analyzed. The first (designated as Ball #1) was tribochemically polished, dipped in chromic acid for 24 hours and kept in air (transit to Arizona etc.) for 7 days before the RBS measurement. The second sample (marked Plate) was polished, dipped in chromic acid for 48 hours and analyzed after 7 days. The third sample (marked Ball #2) was tribochemically polished and analyzed by RBS after 7 days in air. The purpose of the dipping in chromic acid was to determine if there is a risk of chromium embedding occurring in the tribochemically polished surfaces. Previous to the RBS measurements, the sample marked "Plate" was bombarded by cesium ions in a SIMS experiment. The unavoidable presence of Cs in this surface served as a test for the RBS sensitivity. Figure 20 shows the results. Figures 20(A) to (C) present the detected signal for scattered ion energies from 0.4 to 1.9 MeV. Figures 20(D) to (F) present a magnified picture of the significant data in the energy range from 1.2 to 1.9 MeV. The energies of ions scattered by the elements are 0.5 MeV for C, 0.62 MeV for N, 0.72 MeV for O, 1.03 MeV for Mg, 1.10 MeV for Al, 1.13 MeV for Si, 1.34 MeV for Ca, 1.47 MeV for Cr, 1.50 MeV for Fe and 1.77 MeV for Cs. As shown in Figures 20 (A) to (C), N and Si are clearly visible and the amount of oxygen in the disc which experienced 48 hours dipping in solution is higher than for ball #1 which experienced 24 hours dipping. In ball #2, which was removed immediately after tribochemically polishing, the amount of oxygen is almost undetectable. The variation of the amount of oxygen can be assigned to the thickness of the oxidized surface layer. Figures 20(D) to (F) show the result for trace elements. Fe is clearly visible in all samples and the amount of iron in the disc is higher than in the balls. Fe is a known impurity introduced in the processing of silicon nitride. There is no

trace of Cr which was used as the polishing solution. This demonstrates that the chromic acid as a polishing medium does not remain on the surface as contamination or residual trace material. The peak around 1.75 MeV in the disc can be assigned to Cs introduced by the SIMS experiments. The data also show that dipping in chromic acid produces an oxide layer and that the latter is absent or very thin after tribochemical polishing. This verifies our model according to which the silicon nitride is oxidized by the acid and the oxide is dissolved in the solution.

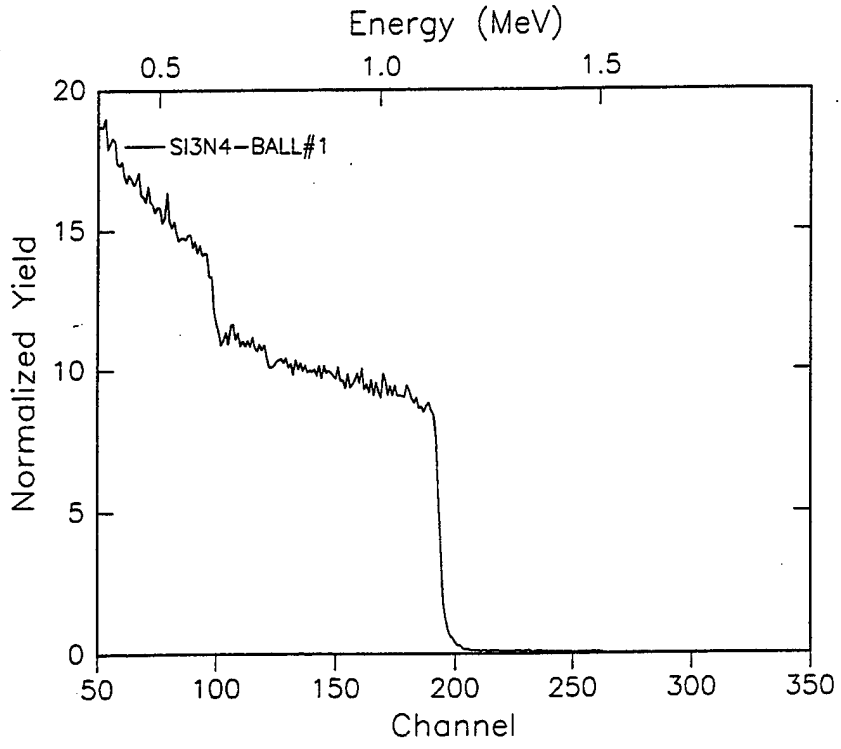

(A)

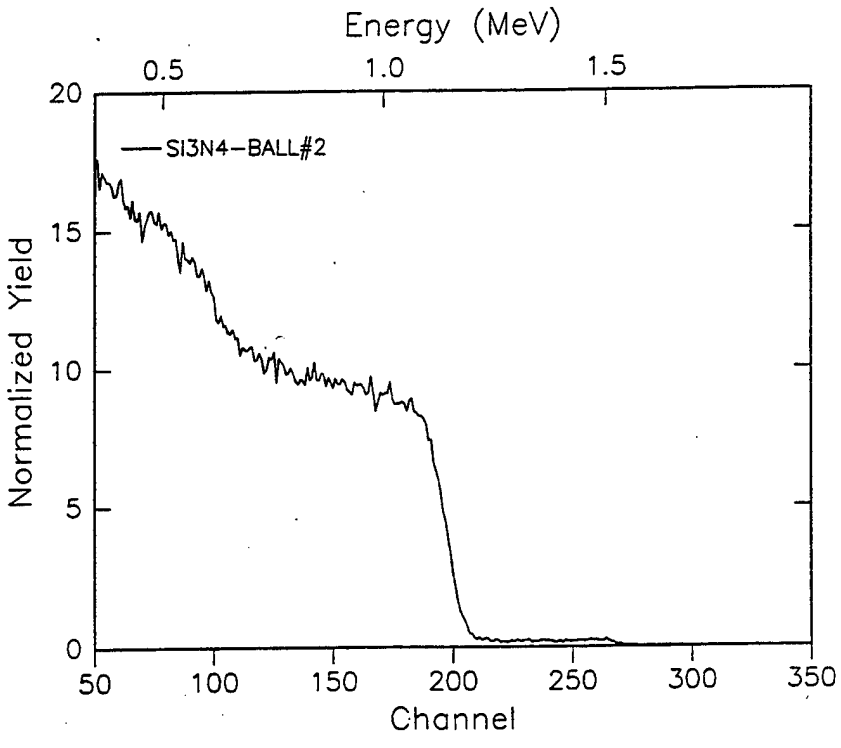

(B)

Figure 20 Rutherford Backscattering Spectroscopy (RBS) measurement of a tribochemically polished 1/4" ball surface in 3 wt.% CrO_3. (A) and (B) detected signal for scattered ion energies are from 0.4 to 1.9 MeV.

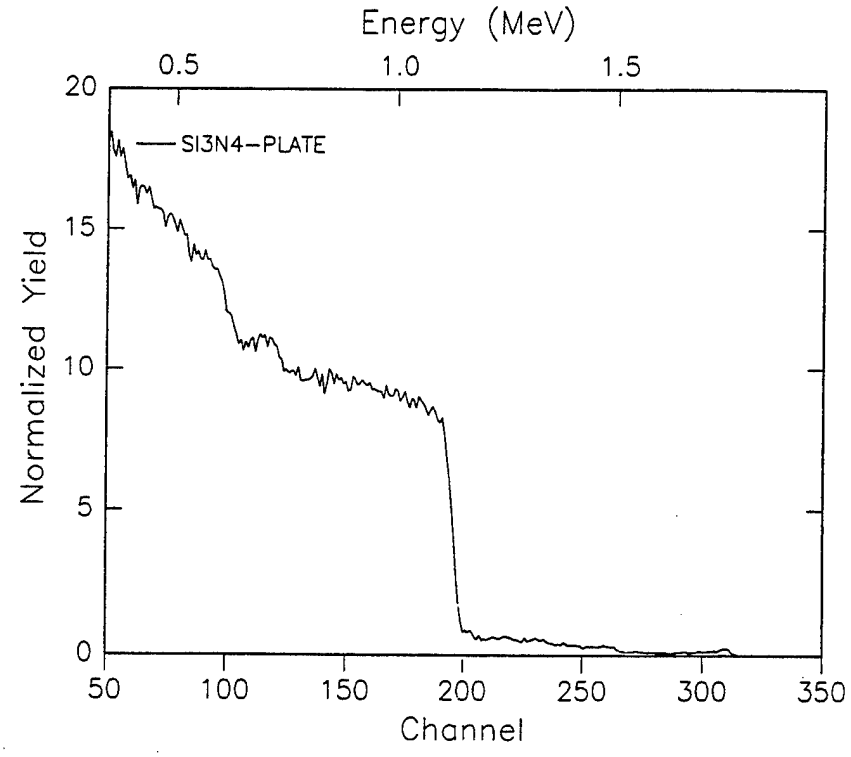

(C)

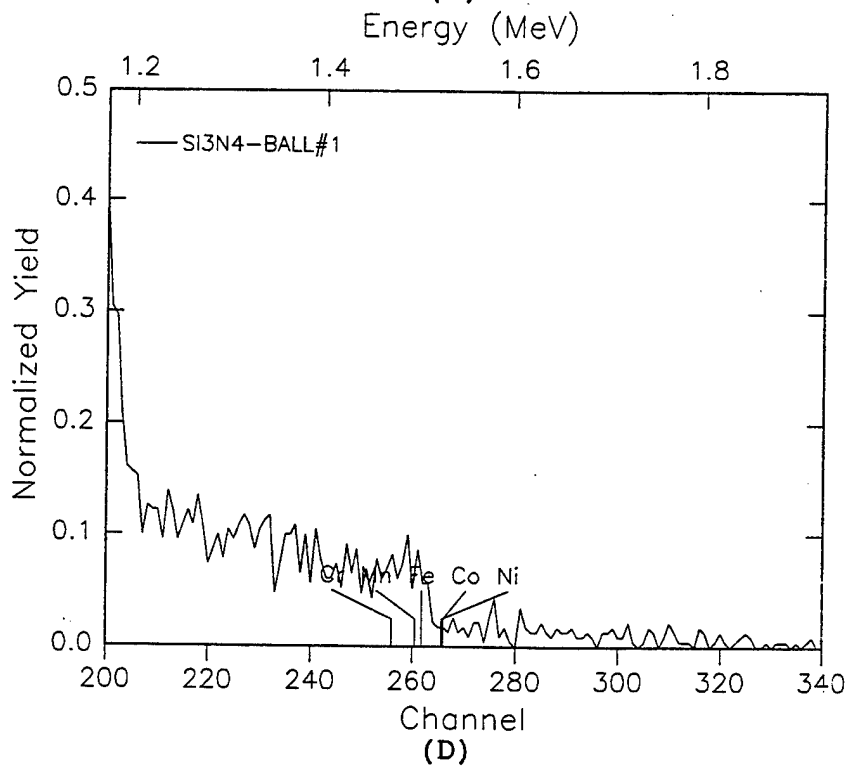

(D)

Figure 20 (continued) Rutherford Backscattering Spectroscopy (RBS) measurement of a tribochemically polished plate and a 1/4" ball surface in 3 wt.% CrO_3. (C) detected signal for scattered ion energies is from 0.4 to 1.9 MeV. (D) is a magnified picture of significant data.

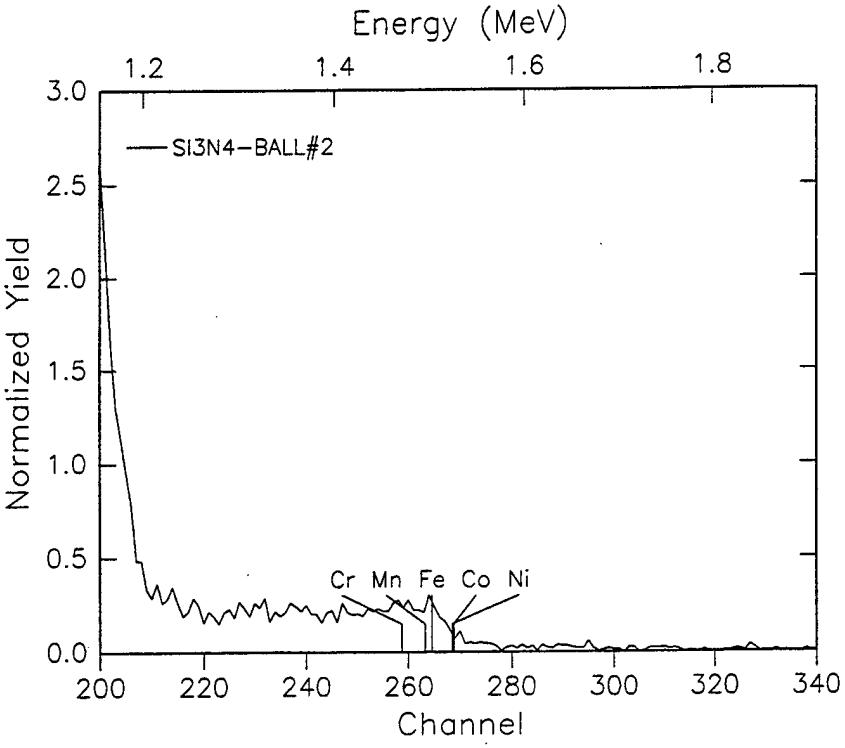

(E)

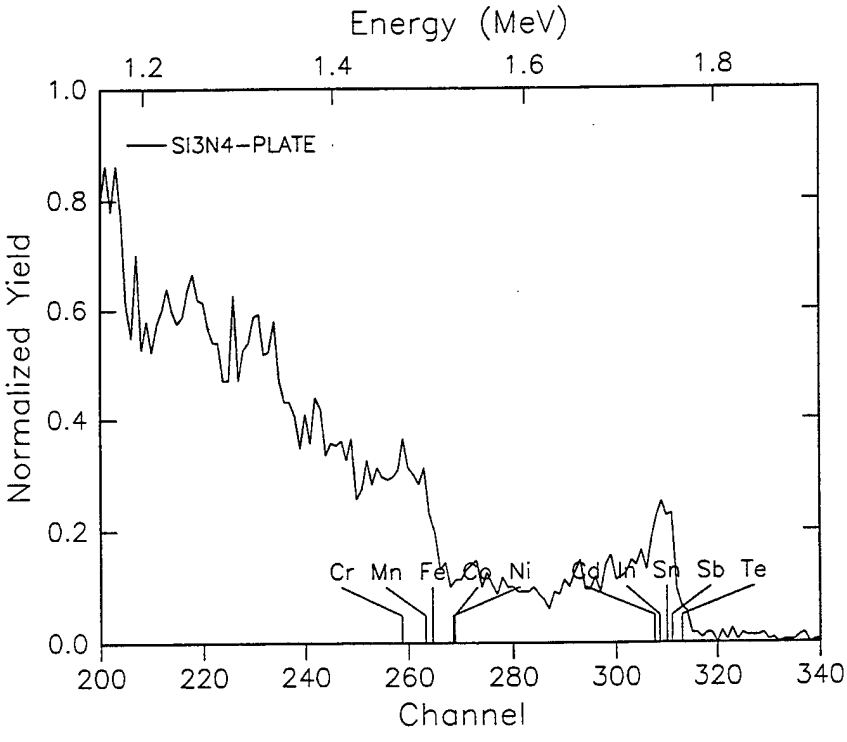

(F)

Figure 20 (continued) Rutherford Backscattering Spectroscopy (RBS) measurement of a tribochemically polished 1/4" ball surface in 3 wt.% CrO_3. (E) and (F) are magnified pictures of significant data.

The most sensitive analysis technique is SIMS. It can detect all elements, including hydrogen, and depth profiling is possible. SIMS is classified by the ion gun types such as positive cesium, argon, and oxygen. For the present investigation, SIMS measurement was performed to search for Cr on the surface. For analytical convenience, a 20mm x 20mm x 3mm disc, instead of a bearing ball, was dipped in chromic acid over 48 hours and analyzed. A Cs^+ ion gun with 500-800 eV kinetic energy and a vacuum pressure of less than 10^{-8} torr were used to enhance the yield of negative secondary ions and to minimize charging effects. The measured sample current was 2-3 μA. Negative secondary ions were detected by quadrupolar mass spectrometer. While the SIMS test was performed, C^-, O^-, Na^-, OH^-, Si^-, N^- and other trace elements were detected. However, no Cr was found. This verifies the absence of residual chromium after tribochemical polishing. Silicon nitride has as excellent oxidation resistance due to the presence of a protective oxide layer. In oxidizing environments, silicon nitride is stable only at very low partial pressures of oxygen, but in air it rapidly forms a silicon oxide layer on the surface. As tribochemical polishing is a simultaneous chemistry and friction process, one can speculate that the reaction is accelerated because the oxide formed on the surface is continuously removed and fresh surface is exposed by friction. One concludes that tribochemical polishing produces a clean silicon nitride surface which, however, will be oxidized in air but not more than a fractured surface would. To verify this speculation, surface analysis was performed before and after tribochemical polishing. Electron spectroscopy for chemical analysis (ESCA), also known as X-ray photoelectron spectroscopy (XPS), is the most effective technique for analysis of the composition of surfaces for all elements except hydrogen, the chemical state of surface species, composition of thin surface layers, and identification of surface layer depth. ESCA is not severely affected by sensitivity variations or matrix effects. The major characteristics of ESCA is to measure the shift of binding energy of core electrons caused by the variation of chemical environments. ESCA analysis was performed to characterize the surface of silicon nitride before and after tribochemical polishing by determining the surface atomic concentration and oxidational state of all detectable elements. One of the as-received 1/4" diameter balls and two tribochemically polished surfaces were analyzed and an air-fractured disc was used as a reference sample.
A Perkin-Elmer 5000 LS instrument was operated with a monochromatic aluminum x-ray source at 600 watts for the surfaces under study and a standard magnesium x-ray source at 400 watts was used for the air-fractured silicon nitride disc. The area analyzed was 0.6 mm diameter for the samples and 1 mm x 3mm for the fractured disc. Emitted electrons were detected at 20°±10° and 60°±10° exit angle. The exit angle is defined as the angle between the sample plane and the electron analyzer lens. Because

the samples were electric insulators, the energies were calibrated by the binding energy of C-(C,H) at 284.6 eV as charge reference. The charge was neutralized by a 5 watt electron flood gun. The samples were examined initially with low resolution survey scans to determine which elements were present. High resolution ESCA multiplex data were taken to determine the atomic concentration and binding energy of the elements of interest. Quantitative analysis was accomplished by using the atomic sensitivity factors for the Perkin-Elmer spectrometer as configured. The approximate sampling depths (3λ) for these experiments were 20Å at 20° exit and 70Å at 65°. Through the preliminary investigation, the surface layer on the silicon nitride samples was found to be too thin to sputter, so angle-resolved ESCA was adopted. High resolution spectra of Si 2p, N 1s and O 1s photoelectrons were obtained and used to calculate the film composition, following the method outlined by Wagner[6] et al (C.D.Wagner, W.M.Riggs, L.E.Davis and J.F.Moulder:pp. 8-22 in Handbook of X-ray Photoelectron Spectroscopy, edited by G. E. Muilenberg, Perkin-Elmer Corp., Eden Prairie, MN,1979).

The atomic fraction of element i was calculated from the equation:

$$C_i = \frac{Ii/Si}{\sum_j (Ij/Sj)} \qquad (5)$$

where I is the area under a spectral peak and S is an areal elemental sensitivity factor. Values for S, determined by the spectrometer manufacturer, of 0.26, 0.43 and 0.67 were used for the Si 2p, N 1s and O 1s photoelectrons, respectively. Figure 21 shows the Si 2p peaks[7] in tribochemically polished surfaces and a commercially lapped ball. The results of the analysis are summarized in Tables 7, 8(A) and (B). Table 7 lists the atomic concentrations as a function of exit angle. Tables 8(A) and (B) are the relative amounts of the silicon and nitrogen species by curve fitting. In all cases, the only elements detected were Si, O, N and C. No Cr was detected on the surface of any sample. All inorganic surfaces that have been exposed to the atmosphere are covered with a certain amount of adsorbed organic material, termed adventitious carbon. The oxygen signal decreased as a function of exit angle indicating the presence of a thin surface layer. Silicon and nitrogen signals increased with exit angle. Insight into the silicon chemistry and chemical state distribution as a function of depth can be derived from the curve fits (Tables 8(A) and(B)) and overlays of the Si 2p spectra collected at different angles.

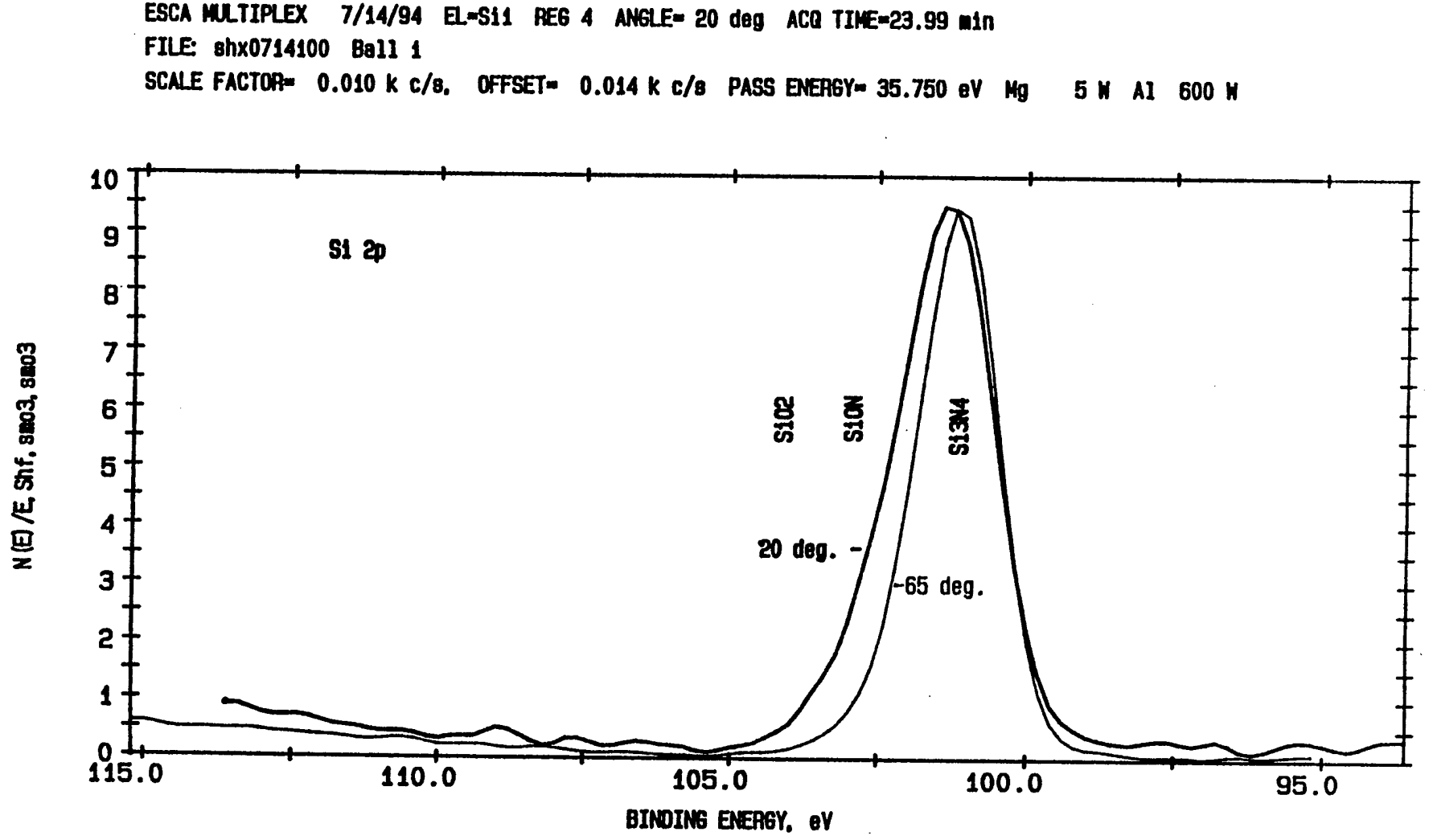

(A)

Figure 21 ESCA analysis of Si 2p peaks: (A) tribochemically polished ball surface.

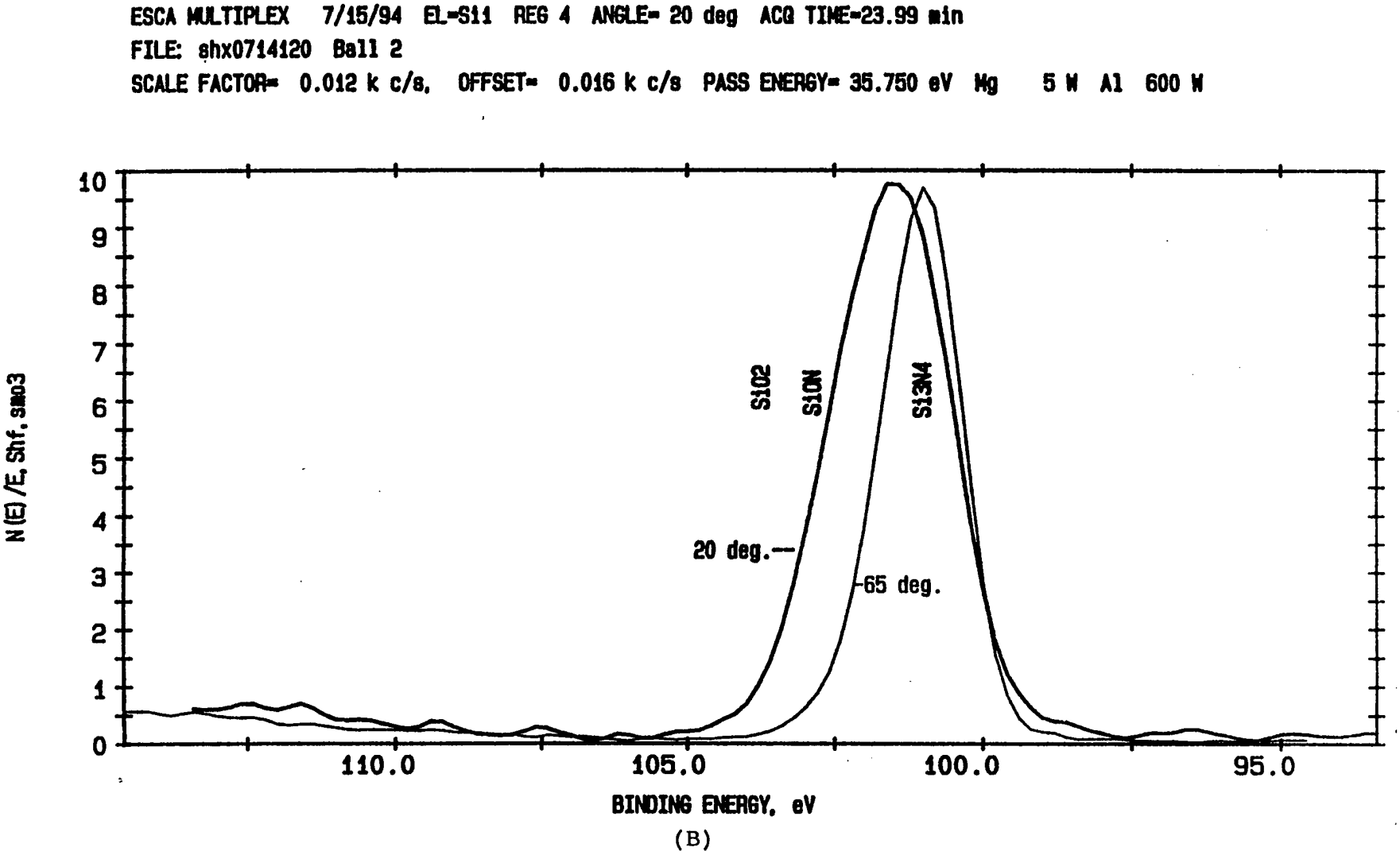

Figure 21 ESCA analysis of Si 2p peaks: (B) tribochemically polished ball (continued) surface.

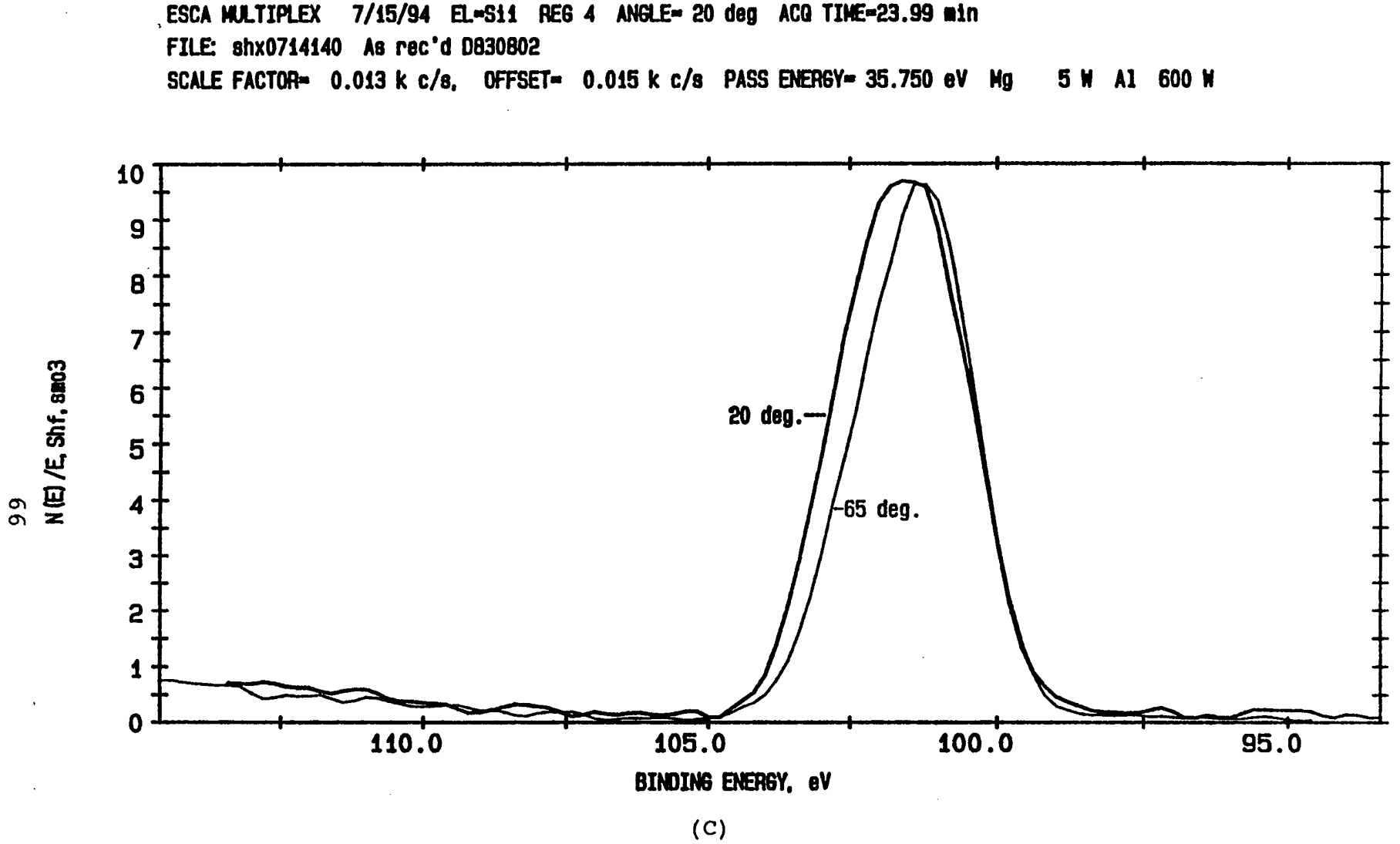

(C)

Figure 21 ESCA analysis of Si 2p peaks: (C) commercially finished ball (continued) surface.

The overlays show that the sample surfaces are enriched with an oxygen-containing species, i.e. SiO_2 and SiO_xN_y. In theory it is possible to determine the SiO_xN_y stoichiometry since we have curve fit the silicon into its three main components and we know the atomic concentration of Si, O, and N. However, the relative sensitivity factors used to calculate the atomic concentrations assume a uniform composition as a function of depth, which clearly is not the case. To determine the exact SiO_xN_y stoichiometry and the layer thickness is virtually impossible due to the complexity of this system. However, we were able to identify three different layers within the top 25 Å: adventitious carbon, SiO_2, and SiO_xN_y on top of Si_3N_4. By comparing the relative amounts of silicon bonded as Si_3N_4 and SiO_2, the relative thicknesses of the oxygen-containing surface layers can be estimated. The oxide layers on the air-fractured disc, and the two tribochemically polished surfaces had very similar thicknesses. The as-received ball has a thicker surface oxide layer. It can be estimated[8] that the total thickness of the surface layers is less than 25 Å on the fractured and tribochemical polished surfaces; this is composed of a monolayer of adventitious carbon, 2-5 Å of SiO_2 as a second layer, 10-15 Å of SiO_xN_y as a third layer and Si_3N_4 substrate. It is generally believed that the natural oxidation layer of silicon nitride at room temperature is no more than 25-30 Å. We can conclude that since the thicknesses of the oxide on the air-fractured disc and on the tribochemically polished surfaces are the same, the tribochemical polishing process does not produce a layer that is chemically different from the substrate silicon nitride and that any oxide layer is subsequently produced by exposure to air.

Table 7.
Atomic Concentration of Detected Elements

Sample	Exit Angle	O	N	Si	C
Tribochemical Surface #1	20°	22.9	7.2	15.7	54.2
	65°	18.7	27.0	26.7	27.6
Tribochemical Surface #1	20°	27.3	6.9	16.1	49.7
	65°	18.6	23.9	24.5	33.0
As-Received 1/4" Diameter Ball	20°	29.4	7.7	17.9	45.0
	60°	29.0	17.7	24.5	28.9
Air Fractured Disc	60°	20.1	22.8	24.8	32.3

Table 8 (A).
Si 2p Curve Fits, Total Percentage of Silicon

Sample	Exit Angle	Si_3N_4	eV	SiO_xN_y	eV	SiO_aN_b SiO_2	eV
Tribochemical Surface #1	20°	72.3	101.2	22.6	102.2	5.1	103.1
	65°	85.3	101.1	13.4	102.0	1.3	103.2
Tribochemical Surface #2	20°	53.0	101.0	41.3	102.1	5.7	103.0
	65°	87.2	101.0	12.1	102.1	0.7	103.5
As-Received 1/4" Diameter Ball	20°	47.1	101.0	42.3	102.1	10.6	102.9
	60°	55.3	100.9	33.9	101.9	10.8	102.8
Air Fractured Disc	60°	78.2	101.5	21.4	102.5	0.4	103.4

Table 8 (B).
N 1s Curve Fits, Total Percentage of Nitrogen

Sample	Exit Angle	N1[a]	eV	N2[b]	eV	C-N	eV
Tribochemical Surface #1	20°	70.8	396.9	14.6	398.1	14.6	399.6
	65°	90.4	397.1	5.7	398.1	3.9	399.8
Tribochemical Surface #2	20°	69.2	396.9	19.0	397.6	11.8	399.2
	65°	91.5	396.9	6.4	397.8	2.1	399.4
As-Received 1/4" Diameter Ball	20°	77.6	396.8	14.2	398.0	8.1	399.5
	60°	92.3	397.0	5.3	397.8	2.4	399.2
Air Fractured Disc	60°	94.9	397.1	2.7	398.4	2.4	399.1

[a] N1 is Si_3N_4 and SiO_xN_y.
[b] N2 is likely a second oxynitride SiO_aN_b, where a>x.

4.1.4 Molecular Analysis

It is thought that tribochemical polishing occurs by the oxidation of the material in water as follows:

$$Si_3N_4 + 6H_2O \xrightarrow{friction} 3SiO_2 + 4NH_3\,(g) \qquad (7)$$

The reacted products form water soluble silicic acid and ammonium hydroxide:

$$SiO_2 + 2H_2O = Si(OH)_4 \qquad (8)$$

$$NH_3 + H_2O = NH_4OH \qquad (9)$$

To identify the chemical reaction as speculated above, chemical titration and micro-Fourier Transformed Infrared Spectroscopy (micro-FTIR) were performed in the tribochemically polished solutions. First, to detect the ammonia, chemical titration by Nessler reagent was performed in some of the solutions used for the tribochemical polishing, namely distilled water, 3 vol.% hydrogen peroxide and so on. The Nessler reagent can be made as follows: Dissolve 50g of potassium iodide in the smallest possible quantity of cold water. Add a saturated solution of mercuric chloride until a faint show of color. Add 400 ml of 50% KOH solution. After the solution has clarified by settling, make up to 1 liter with water, allow to settle and decant. The Nessler reagent is used to detect ammonia in water or solutions. When added to a solution containing ammonia, combined or free, it produces a brown precipitate, $NHg_2I.H_2O$. If the ammoniacal solution is sufficiently dilute, a yellow or reddish-brown color is produced, according to the amount of ammonia present. The representative reaction is as follows :

$$2(2KI, HgI_2) + NH_3 + 3KOH = NHg_2I.H_2O + 7KI + 2H_2O \qquad (10)$$

Figure 22 shows the results of chemical titration in the solutions before and after tribochemical polishing when the same amounts of Nessler reagent were added. The solutions used in tribochemical polishing have a yellow color and the solutions which were not used in tribochemical polishing retain their original appearance. It is concluded that the tribochemical polishing produces ammonia in solution, which verifies the chemical reaction (9). Micro-FTIR reflectance spectroscopy is effective for the identification of molecular species on surfaces.

True transmittance (T) and absorbance (A) of light in a substance are defined as follows :

$$T = \left(\frac{Is}{Io}\right)'_{\nu} \qquad A = -\log_{10}\left(\frac{T}{100}\right) \tag{11}$$

where *Is* is the instrument response function (single beam spectrum) with sample, Io is the instrument response function without sample and v is the frequency.

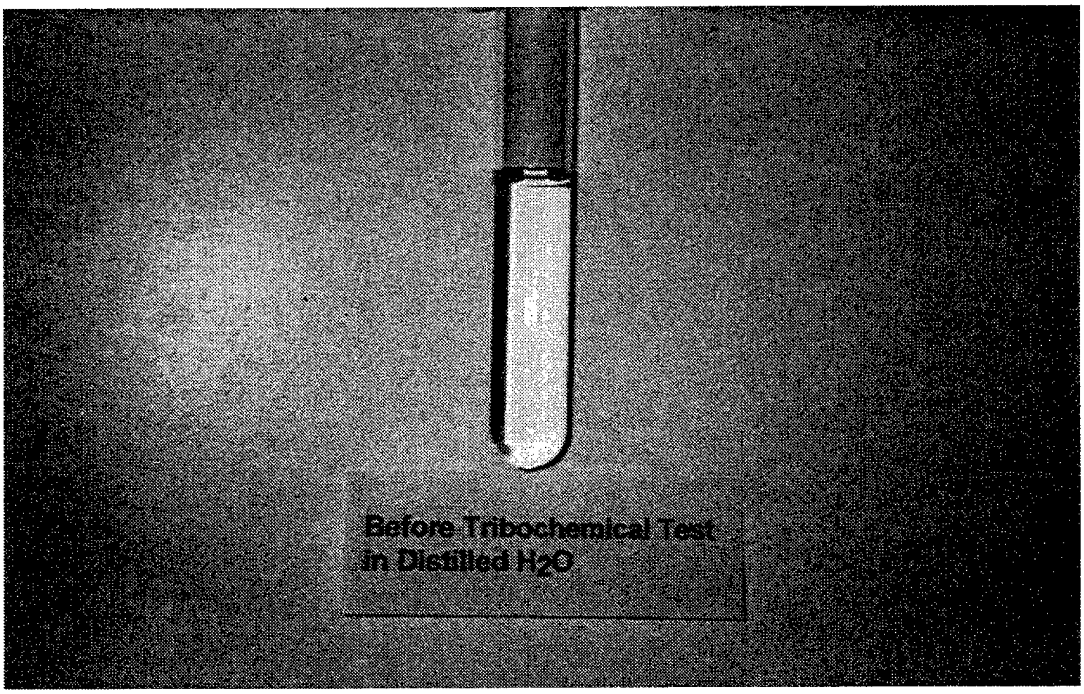

(A)

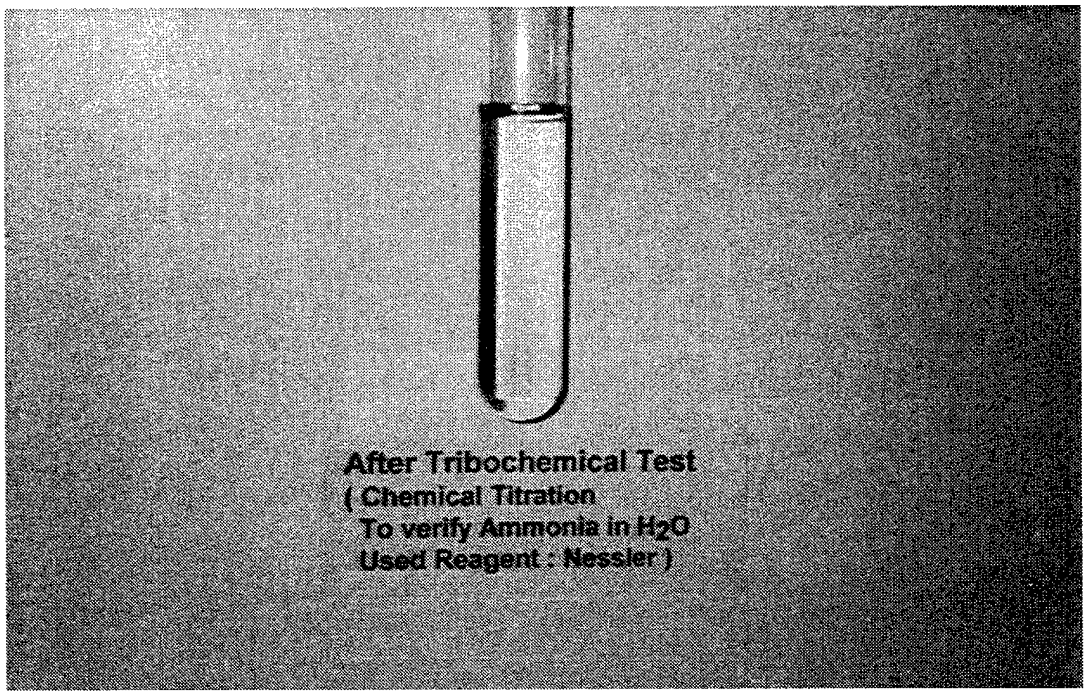

(B)

Figure 22 Chemical titration by Nessler's reagent, before and after tribochemical polishing, to verify the chemical reaction proposed by the present investigators: (A) and (B) in distilled water.

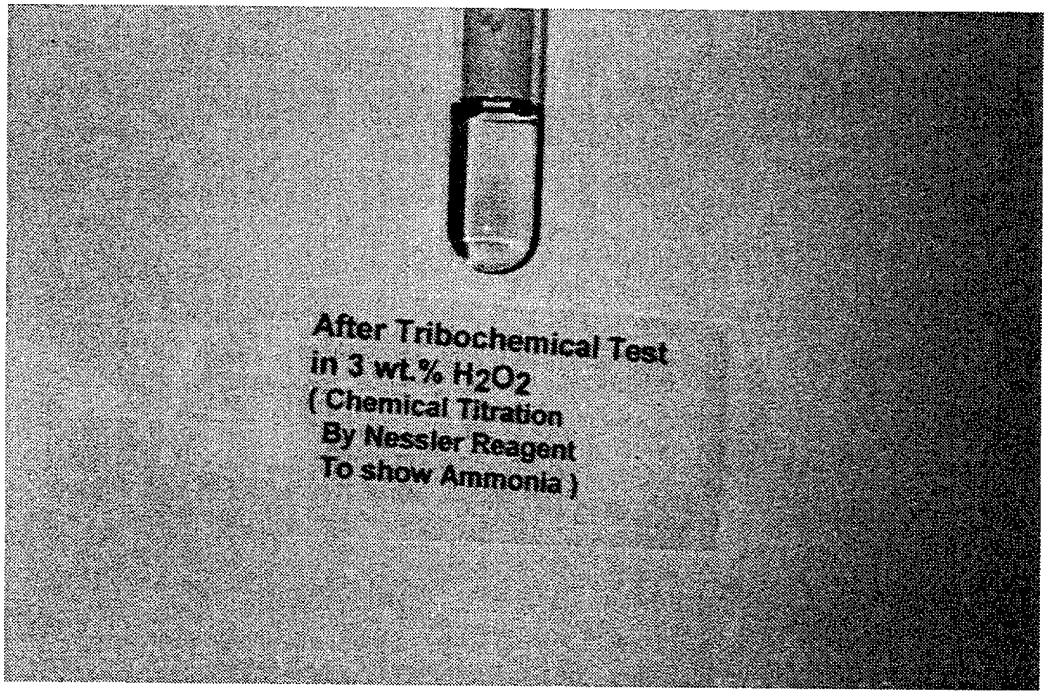

(C)

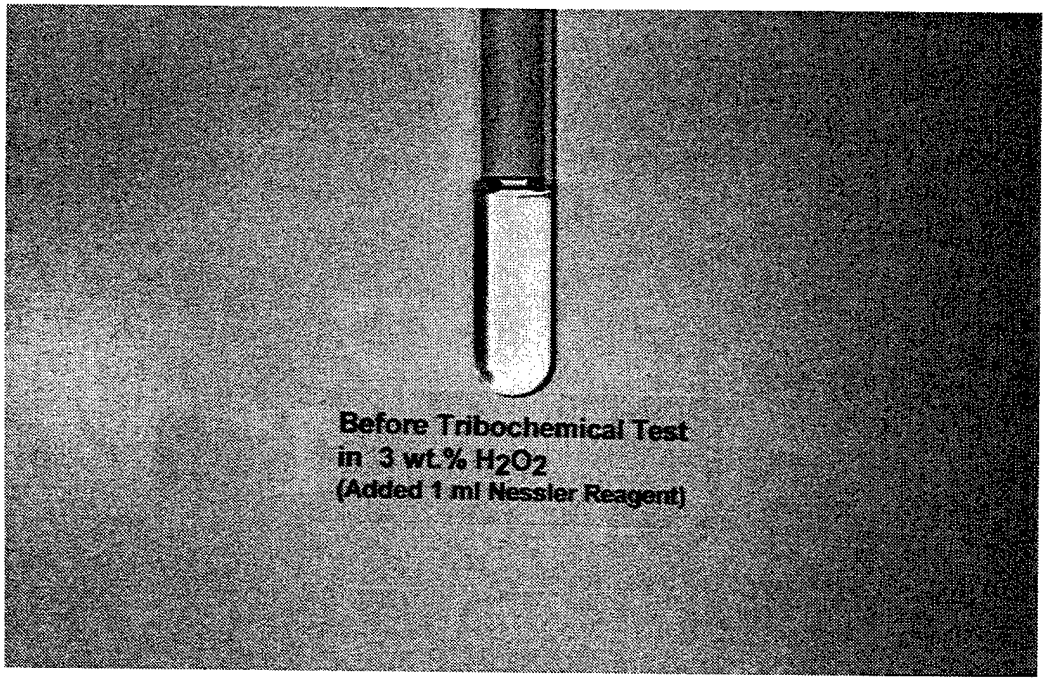

(D)

Figure 22 (continued) Chemical titration by Nessler's reagent, before and after tribochemical polishing, to verify the chemical reaction proposed by the present investigators: (C) and (D) in 3 wt.% hydrogen peroxide.

Micro-FTIR spectra were recorded from 4000 to 400 cm^{-1} by a Nicolet 800 spectrometer. To reduce the noise, up to 300 scans have been averaged. Bearing balls, discs, and chemical solutions before and after tribochemical polishing were measured with KBr crystal as a beam splitter for mid-IR, Mercury Cadmium Telluride (MCT-A) detector for the reflectance mode and 4 cm^{-1} resolution. Figures 23(A, B) show the results of micro-FTIR of a 30 vol.% hydrogen peroxide solution before and after tribochemical polishing. Figure 23(A) shows the FTIR data of a commercially lapped silicon nitride disc. The surface consists of silicon oxide and hydrated silica. The high intensity at 1211 cm^{-1} and very weak peak at 1589 cm^{-1} can be assigned to asymmetric Si-O-H bonding characteristic of hydrated silica ($SiO_2.xH_2O$). The sharp peak at 1026 cm^{-1} and weak peak at 1080 cm^{-1} present symmetric Si-O bonding. The peak at 847 cm^{-1} indicates an asymmetric Si-N stretching bond of β-Si_3N_4. The peak at 940 cm^{-1} can be assigned either to an asymmetric stretching bond of Si-N-Si or Si-O-Nx. Figure 23(B) is the spectrum from pure 30 vol.% hydrogen peroxide solution on a silicon nitride plate and (C) is the same solution's data after tribochemical polishing. The strong and sharp peaks at 3848 cm^{-1} correspond to O-H stretching vibrations and the peak at 1640 cm^{-1} is a mixture of bending O-H and hydrogen peroxide. The peak at 1430 cm^{-1} indicates O-H in-plane deformational vibrations.

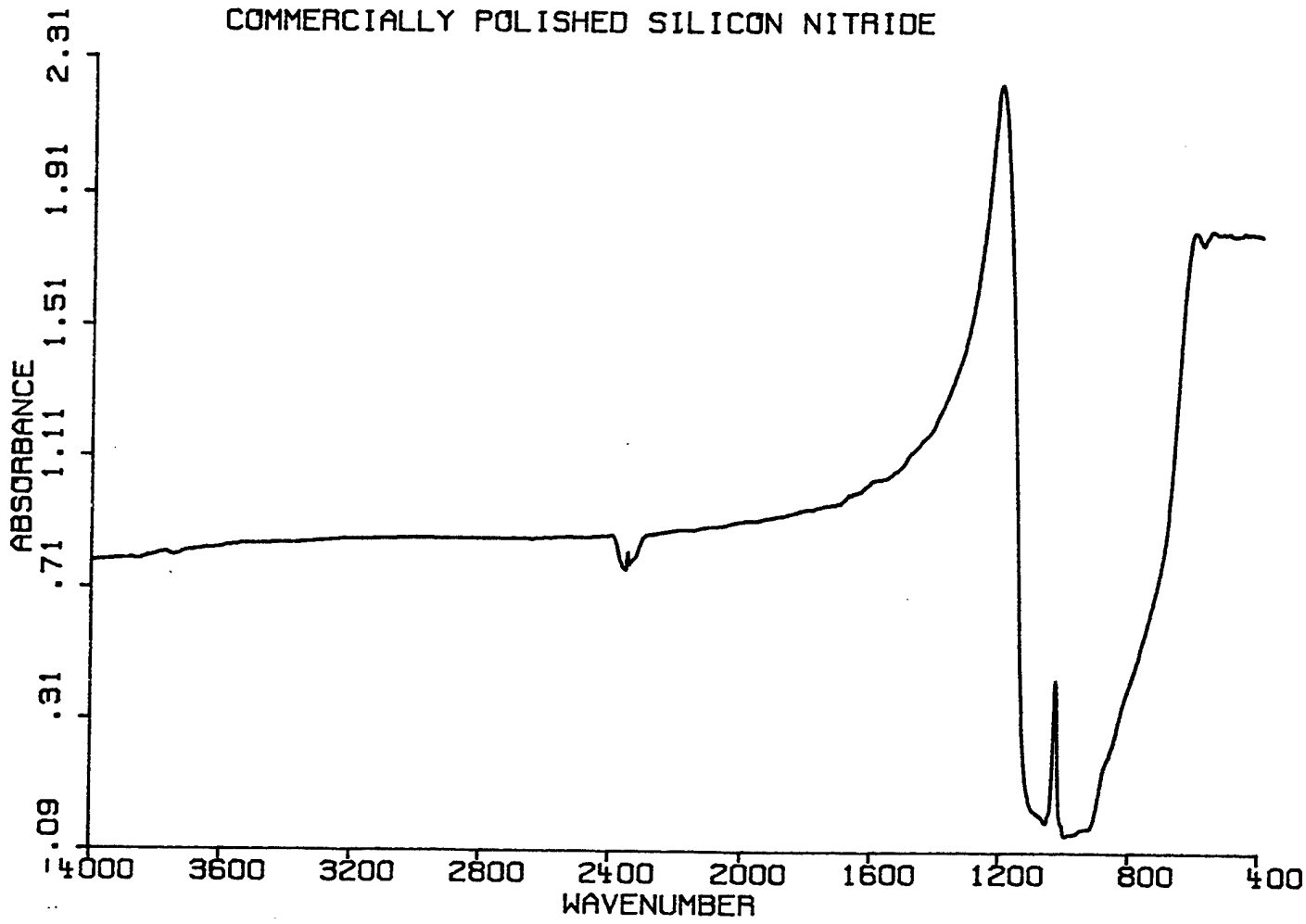

(A)

Figure 23 Micro-Fourier Transformed Infrared Spectroscopy (micro-FTIR) measured result of a 30 vol.% hydrogen peroxide solution on: (A) a commercially polished silicon nitride disc.

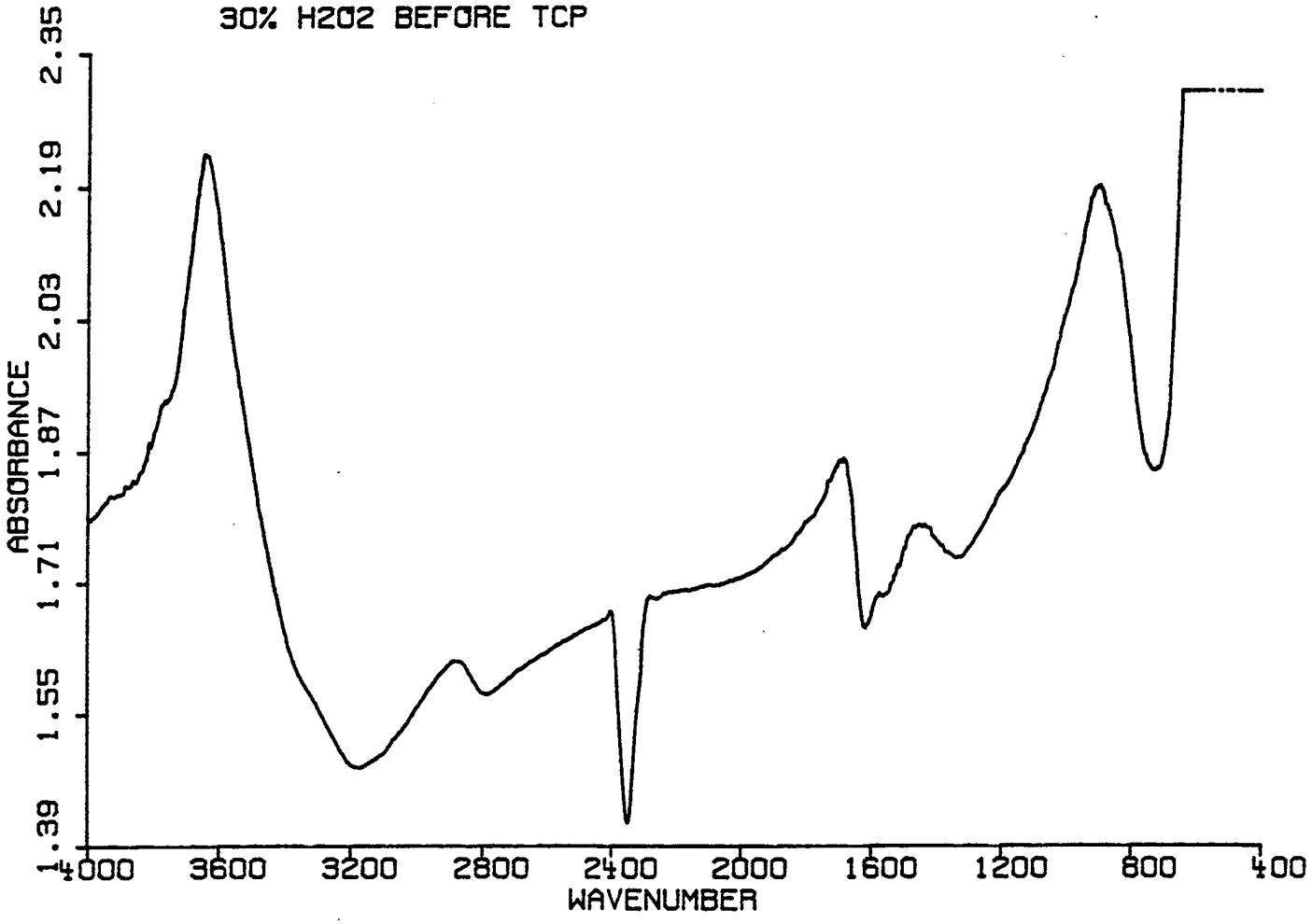

(B)

Figure 23 (continued) Micro-Fourier Transformed Infrared Spectroscopy (micro-FTIR) measured result of a 30 vol.% hydrogen peroxide solution on: (B) an unpolished silicon nitride disc.

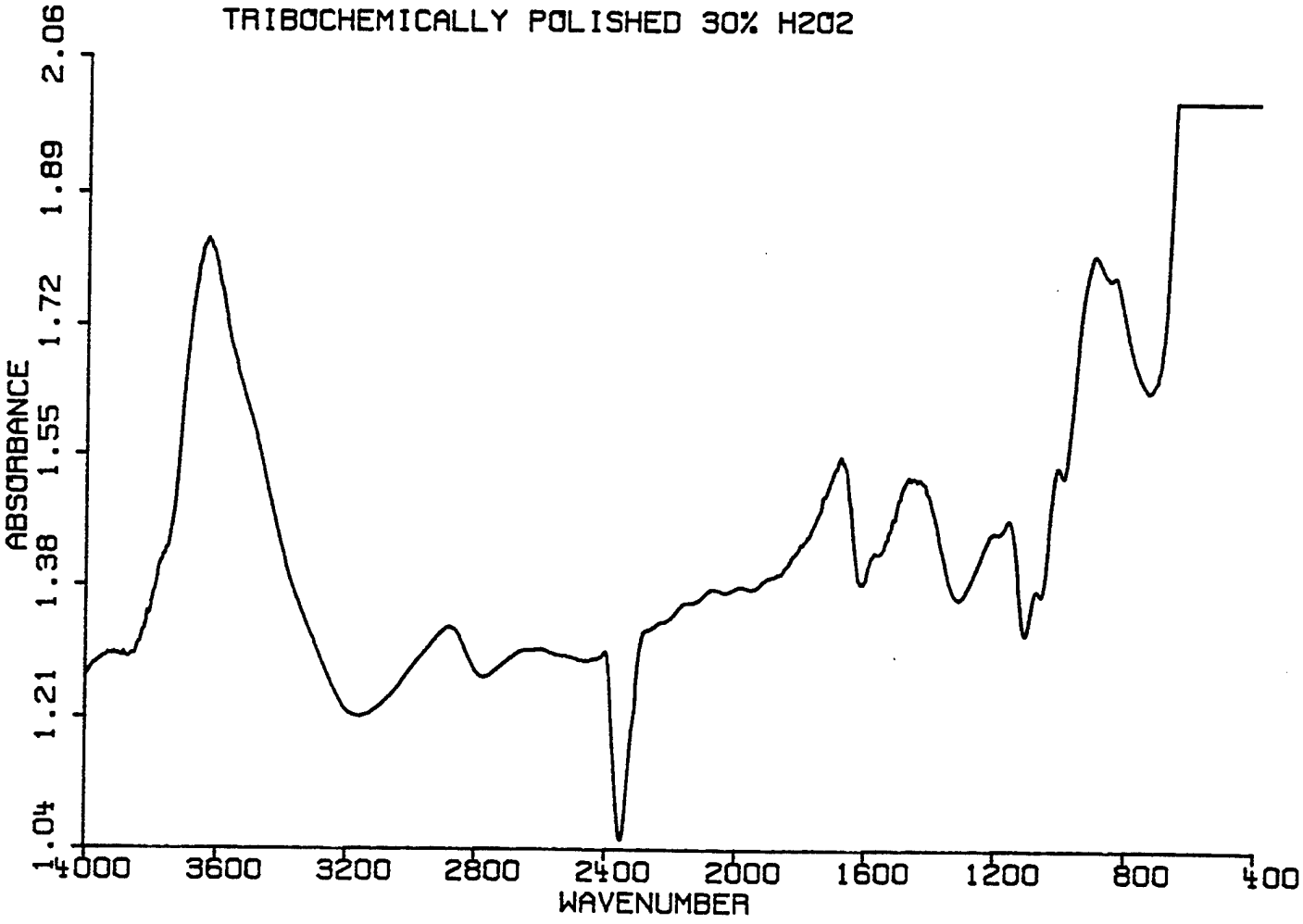

(C)

Figure 23 (continued) Micro-Fourier Transformed Infrared Spectroscopy (micro-FTIR) measured result of a 30 vol.% hydrogen peroxide solution on: (C) a tribochemically polished silicon nitride disc.

The peaks at 3360 cm^{-1}, 2780 cm^{-1} and 1640 cm^{-1} are the absorption bands of hydrogen peroxide. The peaks at 1576 cm^{-1} and 1204 cm^{-1} indicate asymmetric Si-O-H bonding of hydrated silica. The peaks below 1080 cm^{-1} indicate Si-O, Si-N and/or Si-O-N_x. Subtracting Figure 23(C) from (B) leaves two peaks at 3500 cm^{-1} and 1170 cm^{-1}. The residual peak at 3500 cm^{-1} can be assigned to asymmetric stretching vibrations (v3) of the ammonium tetrahedral cation (NH_4^+) and the peak at 1170 cm^{-1} can be assigned to symmetrical bending vibration modes of N-H. As the specific peaks at 3500 cm^{-1} and 1170 cm^{-1} are only detected from the tribochemically polished 30 vol.% H_2O_2 solution, the presence of ammonia in the solutions is verified through micro-FTIR and chemical titration.

4.1.5 Exploration Tribochemical Polishing Mechanisms

We have proposed earlier that the tribochemical polishing mechanism in aqueous solutions occurs by simultaneous chemical reaction of excess oxygen and removal of the nascent SiO_2 scale by friction as shown in the following equations:

$$Si_3N_4 + 6H_2O \xrightarrow{friction} 3SiO_2 + 4NH_3(g) \quad (12)$$

$$SiO_2 + 2H_2O = Si(OH)_4 \quad (13)$$

$$NH_3 + H_2O = NH_4OH \quad (14)$$

Tables 9 and 10 show the thermodynamics of some relevant chemical reactions of silicon nitride at room temperature (25°C) and at 100°C.

Table 9.
Thermodynamics of Si_3N_4 Reactions at 25°C

Chemical reaction	ΔH (Kcal)	ΔG (Kcal)	K
$Si_3N_4+3O_2(g)=3SiO_2+2N_2(g)$	-475.1	-459.4	$1.000x10^{+308}$
$Si_3N_4+6H_2O_2(l)=3SiO_2+4NH_3(g)+3O_2(g)$	-249.7	-302.5	$5.700x10^{+221}$
$Si_3N_4+6H_2O(l)=3SiO_2+4NH_3(g)$	-109.1	-135.0	$9.018x10^{+098}$

Table 10.
Thermodynamics of Si_3N_4 Reactions at 100°C

Chemical Reaction	ΔH (Kcal)	ΔG (Kcal)	K
$Si_3N_4+3O_2(g)=3SiO_2+2N_2(g)$	-474.9	-455.4	$5.758x10^{+266}$
$Si_3N_4+6H_2O_2(l)=3SiO_2+4NH_3(g)+3O_2(g)$	-254.3	-315.2	$4.351x10^{+184}$
$Si_3N_4+6H_2O(l)=3SiO_2+4NH_3(g)$	-113.9	-140.9	$3.533x10^{+082}$

The proposed reactions are strongly exothermic and their equilibrium constants "K" are very high. Thus, two questions arise:

1). What is the slow step in this reaction?

2). Which step is accelerated by friction?

Because oxidation is exothermic and is classically limited by the oxide scale, we conclude that the tribochemical acceleration resides in the removal of the SiO_2 as it is formed. Experiments have shown that the tribochemical reactions are faster in hydrogen peroxide than in water. This is an indication that the slow step is the oxidation of the silicon nitride. The reaction with hydrogen peroxide is more exothermic and has been seen above to be more rapid than with water. Hydrogen peroxide is an unstable oxidant. The instability of hydrogen peroxide with respect to decomposition into water and oxygen is due to its simultaneous ability to oxidize and to reduce itself. Although the exact positions of the hydrogens are not known, it appears that one is associated with each oxygen at a bond angle of 101.5° (96° 52' for liquid state hydrogen peroxide) that the other lies at a 106° (93° 51' for liquid state) angle to each other in the case of crystalline form. In aqueous solutions, hydrogen peroxide is more acidic than water. The oxidation of hydrogen peroxide in acidic solutions is faster than in alkaline solutions. In combination with certain organic materials, it yields highly explosive mixtures. Chromic (VI) acid (CrO_3) is hygroscopic and has large solubility in water. In the range of temperature from 0°C to 100°C, the solubility in water varies from 61.70 wt.% to 67.46wt.%. Silicon and silicon nitride are not attacked by chromic acid. Chromate (VI) ions are polymerized; the degree of polymerization depends on pH and can be classified by the color: Yellow corresponds to chromate ($HCrO_4^-$), orange to dichromate ($HCr_2O_7^-$), red to trichromate ($Hcr_3O_{10}^-$), and brown to tetrachromate[9] ($HCr_4O_{13}^-$). As the color becomes darker, the pH and the degree of polymerization increase. The orange color of 3 wt.% chromic acid means that the chromate ion is $Cr_2O_7^{-2}$. The

role of chromic acid in the polishing is still somewhat of a mystery. It does not accelerate the material removal rate but increases the surface quality, which means that it suppresses the mechanical form of wear.

4.2 Exploration of Tool Materials

The results of tribochemical polishing in various aqueous solutions suggested some suitable polishing media, such as hydrogen peroxide, chromic acid, chromates, and nonahydrated iron nitrate, which gave perfectly smooth and ultraflat surfaces. For the selection of tool materials, the following arguments were used: Since chromic acids and chromates give good surface qualities, stainless steels containing high chromium concentrations, such as 440C stainless steel, can be considered as promising tool materials. Nonahydrated iron nitrate also gave good surface quality, so cast iron might be considered as a promising candidate. 440C stainless steel and ASTM class 25 grey cast iron were selected and shaped as tool materials. Alumina and oxidized silicon nitride were also evaluated in order to explore whether the chemical considerations above are relevant. Tables 11 and 12 show the chemical and mechanical properties of these materials. The silicon nitride disc was oxidized at 1100°C during 12 hours in room air; heating and cooling rates were kept at 200°C/hour in order to prevent cracking due to rapid degassing. Figure 24(A, B, C) shows material removal, friction coefficient, and polishing rate (or wear rate) in various tool materials. Figure 24(B) indicates friction coefficients. Figure 25(A) shows the microstructure of a candidate tool material, ASTM class 25 grey cast iron[10], used before tribochemical polishing. As shown in Figure 25(B), the thickness of the oxidized layer on silicon nitride was about 2.8μm, which was sufficient for one tribochemical polishing process. We have used the various tool materials without giving them a high polish. We have relied on the movement and rotation of the surfaces to be polished in order to even out the effect of surface roughness and obtain a good polish on the silicon nitride. This is easily achieved because the role of the rubbing tool is not to remove material directly but only to stimulate the tribochemical reaction. The most favorable tool materials investigated in the study were ASTM class 25 cast iron and 440C stainless steel. Since tribochemical finishing uses the simultaneous action of mechanical friction and chemical action to remove material at asperity contacts, almost any tool material of reasonable stiffness and rigidity could be used.

Table 11.
Specifications of Alumina Tool Materials

Code	Dopant Concentration (ppm)	Grain Size (m)	Hardness (Hv)
1104	500 MgO	0.68	2000±50
1318	500 MgO+1500Y_2O_3	0.68	2000±50

Table 12.
Specifications of Metallic Tool Materials

Item		440C Stainless Steel	Grey Cast Iron
Chemical Composition (wt.%)	C	1.02	3.07
	Si	0.41	2.21
	Mn	0.71	0.78
	P	0.022	residual
	S	0.003	0.054
	Mo	0.46	residual
	Ni	0.44	residual
	Cr	16.39	residual
	Cu	0.098	0.112
Classification		Isothermally Annealed	ASTM Class 25
Hardness		H_{RC}=25±1 H_B=229/235	H_B=201-207

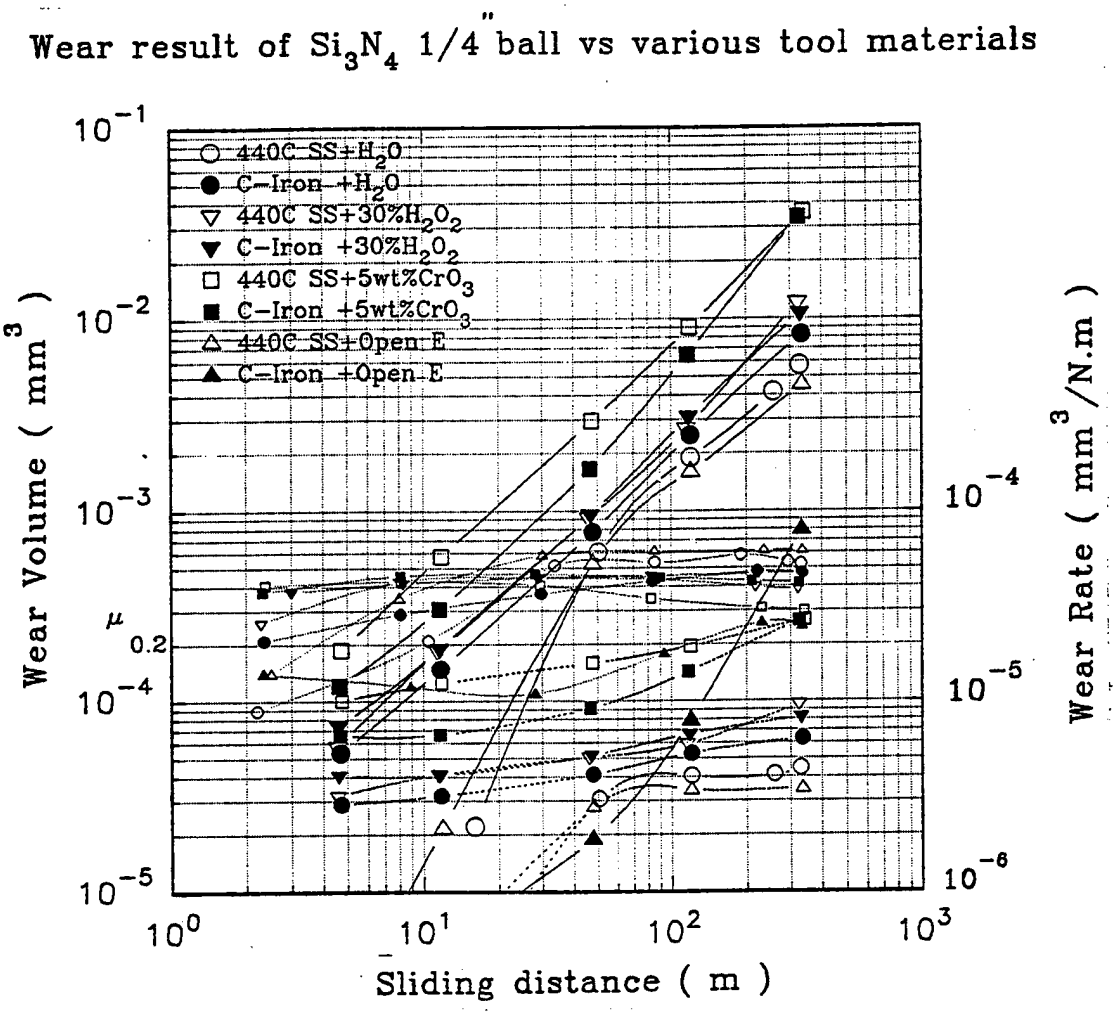

(A)

NOTE: "Open E" indicates the following conditions: without the use of a lubricant, at a temperature of 20±5°C and a Relative Humidity of 40 to 60%.

Figure 24 Material removal, friction coefficient, and polishing rate for tribochemically polished surfaces with tool materials used as counter pieces: (A) 440C stainless steel and ASTM class 25 grey cast iron.

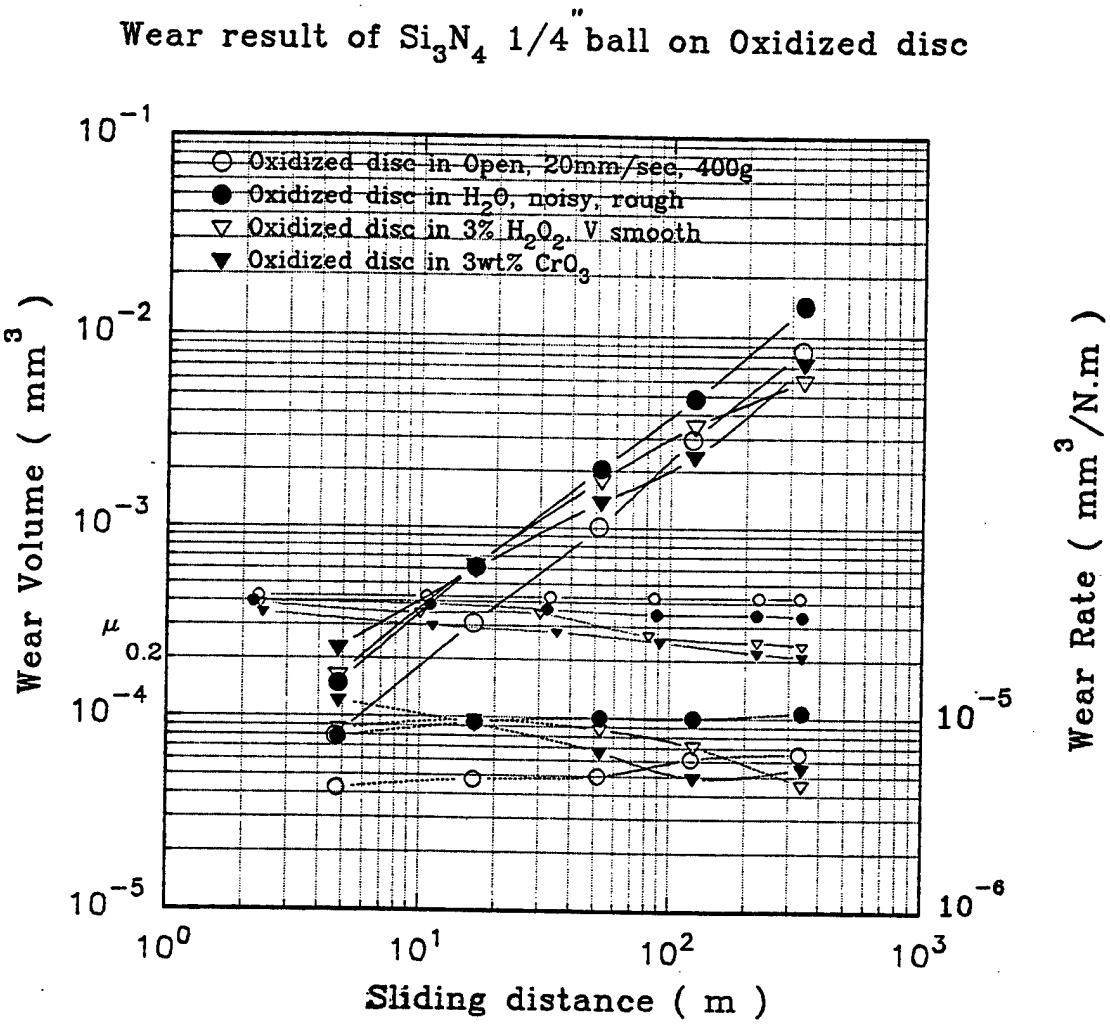

(B)

NOTE: "In Open" indicates the following conditions: the use of a lubricant, at a temperature of 20±5°C and a Relative Humidity of 40 to 60%.

Figure 24 (continued) Material removal, friction coefficient, and polishing rate for tribochemically polished surfaces with tool materials used as counter pieces: (B) oxidized silicon nitride disc.

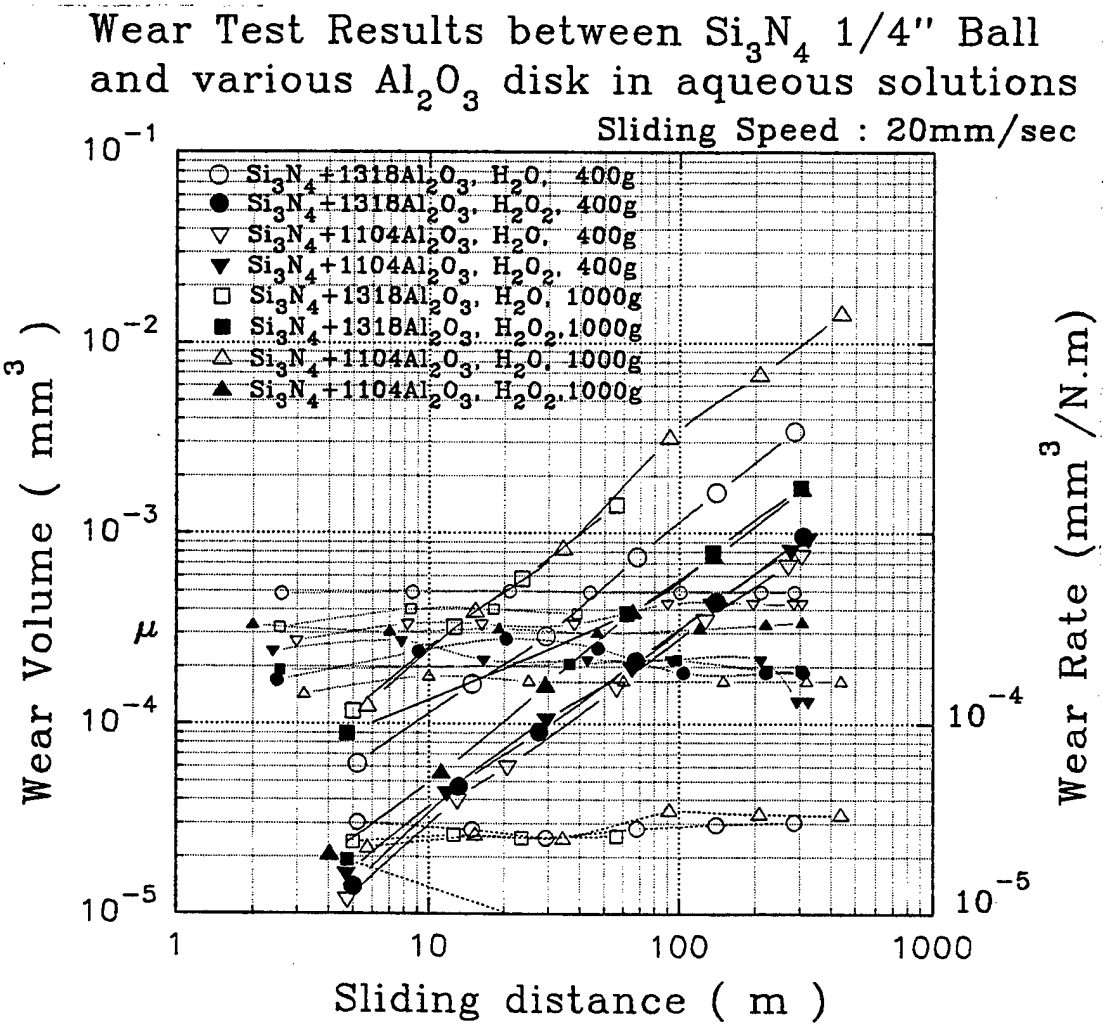

(C)

Figure 24 (continued) Material removal, friction coefficient, and polishing rate for tribochemically polished surfaces with tool materials used as counter pieces: (C) highly purified alumina.

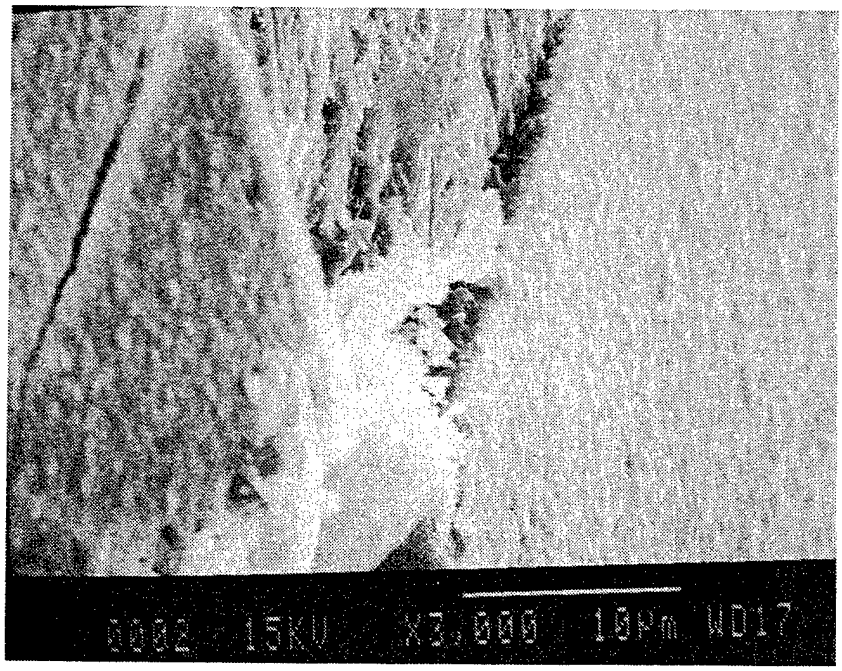

(A)

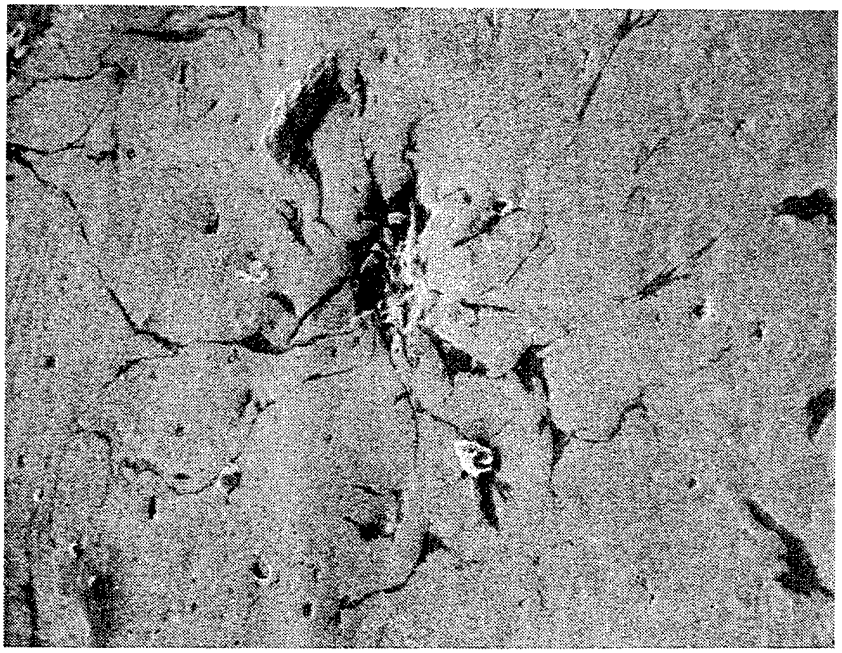

(B)

Figure 25 Surface morphology by SEM in: (A) ASTM class 25 grey cast iron (350x, tilting = 45°) and (B) Oxidized silicon nitride (3,000x, tilting = 62.2°, thickness of oxidized layer is about 2.8μm.

Figure 26 shows the surface qualities of the silicon nitride samples polished with the help of the different tool materials. Generally, the surfaces are quite smooth even when the metallic surface was rough. The grainy roughness on Figure 26(C) is surface contamination.

4.3 Producing Flat Surfaces With the Tribochemical Polishing Method.

The exploration has shown that it is possible to obtain silicon nitride surfaces with extremely high polish and a lack of surface defects with the use of several different oxidizing fluids and metallic or ceramic counter surfaces. The next task is to produce larger flat lapped surfaces. For this purpose, larger, rigid versions of the pin-on-disc apparatus were designed and built. Six inch (150 mm) diameter rotating discs of 440C stainless steel and ASTM class 25 cast iron were fabricated. As above, no special care was taken to polish the surfaces of the metallic discs. A modified sample holder was designed and built to adapt the attitude of the sample to the disc surface even when the latter was not precisely true.

Silicon nitride rectangular plates 22mm x 34mm x 3mm (0.873 in x 1.350in x 0.119in) were provided by Norton Advanced Ceramics.

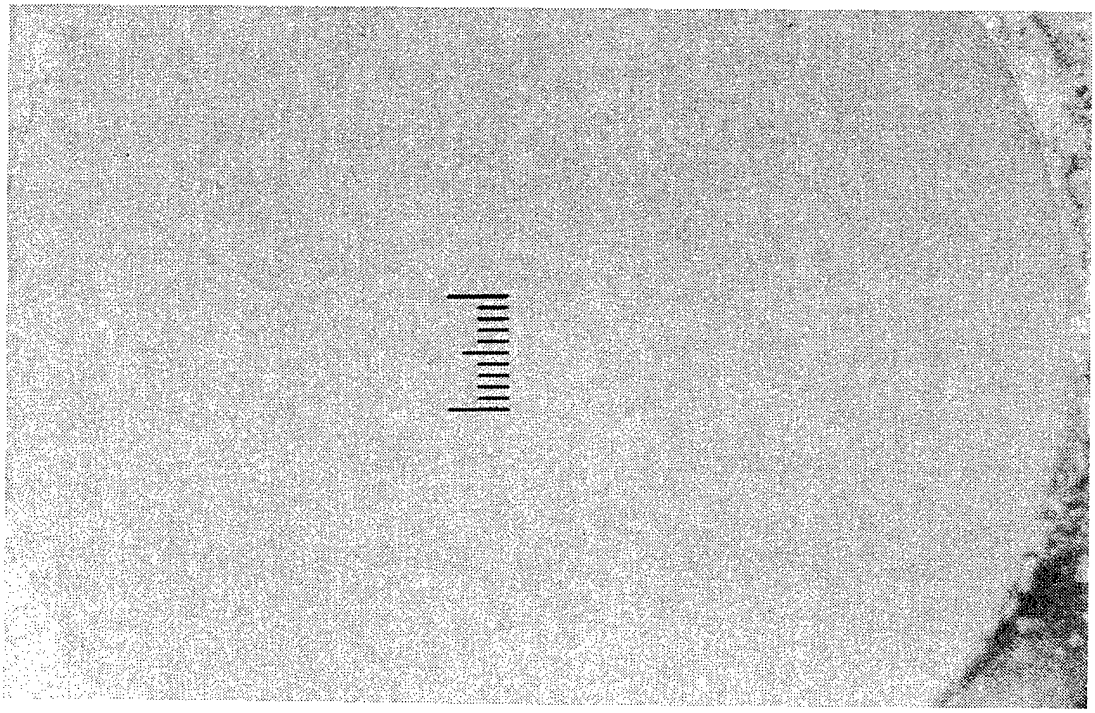

(A)

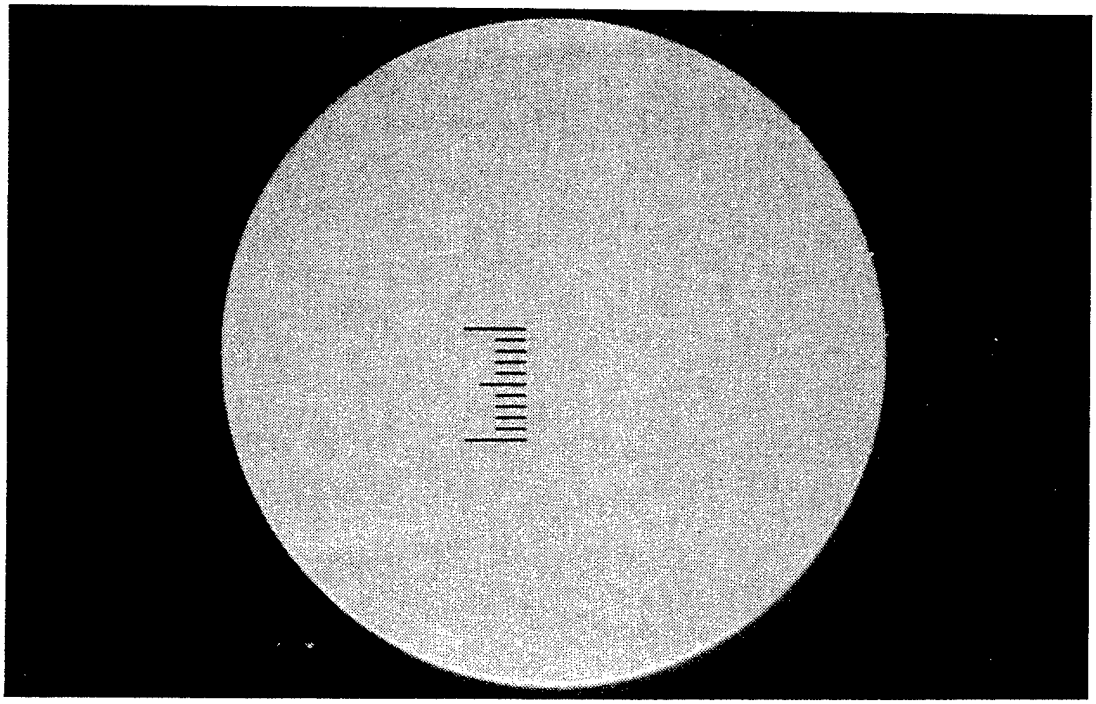

(B)

Figure 26 Surface qualities of tribochemical polished samples with different counter tool materials: (A) 1104 alumina in a 3 vol.% H_2O_2, 3.92 N, x200, 20mm/sec, at 300m. (B) 440C stainless steel in 5 wt.% C_rO_3, x50, 20mm/sec, at 340m.

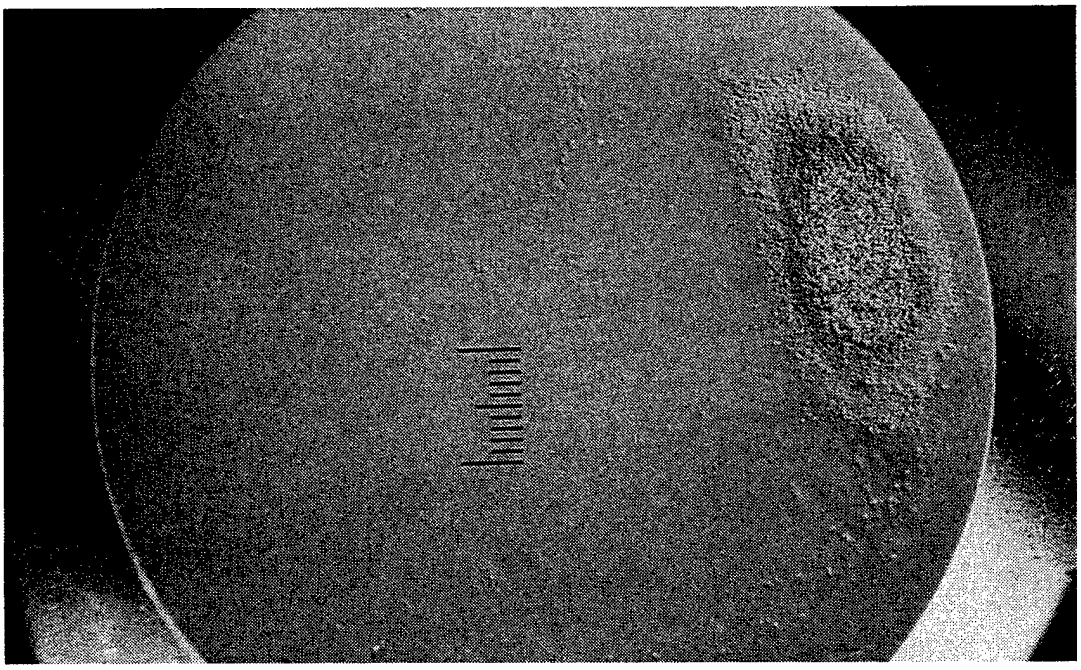

(C)

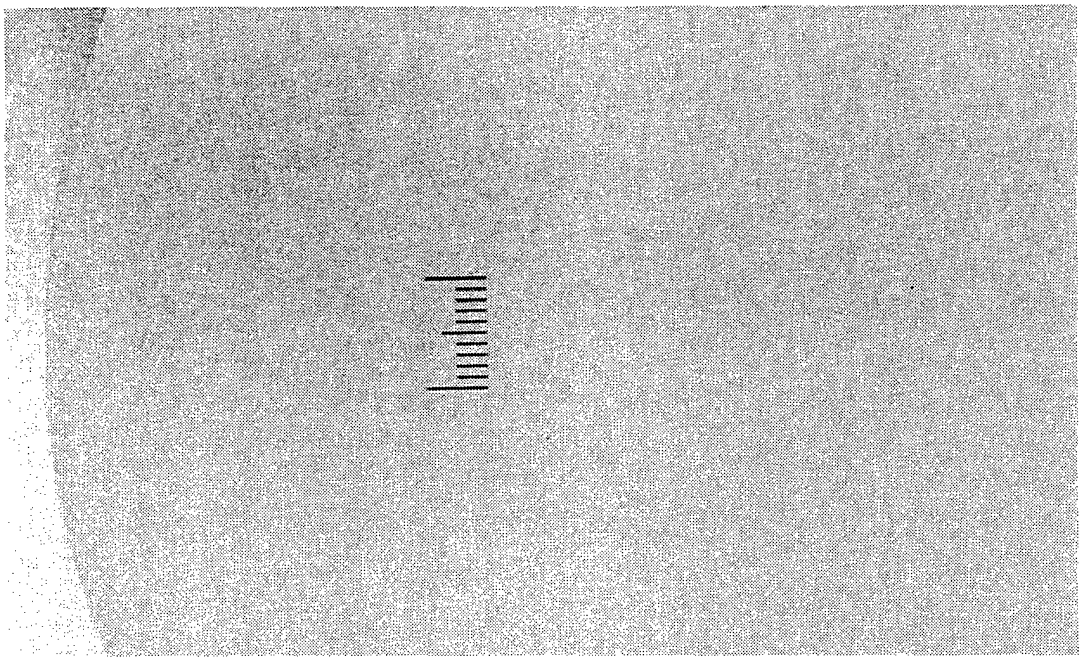

(D)

Figure 26 (continued) Surface qualities of tribochemical polished samples with different counter tool materials: (C) ASTM class 25 grey cast iron in 5 wt.% CrO_3, x100, 20mm/sec, at 116m. (D) oxidized silicon nitride disc in 3 wt.% CrO_3, 200x, 20mm/sec.

They were polished in the larger machines, using stainless steel and cast iron discs as tools. The fluids were hydrogen peroxide and chromic acid because of the superior surface quality they produce.

When the surface polish is good enough, hydrodynamic lubrication is established even with a low sliding speed and high load in the low viscosity of aqueous solutions. When this occurs, the surfaces are separated by a fluid film, the sample slides with a vanishing friction coefficient, and material removal (wear) ceases. This well known fact has baffled many researchers in the measurement of wear rates of silicon nitride. The rotating speed of the discs and load on the samples were selected in a way to provide fast enough material removal to prevent hydrodynamic lubrication.

It is a characteristic of the present configuration that the tribochemical surfaces are extremely flat. This is at the same time an advantage and a limitation of the process, depending on the application. The surface roughness of the large samples has been measured by Talysurf profilometer and atomic force microscopy. Figure 27(A) is a profilometer trace of one (22mm x 34mm x 3mm) rectangular plate. An Ra of 4 to 6 nm (0.016 μin to 0.024 μin) was measured with cutoffs of 0.8 and 8 mm. We believe that this is a measure of the macroscopic curvature and not of microscopic roughness. This Ra compares favorably with that of a silicon wafer polished by Chemomechanical Polishing (CMP) in the semiconductor[11] industry as shown in Figure 27 (B). Such a wafer, provided by IBM, which is considered of the highest quality, suitable for IC chip processing, measured an Ra of 4 to 6 nm (0.016 μin to 0.024 μin) over the cutoff lengths of 0.8 and 2.5 mm. In a cut-off length of 8mm and 25 mm, the Ra of the wafer is 6 to 12 nm (0.024 to 0.048 μin). In other words, the planarity of the tribochemically polished silicon nitride is better. Consider that this result was achieved with a very simple machine, at room temperature and in one step.

The material removal rate was sufficient to allow the total polishing, in one step of a 22mm x 34mm x 3mm sample in less than 8 hours, starting with a rough ground surface. This corresponds to a removal rate of 180 nm (7.2 μin) per hour.

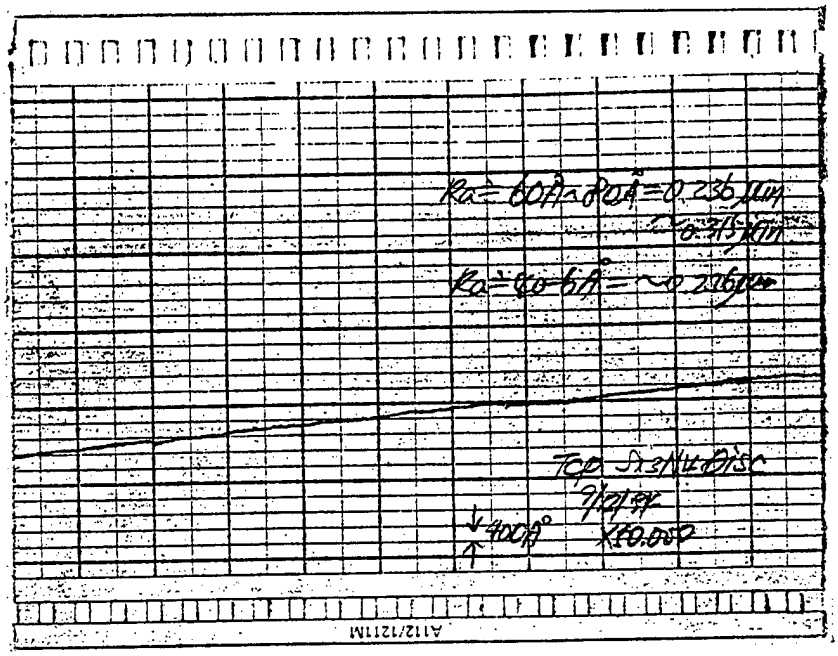

(A)

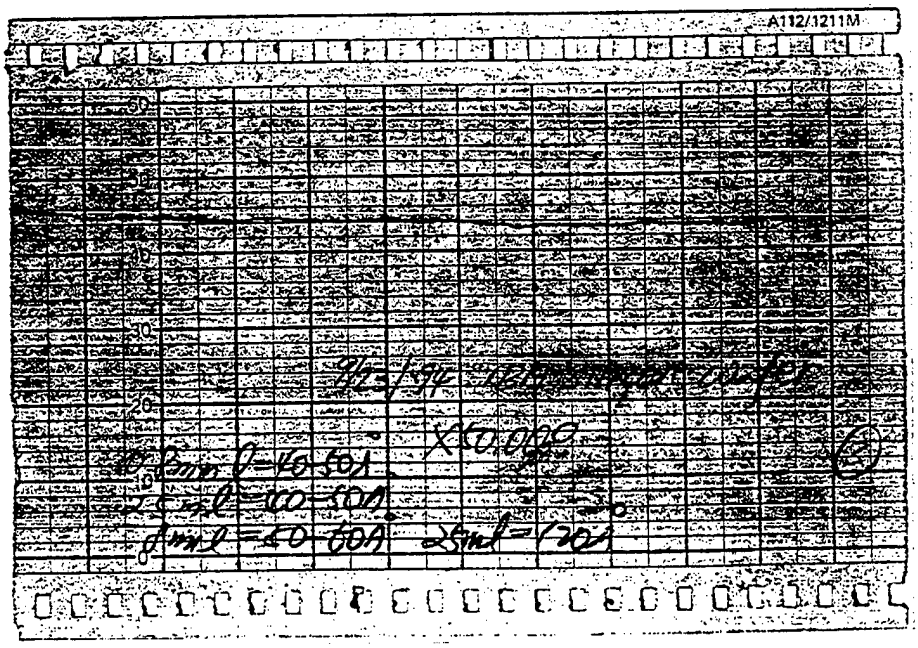

(B)

Figure 27 Profilometer trace: (A) tribochemically polished large plate (22mm x 34mm x 3mm), Vertical scale=x50,000, resolution= 0.04μm, Ra≤6nm, (B) 4" silicon wafer provided by IBM, Vertical scale=x50,000, resolution=0.04μm, Ra=4-12nm.

This is comparable to commercial finish polishing rates. Optimal process parameters for maximum material removal rate have not yet been determined. Considering the flatness of the surfaces produced, the total lapping time will depend mostly on the flatness of the initial piece.

4.4 Test and Evaluation of Biaxial Stress Specimens

Thirty biaxial stress test specimens of NDB-200 silicon nitride material were produced by Norton Advanced Ceramics. These were disks 25 mm (0.993 in) in diameter and 2 mm (0.794 in) thick. These were surface ground by low stress grinding techniques. The samples were then polished by three methods as follows:

Samples	1-10	Coarse diamond abrasive Medium diamond abrasive Tribochemical polishing
Samples	11-20	Coarse diamond abrasive Medium diamond abrasive Fine diamond abrasive
Samples	21-30	Tribochemical polishing

Surface finish and characterization of the 30 samples was done on a ZYGO interferometer. Table 13 shows the Ra and PV values for the samples. Samples were loaded to fracture in biaxial stress on a test rig shown schematically in Figure 28. Fracture origins were examined and all fractured pieces retained for further study.

Table 13.
Biaxial Stress Test Specimen
Surface Characterization

Surface Condition	Specimen[a]	R_A nm (μin)	PV nm (μin)
Grind, Polish, Tribo-chemical Finish	1	0.53 (0.021)	3.58 (0.143)
	2	4.71 (0.188)	21.91 (0.876)
	3	0.79 (0.032)	5.54 (0.222)
	4	0.63 (0.025)	4.24 (0.170)
	5	0.62 (0.025)	4.12 (0.165)
	6	0.74 (0.030)	4.30 (0.172)
	7	0.63 (0.025)	3.89 (0.156)
	8	2.36 (0.094)	12.20 (0.488)
	9	1.1 (0.44)	9.70 (0.388)
	10	0.49 (0.020)	3.74 (0.150)
	Average Deviation	2.54 (0.01)	16.92 (0.67)
	Standard Deviation	1.49 (0.06)	10.34 (0.41)
Grind, Polish, Final Polish	11	8.2 (0.033)	5.97 (0.239)
	12	9.2 (0.037)	7.91 (0.316)
	13	46.0 (0.184)	26.85 (1.074)
	14	19.6 (0.078)	13.53 (0.541)
	15	48.8 (0.020)	41.46 (1.658)
	16	16.8 (0.067)	9.85 (0.394)
	17	17.8 (0.071)	16.71 (0.668)
	18	13.9 (0.056)	7.88 (0.315)
	19	45.1 (0.180)	21.78 (0.871)
	20	28.4 (0.114)	17.29 (0.692)
	Average Deviation	1.26 (0.496)	7.32 (0.288)
	Standard Deviation	1.26 (0.496)	5.59 (0.022)

Table 13. (continued)
Biaxial Stress Test Specimen
Surface Characterization

Surface Condition	Specimen[a]	R_A nm (μin)	PV nm (μin)
Grind, Tribo-chemical Finish	21	1.70 (0.068)	10.09 (0.404)
	22	0.83 (0.033)	6.65 (0.266)
	23	0.59 (0.024)	3.85 (0.154)
	24	0.63 (0.025)	4.86 (0.194)
	25	0.482 (0.193)	26.49 (1.060)
	26	0.52 (0.021)	4.88 (0.195)
	27	0.58 (0.023)	4.68 (0.187)
	28	1.16 (0.046)	5.80 (0.232)
	29	1.18 (0.047)	6.78 (0.271)
	30	1.57 (0.063)	7.80 (0.312)
	Average Deviation	1.36 (0.054)	8.19 (0.322)
	Standard Deviation	1.22 (0.048)	6.34 (0.249)

[a] The Wyko interferometer spot size of the specimen is 0.26 x 0.32 mm (0.102 x 0.126 μin)

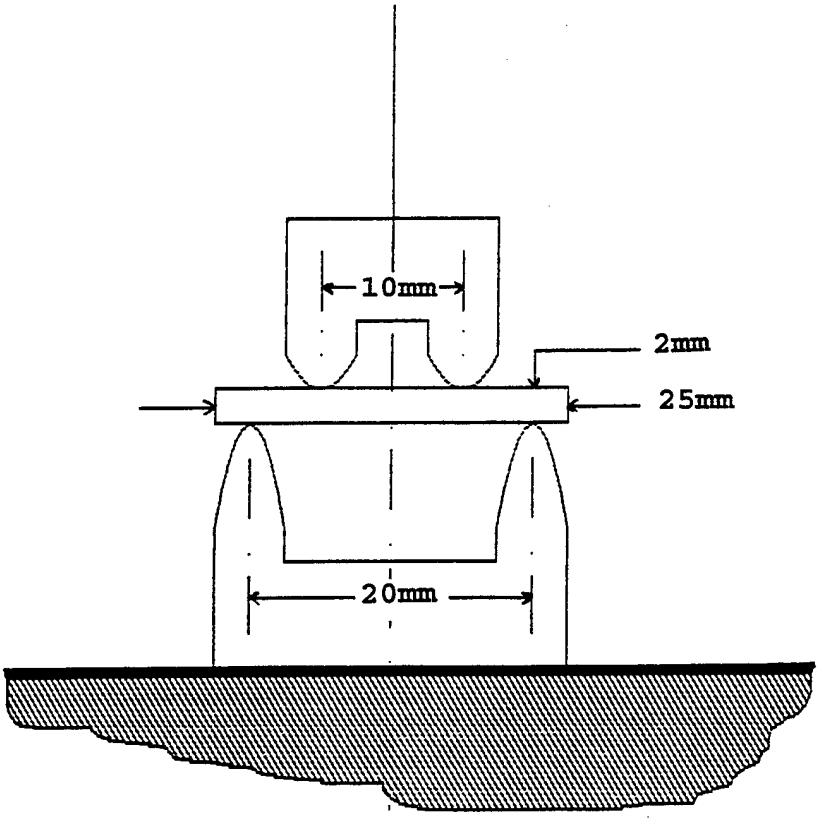

Figure 28 Schematic of an NBD-200 silicon nitride sample disk mounted in a biaxial stress load fracture test rig.

Table 14. shows the stress test results. No significant difference in fracture strength was observed between the three sample groups. Typical test values ranged from 500 to 1000 MPA (72.5 to 145 ksi). Surface finish of the TCP samples are significantly better than the abrasive polished surfaces, averaging 1.3 mm (0.052 in) for the TCP surfaces and 2.5 mm (0.100 μin) for the abrasive polished surfaces.

Table 14
Biaxial Stress Test Results

Surface Condition	Number of Samples Tested	Average Fracture Strength MPA (Ksi)	Standard Deviation MPA (Ksi)
Grind, Polish, Tribochemical Finish	10	711.1 (103.1)	284.8 (41.3)
Grind, Polish, Final Polish	10	702.8 (101.9)	115.4 (16.7)
Grind, Tribochemical Finish	10	771.4 (111.8)	104.6 (15.17)

5.0 Application of Tribochemical Polishing for Commercial Finishing of Silicon Nitride, Subtask 3.4.3

The removal rates and the surface qualities obtained with the stainless steel and cast iron plates were the same. This result indicates that tribochemical polishing can be considered a "drop in" development that does not require difficult modifications of lapping equipment or costly materials.

The shape limitations (i.e. very flat surfaces) are not an intrinsic limitation of tribochemical polishing, but are determined by the simple design of the machine. We do not see any obstacle to the tribochemical finishing of ceramic bearing balls. It was planned to research tribochemical finishing of ceramic bearing balls, but it could not be achieved within the time and resources of the present contract.

5.1 Health Considerations and Environmental Compatibility of Substances Used in Tribochemical Polishing

A low concentration solution of Hydrogen peroxide is not generally regarded as harmful. A 50 percent solution of hydrogen peroxide can be harmful because it is hygroscopic and can oxidize living tissue.

Solid chromic acid is regarded as a health hazard according to Lab Safety Supply (LSS). The preparation of a dilute solution of chromic acid from solid CrO_3 can be a dangerous process. The low-concentration aqueous solutions of chromic acid used in the tribochemical polishing investigation were not considered dangerous to use.

LSS classifies solid chromic acid as a strong oxidizer and a class 3 health hazard material. Short exposure to solid chromic acid may result in injury and could be life threatening. Chromic acid is a minor reactive material that will not burn in air. It is unstable at high temperatures and pressures. When chromic acid comes in contact with water, it can cause a reaction that will release some energy. Chromic acid is regarded as a highly toxic material; inhalation or ingestion can cause cancer. It is corrosive to live tissues and can cause irritation to eyes, lungs, and skin. Chromic acid cannot be stored near oxidizable materials such as flammables, combustibles or reducing agents. Chromic acid attacks many different kinds of plastics.

The permissible exposure limit (PEL) for chromic acid listed in 29 CFR 1910.1000, as of January 19, 1989, is 0.1 mg/m^3 of laboratory space. A PEL is a work-shift, time-weighted average (TWA) level. The "Immediately Dangerous to Life or

Health" (IDLH) concentration of chromic acid, as defined by the SCP for the purpose of respirator selection, is noted in either ppm or mg/m^3. This concentration represents a maximum level from which one could escape within 30 minutes without any physical symptoms or irreversible health effects. Concerning the chromic acid IDLH level of 30 mg/m^3 in a reasonably well ventilated area, the use of a 3 wt.% solution of CrO_3 does not present a danger. Chromic acid must be considered a dangerous pollutant if discharged into ground water. According to LSS, used solutions of chromic acid must be disposed of as follows:

Adjust the acidity of 3% solution or suspension to pH=2 with sulfuric acid. Gradually add aqueous sodium bisulfide in excess while stirring at room temperature. An increase in temperature indicates the reaction is going to completion. If no reaction appears to occur after the addition of about 10% sodium bisulfite solution, cautiously add more acid to initiate a reaction. If manganese chromium or molybdenum is present, adjust the pH of the solution to 7 and treat with sulfide to precipitate metal sulfide. Separate for burial in chemical landfill. Destroy excess sulfide, neutralize and flush the solution down the drain with large amounts of water.

The amount of chromic acid consumed by the process is small; it corresponds to the amount of silicon nitride removed by equations (12) to (14) in the text.

6.0 Conclusions and Results

1) Tribochemical polishing is a viable process that can produce extremely smooth surfaces devoid of surface defects detectable by optical, scanning electron, and atomic force microscopy.

2) Tribochemical polishing of silicon nitride produces a clean surface, devoid of a distorted "polishing layer" and of the surface contaminations that are encountered in chemomechanical polishing.

3) The Tribochemical polishing process is scalable and can be used with standard machinery and materials. The polishing fluids can be selected to be environmentally benign or, in the case of chromic acid, can be disposed of in an environmentally acceptable way without excessive cost or difficulty.

4) Tribochemical polishing can produce a very low roughness of 0.5 nm (0.02 μin) with excellent planarity of 4-6 nm. It is adaptable, with suitable change of machinery, to the finishing of bearing balls.

5) The material removal rate for tribochemical polishing of silicon nitride, although not yet optimized in our research, is comparable to that of the final finishing step in ceramic polishing.

6) Tribochemical polishing in appropriate chemical solutions does not produce residual stresses in silicon nitride.

7) 440C stainless steel and grey cast iron are effective polishing tool materials. In fact, any kind of material producing friction in the correct range can be effective.

8) There is an optimal friction coefficient for tribochemical polishing. A high friction coefficient introduces mechanical wear with surface defects. A low friction coefficient results in small material removal rates.

9) The material removal rate in H_2O_2 is higher and the friction coefficient (μ) is lower (0.3 - 0.4) than in distilled water (μ = 0.4 - 0.6). The result confirms that oxidation is the slow step in tribochemical polishing of silicon nitride. The material removal rate in CrO_3 is almost the same as in H_2O and the friction coefficient (μ) is lower (μ = 0.2 - 0.3) than in distilled water and hydrogen peroxide. CrO_3 produces the bestcombination of material removal rate and surface quality. These results are the subject of a patent application.

10) The above results show that oxidation is the slow step in tribochemical polishing of silicon nitride.

11) Generally, basic solutions show low removal rate and rough surface.

12) Acid solutions show relatively higher volume removal rate than bases, but most of them attack the grain boundaries and cause grain pull-out and rough surfaces.

7.0 References

1. X. Dong and S. Jahanmir, "Wear Transition Diagram for Silicon Nitride"; Wear, Vol. 165, pp. 169-180, 1993.

2. H. Tomizawa and T. E. Fischer, "ASLE Transactions,Friction and Wear of Silicon Nitride and Silicon Carbide in Water; Hydrodynamic Lubrication at Low Sliding Speed Obtained by Tribochemical Wear" ; Vol. 30, No. 1. pp. 41-46, 1986.

3. R. Kolenkow, R. Nagahara, "Chemical-Mechanical Wafer Polishing and Planarization in Batch Systems"; Solid State Technology, June, pp. 112-114, 1992.

4. W. J. Patrick, W. L. Guthrie, C. L. Standley and P. M. Schiable, "Application of Chemical Mechanical polishing to the fabrication of VLSI circuit interconnections"; J. Electrochem. Soc., Vol. 138, No. 6, pp. 1778-1787, 1991.

5. W. L. C. M. Heyboer, G. A. C. M. Spierings and J. E. A. M. van den Meerakker, "Chemomechanical silicon polishing-Electrochemical in situ measurements"; J. Electrochem. Soc., Vol. 138, No. 3, pp. 774-777, 1991.

6. C. D. Wagner, W. M. Riggs, L. E. Davis, J. E., edited by G.E. Muilenberg "Handbook of X-Ray Photoelectron Spectroscopy"; Perkin-Elmer Corp., 1979.

7. R. K. Brow and C. G. Pantano, "Thermochemical nitridation of microporous silica films in ammonia"; J. Amer. Ceram. Soc., Vol. 70, No. 1, pp. 9-14, 1987.

8. D. Roβ and M. Maier, Fresenius Z. "Thickness measurement of thin dielectrics with electron spectroscopy"; Anal. Chem., Vol. 333, pp. 488-491, 1989.

9. T. E. Fischer and H. Tomizawa, "Interaction of tribochemistry and microfracture in the friction and wear of silicon nitride"; Wear, Vol. 105, pp. 29-45, 1985.

10. J. P. Hoare, Plating and Surface finishing, "An electrochemical mystery story : A scientific approach to chromium plating"; Sep., pp. 46-52, 1989.

11. L. Fang, Y. Gao, L. Zhou and P. Li, "Unlubricated sliding wear of ceramics against graphitized cast iron"; Wear, 1993.